Summer 1997

Characterization of the Fast Axonally Transported Proteins in the Rat Optic Pathway

Surafel Mulugeta
Old Dominion University

CHARACTERIZATION OF THE FAST AXONALLY TRANSPORTED PROTEINS IN THE RAT OPTIC PATHWAY

by

Surafel Mulugeta
B. A. May 1982, Bluffton College

A Dissertation Submitted to the Faculty of
Eastern Virginia Medical School and Old Dominion University
in Partial Fulfillment of the Requirements for the Degree of

DOCTOR OF PHILOSOPHY

BIOMEDICAL SCIENCES

EASTERN VIRGINIA MEDICAL SCHOOL
and
OLD DOMINION UNIVERSITY
July 1997

Approved by:

Bruce W. Tedeschi, Ph.D. (Director)

Paul F. Aravich, Ph.D. (Member)

Keith A. Carson, Ph.D. (Member)

Francis J. Liuzzi, Ph.D. (Member)

Charles W. Morgan, Ph.D. (Member)

ABSTRACT

CHARACTERIZATION OF THE FAST AXONALLY TRANSPORTED PROTEINS IN THE RAT OPTIC PATHWAY

Surafel Mulugeta
Eastern Virginia Medical School and Old Dominion University, 1997
Director: Bruce W. Tedeschi

The fast axonally transported proteins represent a subset of neuronal proteins that are conveyed anterogradely as secretory vesicle constituents from the perikarya. Although fast transport displays properties consistent with the general secretory pathway, neuronal structure presents special problems which may require modifications of the general pathway. The elucidation of these special modifications is essential for a more complete understanding of neuronal function both in normal and pathological conditions. In order to characterize the fast transported (FT) proteins and to better understand fast transport trafficking, the FT of radiolabeled retinal ganglion cell (RGC) proteins in the adult rat optic pathway was studied. The optic pathway model system afforded the opportunity to delineate FT trafficking in the axon from FT trafficking at pre-synaptic terminals. Radiolabel studies of FT proteins revealed six distinct classes of proteins. The first class of FT proteins were found to have little or no trafficking preference for axons or pre-synaptic terminals. The second class of FT proteins exhibited no compartmental trafficking preference and decreased in specific activity from 4-48 hr post-labeling. Such decrease could suggest rapid turnover of these FT proteins. A third class of FT proteins showed increased specific activity only in the axon compartment at 24 hour post intra-ocular labeling (PIL). A fourth class of FT proteins appeared to be

trafficked to both compartments, but with a slower time course than the general FT population. The fifth and sixth classes of proteins represent those proteins that were preferentially localized to the terminal and axon compartments, respectively. Fractionation of synaptosomal membranes revealed that the majority, but not all, of FT proteins were conveyed as integral membrane proteins. Immunoprecipitation revealed the major ^{35}S-methionine labeled protein in the rat optic pathway (SNAP-25) was found to be associated with specific subsets of FT and slow transported (SCb) proteins. In summary, the FT proteins in the rat optic pathway displayed heterogenous transport initiation, kinetics, compartmentation, and intermolecular association. Since axons lack sorting organelles (e.g., Golgi), these results suggest that neurons have evolved complex mechanisms for differential delivery of FT proteins from the perikarya.

This work is dedicated to my parents. To my loving mother, Yeshihareg Sebsebé, and in memory of my dear father, Mulugeta Akalu.

ACKNOWLEDGMENT

This project would not have been possible without the assistant and support of many people. I am sincerely grateful to Dr. Paul Aravich, Dr. Keith Carson, Dr. Frank Liuzzi, Dr. Charles Morgan, and Dr. Bruce Tedeschi for serving on my committee and providing me with the guidance during the course of this project. I would also like to thank Dr. Aravich for his help in the presentation of my defense; David Haddaway for his skilled editorial help; Michael Brown for his skills in the electron microscope; Diane Carroll for her office-work assistance; and Dr. Paul Kolm for his statistical expertise. It was a privilege and an honor to have been among such caring and supportive people.

Most of all, I express my earnest gratitude to my advisor, Dr. Tedeschi, who has been my inspiration throughout the course of my studies. His encouragement, guidance, tremendous patience, and genuine concern for the welfare of my education, have been most invaluable and for which I am forever indebted.

TABLE OF CONTENTS

Page

Page

Page

LIST OF TABLES

LIST OF FIGURES

Page

Page

Page

CHAPTER I

INTRODUCTION

A. REVIEW OF THE LITERATURE

A key question in cellular neurobiology is how proteins are directed to the various specialized regions of the neuronal cell. Neurons are characterized by highly elongated extensions, i.e., the dendritic and axonal processes, that can extend over distances thousands of times greater than the cell body diameter and comprise a total volume of cytoplasm hundreds of times greater than the cell body volume (1, 2). Nevertheless, it is the cell body, containing the protein synthesizing machinery, that is responsible for the maintenance of the whole neuronal mass. Thus, during development, maturity, and regeneration, proteins making up the axon and terminal, as well as those that are secreted, are essentially generated in the cell body and then conveyed by axonal transport to their axonal and terminal targets (3). The neuron's normal operation, therefore, depends on the accurate delivery of these proteins from the cell body to the specific axonal and terminal destinations by specialized transport systems. Discerning the complex series of events that are involved in the transport of these proteins is fundamental to understanding the normal function of neurons. The current study examines the kinetics and compartmentation of one population of the axonally transported proteins, the *anterograde fast axonally transported proteins.*

The Model Journal used for this dissertation was The Journal of Cell Biology.

1. BASIC PRINCIPLES OF NEURONAL PROTEIN SYNTHESIS AND TRAFFICKING

With the exception of axonally transported mitochondrial proteins, essentially all of the neuronal proteins are translated in the cell body and dendrites (4, 5). Each protein bears targeting sequences which initially direct the protein to one of four destinations: the cell nucleus, mitochondria, peroxisomes, or rough endoplasmic reticulum (RER). Proteins that are destined to the nucleus, mitochondria, and peroxisomes, along with cytoplasmic proteins, are synthesized on free polysomes. Proteins destined for the secretory pathway or lysosomes are co-translationally directed to the RER.

Proteins, directed to the RER via a signal sequence, are either completely inserted into the RER lumen or tethered to RER membrane by hydrophobic transmembrane domain(s). The fate of lumen-soluble or membrane-bound proteins depends on the signal sequence within each protein (6). Proteins, that contain retention signals, remain in the ER and Golgi apparatus (GA) as membrane-bound or soluble luminal constituents. Proteins, lacking retention or lysosomal targeting signals, are packaged in the trans-Golgi network (TGN) for the secretory pathway.

Transfer to the secretory pathway takes place from the RER either via transition vesicles which shuttle to the cis-face of the GA (7, 8) or via a system of tubules that are continuous between RER and GA (9). Within the RER and GA, proteins are altered by a series of proteolytic cleavages, glycosylations, sulfations, or other post-translational modifications. These modifications depend on the specific enzyme content within the RER and the cis-, medial-, and trans-segments of the GA (10, 11).

As in other non-neuronal cell types, two secretory pathways, known as constitutive and regulated pathways, exist in neurons (12, 13, 106, 108). The constitutive pathway refers to Golgi-derived vesicles that continuously 1) refurbish the plasmalemma by bringing newly-formed membrane and membrane-associated molecules to plasma membrane 2) recycle existing membrane back into the cell, primarily through endosomes and 3) secrete viral proteins, enzymes, growth factors, and extracellular matrix molecules by fusion with the plasma membrane. This pathway occurs in the absence of signals (e.g., calcium/depolarization). In contrast, the regulated pathway refers to secretory and synaptic vesicles that fuse with the plasmalemma and release their contents (neuroactive peptides, neurotransmitters, neruomodulators) in response to external stimuli.

Membranous organelles of the secretory pathway, therefore, carry a number of different type of proteins: integral and peripheral membrane proteins that are destined to the plasmalemma, soluble proteins that are destined for secretion at the plasma membrane, and motor proteins that carry the vesicles on slower moving microtubules (14, 15, 16, 17, 18). Among the integral and peripheral proteins, uncharacterized proteins may exist to code the vesicles for their final destination (19). Thus, transfer of membrane and membrane-associated molecules between the protein synthesizing machinery and the plasmalemma is accomplished by a directed transport of vesicles.

2. TOPOLOGY OF VESICLES

During their synthesis and sorting, proteins of the secretory pathway are segregated from proteins of the cytoplasm (37, 43, 44). Studies have demonstrated that

the side of internal membranes facing the vesicle lumen is topologically equivalent to the side that will be facing the outside of the cell when the vesicle fuses with the cell surface. For vesicle integral membrane proteins, the lumenal domain of the internal protein will be exposed on the extracellular membrane surface upon exocytosis, and the cytoplasmic domain will be exposed on the cytoplasmic membrane surface. Evidence for this topology was determined in the studies of newly synthesized glycoproteins. The glycotransferase enzymes responsible for the glycosylation of polypeptide chains are restricted to lumenal domains. Thus, while the glycoproteins face the lumen during vesicular intracellular transport, they emerge as extrinsic cell surface determinants when they reach the plasmalemma (45, 46, 47).

3. AXONAL TRANSPORT

Radioisotopic studies of the axonal transport system have revealed the simultaneous movement of at least five distinct categories of proteins, each transported at a different rate and/or direction (20, 21). The first four groups of transport represent the anterograde transport from the cell body to the periphery of the neuron. Two groups of proteins are carried by slow axonal transport at rates of 0.2 to 1 mm/day and 2 to 5 mm/day and are designated slow component a (SCa) and slow component b (SCb), respectively. Slow axonal transport proteins include components of the cytoplasmic matrix and associated proteins, including cytoplasmic enzymes of intermediary metabolism (22, 23). SCa proteins include tubulin, neurofilament triplet, tau proteins, and spectrin. SCb proteins include actin, clathrin, spectrin, myosin and myosin-like proteins, nerve-specific enolase, creatine kinase, calmodulin, aldolase, and pyruvate

kinase. These slow transported proteins may serve to replenish worn out structural proteins and to supply such proteins to growing axons.

Two groups of proteins are transported by fast axonal transport at rates ranging from 50 to 400 mm/day. Mitochondria, and associated proteins such as F1 ATPase, are transported at rates of 50 to 100 mm/day. The major population of anterograde fast transported (FT) proteins are transported as constituents of membranous organelles at rates of 200 to 400 mm/day (21). These organelles include secretory vesicles, synaptic vesicles, large dense cored vesicles, multivesicular bodies, and lysosomes or prelysosome-like organelles (25, 26, 27, 28). The membranous FT organelles are predominantly small vesicles with an average diameter of 80 nm. However, neurosecretion is mediated by several types of vesicles (29, 30, 31, 32). Large dense cored vesicles appear to typically contain neuropeptides and secretory proteins. Small dense cored vesicles contain transmitter-associated enzymes (e.g., dopamine ß-hydroxylase for adrenergic neurotransmitters). Small clear vesicles contain neurotransmitters such as glutamate, γ-aminobutyric acid (GABA), and acetylcholine. Other proteins that have been shown to be fast transported include Na^+-K^+ ATPase and growth associated proteins (GAPs). The relative number of these vesicles varies depending on the cell type. No proteins of the cytoplasmic matrix have been detected moving with the FT membranous organelles, while the membranous organelles of the smooth endoplasmic reticulum appear to be moving at a rate slower than FT proteins (24, 97). In addition, the movements of these FT organelles have been directly observed using video enhanced microscopy, and the rate of their movement is consistent with studies performed with radioisotopes (51, 52, 53).

The fifth and last group, categorized as fast retrograde axonal transport (RT), represents directed movement of organelles from the neuronal periphery to the cell body at rates of about 100 to 200 mm/day (1 to 2 μm/s). Similar to anterograde FT proteins, the RT proteins are components of membranous organelles. These RT organelles appear to be morphologically similar to many of the organelles associated with endocytosis. These organelles include multi-vesicular bodies, lysosomes, pinocytic vesicles and receptor-mediated endocytic vesicles. In addition, a substantial proportion of the organelles is composed of vesicles that are morphologically indistinguishable from the anterogradely transported vesicles (25, 26). Retrograde transport may also serve to remove worn-out or old membrane constituents from the plasma membrane while anterograde fast transport replenishes such constituents.

This brief account describes the nature of organelles and most proteins that are destined for axonal transport. The following section will outline, in greater detail, the complex series of events that are involved in sorting and trafficking of the anterograde fast axonal transported proteins.

4. FT PROTEINS

As described earlier, proteins destined for the cell surface membrane or secretion are synthesized in polysomes coupled to the RER. They then pass, via vesicle shuttle or direct membrane continuities, to the GA for post-translational modification/sorting and leave the GA as constituents of secretory vesicles. Since FT involves the translocation of vesicles, a prediction would be that the FT proteins are initiated from the RER-GA system.

Evidence for the initiation of FT in the RER-GA has been described in numerous studies (25, 26, 27, 28). For example, autoradiographic electron microscopy has revealed that radiolabeled proteins appeared to pass sequentially from the RER to GA to the axon (33). Upon entering the axon, the membrane-associated proteins are presumably conveyed by a fast axonal transport microtubule-based mechanism (34, 35). RER-GA dependence of FT proteins has also been shown in pharmacological-based studies. Monensin, a Na^+ ionophore that is known to interfere with intracellular traffic through the GA (36), significantly reduced accumulation of FT proteins in the axon. Further, Co^{2+}, an antagonist of Ca^{2+}-mediated events (vesicle transfer from RER to GA and release of vesicles at the trans-GA), and brefeldin A, which disrupts the cis- and medial-GA, both appeared to also decrease the amount of radiolabeled FT proteins delivered to the axon (36,105). Similar pharmacological studies in non-neuronal systems have demonstrated a reduction of radiolabeled integral membrane cell surface proteins and released secretory proteins (48, 49, 50). Thus, routes, by which membrane and secretory proteins reach the axon, appear as variations of a common pathway. One variation is that proteins destined to the axon appear to be routed at a steady rate through the constitutive pathway rather than the regulated pathway which requires extracellular stimuli.

Since the membrane-bound transport of FT proteins as vesicle components requires the assembly of a protein-lipid complex, inhibiting lipid synthesis might be expected to decrease transport of FT proteins. Experimental drug studies support this proposition. Both fenfluramine, an agent that affects phospholipid biosynthesis, and diazacholestrol, an agent that blocks the final step of cholesterol biosynthesis, have been

shown to inhibit protein or phospholipid fast transport (109).

5. INITIATION OF FAST TRANSPORT

Some FT proteins may enter a storage pool in the cell body prior to entering the axon. Studies have shown prolonged release of lipids (58, 59), proteins (60, 61, 62, 65, 66), and glycoproteins (63) from the neuronal soma. These results have been interpreted to suggest that some material may enter a storage pool from which they are slowly released and then conveyed by fast transport once they enter the axon. Other FT proteins may display even more complex kinetics. For example, some synapsin I, a neuron-specific FT phosphoprotein that is found associated with the surfaces of small synaptic vesicles, displays a rapid initiation profile; while a second synapsin I subpopulation seems to enter a delayed release storage pool (62, 64, 107).

6. PROTEIN TARGETING

As previously described, proteins are encoded with sorting sequences which target them to specific intracellular organelles. The pharmacological studies suggest that most FT proteins contain a signal sequence targeting them to the RER. The first evidence for such sorting signal sequences came from studies utilizing mRNA-directed cell-free systems. When translated *in vitro*, many eucaryotic proteins, hormones, and immunoglobulin light chains appear to have higher molecular weights than their *in situ* molecular size (39, 40, 41, 42). In each case, the difference was found to be at the N-terminal region of the protein and corresponded to the first 18-30 amino acid residues. This N-terminal leader or signal sequence was subsequently shown to attach the polysome

to the RER and lead the growing polypeptide chain through the membrane into the lumen of the RER. The signal sequence is eventually cleaved from the protein in the RER prior to chain completion. Do neuronal proteins contain additional structural signals necessary to initiate their FT, as well as, target them to specific final destinations?

Post-translational modification may play an important role in determining the fate of newly synthesized FT proteins. For example, glycosylation has been shown to: (1) protect its protein moiety against proteolysis; (2) assist in determining the glycoproteins' final destination (54); and (3) serve as a membrane functional determinant at the cell surface (55). Axonal transport studies, using metabolic isotopic sugar labeling, have shown that glycoproteins are specifically conveyed with the FT protein population and are not conveyed among the slow transported proteins. In addition, the molecular weight of these glycoproteins are predominantly greater than 35 kDa as estimated by sodium dodecyl sulfate-polyacrilamide gel electrophresis (SDS-PAGE) (56).

When visualized by 2D fluorography, most of the carbohydrate-containing species line up as groups or families of spots, each group having a similar molecular weight but different isoelectric points. Studies utilizing neuraminidase treatment of FT proteins, an enzyme that removes sialic acid residues from glycosylated proteins, have demonstrated that each group can represent a single protein type with individual species bearing different sialic acid charge units. Many of the spots in a group collapse to a single larger spot, following neuraminidase treatment, while other spots are either unaffected or shifted to more basic isoelectric points (56).

Sulfation is another post-translational modification which appears to play a role in assisting FT proteins to their destinations. Sulfated glycoproteins have been shown

to travel among FT proteins (57) and may be involved in directing FT proteins to the terminal region of the neuron.

Thus, in neurons, FT proteins display behavior characteristic of secretory pathway proteins.

7. DIFFERENTIAL DELIVERY OF FT PROTEINS

Preferential delivery of FT proteins either to the axon or terminals has been reported in several studies (63, 67, 110, 111, 112, 113, 114, 115). Cancalon and Beidler, using the long unmyelinated axons of the garfish olfactory nerve, demonstrated the preferential delivery of FT protein to the axon and pre-synaptic terminal (67). One- and two-dimensional electrophoretic of FT proteins in both garfish and bullfrog systems (67, 68) have shown that, while predominantly lower molecular weight species tend to be preferentially deposited in the axon, higher molecular weight species are transported to the terminal. Further, some of the FT proteins that appeared to be destined for pre-synaptic terminals contained sulfated tyrosine residues. This result suggests that the presence of sulfation on tyrosine residues may play a role in sorting some FT proteins to the nerve terminal (69, 77). Support for this hypothesis came from tissue culture studies showing that K^+ stimulation of pheochromocytoma cells (PC-12 cells) resulted in secretion of sulfate-containing proteins (70, 78).

In support of differential routing of FT proteins, a recent study has presented evidence for heterogenous populations of FT membranous organelles (71). Subcellular fractionation of the rabbit optic nerve after intraocular labeling revealed three populations of organelle that were transported into the axon. The lightest density membrane fraction

population (diameters >200nm) appeared to be stationary in the axolemma. Immunological studies of this population revealed the presence of glucose transporters, which are normally abundant in the axolemma. The intermediate density fraction population (vesicular diameters ~84 nm) appeared to be mobile and disappeared from the axon with kinetics consistent with fast transport. The protein contents (glucose transporters, synaptophysin, and kinesin) of this population suggested that this population of organelles is destined to both axons and terminals. The heaviest fraction population contained FT synaptophysin and tachykinin neuromodulators which are pre-synaptic terminal proteins suggesting that this population of organelles is destined to the terminals. Thus, the results of such studies suggest that not all FT proteins are routed to the same destination following initiation from the soma.

8. SNAP-25

Perhaps the most intensively investigated organelles at the pre-synaptic terminals are the synaptic vesicles (72, 73, 74), owing to their unique functional properties in the storage and release of chemical messengers (e.g., neurotransmitters and neuromodulators). Most synaptic vesicle-associated proteins have been purified and are well characterized (72, 75). These vesicle-associated proteins play important roles in the targeting, docking, and fusion of the synaptic vesicles at pre-synaptic terminals (76).

The 25 kDa synaptosomal associated protein (SNAP-25) and syntaxin are neuronal-specific plasma membrane proteins that act in concert with other pre-synaptic terminal proteins, including the synaptic vesicle proteins, to mediate exocytotic membrane fusion and neurotransmitter/neuromodulator release (79). SNAP-25 and

syntaxin function as target synaptic vesicle receptors (t-SNARES) by binding to specific vesicle-associated proteins, the vesicle synaptic vesicle receptors (v-SNARES). In neurons, the v-SNARES are synaptobrevin (also known as VAMP) and synaptotagmin. Recent evidence suggests that the t-SNARES and v-SNARES form a precomplex, followed by a displacement of synaptotagmin for a core fusion complex comprised of N-ethylmaleimide-sensitive factor (NSF) and three isoforms of soluble NSF-associated proteins (α-, ß-, and γ-SNAPs) (80). The important roles of the t-SNAREs and v-SNARES in exocytosis have been demonstrated by studies utilizing botulinum neurotoxins (BoNTs), which specifically act on the SNAREs. BoNTs penetrate motorneurons at the neuromuscular junction where they block acetylcholine release. These toxins are zinc-dependent endopeptidases that selectively cleave SNARE proteins, thereby inhibiting the docking and fusion of synaptic vesicles (81, 82, 83). The particular botulinum neurotoxins that cleave SNAP-25 include serotypes A, C, D, and E (82, 83, 84).

Evidence suggests that SNAP-25 may also be involved in axonal growth and differentiation. SNAP-25 is expressed in axonal growth cones during elongation, and this elongation can be halted by selective inhibition of SNAP-25 (85). Two isoforms of SNAP-25 (SNAP-25a and SNAP-25b) can be generated by alternative splicing of exons (86, 87). The two isoforms are characterized by a different clustering of cysteine residues involved in post-translational palmitoylation, an important mechanism for membrane anchoring of SNAP-25. These isoforms are differentially regulated during development (88). In the neonatal rodent brain, the low levels of SNAP-25 mRNA consist predominantly of the SNAP-25a isoform, whereas during synaptogenesis and

brain maturation, there is a dramatic induction of SNAP-25 mRNA principally by the upregulation and preferential expression of the SNAP-25b isoform (88, 89).

The sequence of SNAP-25 is known and displays several important properties. First, SNAP-25 has a large number of methionine residues. In fact, it is the most prominent species among methionine-labeled proteins conveyed by fast axonal transport. Its conspicuous appearance among methionine-containing proteins has lead to the designation, *superprotein*. Radiolabel studies have shown that SNAP-25 incorporates greater than 14% of total FT ^{35}S-methionine, more than 20 times the average incorporation, in rabbit retinal ganglion cells (62, 90, 91). Although SNAP-25 may be methionine-rich, its abundance is relatively low. For example, SNAP-25 has not been detected by staining of electrophoretically separated proteins with Coomassie blue or silver (92).

Second, SNAP-25 is a major substrate for palmitoylation (93). Unlike most integral membrane proteins, SNAP-25 lacks a sufficient hydrophobic domain for insertion into the membrane. Instead, it is anchored to the membrane on the cytoplasmic face by palmitoyl side chains attached to four tandem cysteine residues. SNAP-25 appears to be palmitoylated in the cell soma prior to transport initiation.

Finally, lowered SNAP-25 expression has been shown to be associated with certain behavioral abnormalities. Locomotor hyperactivity and delayed neurobehavioral development have been observed in the mouse heterozygous SNAP-25 mutant (coloboma) (94, 95). Moreover, the relative abundance of FT SNAP-25 in rat motorneuron has been shown to increase after chronic exercise (96). This result has been interpreted to suggest that SNAP-25 may play a role in the exercise-induced changes of neuronal morphology

and physiology.

B. STATEMENT OF THE CURRENT INVESTIGATION

As stated in the brief account outlined in part A, the anterograde fast axonal transported proteins are believed to be conveyed as components of membranous organelles (vesicles) from the neuronal perikarya to their axonal and pre-synaptic terminal compartments. The basic cellular mechanisms of vesicular packaging and sorting of the secretory pathway have been resolved (4, 5, 9, 11, 12, 13, 15). However, the neuronal mechanisms underlying the specialized axonal secretory pathway are not well understood. It is not clear how FT proteins arrive at specific destination sites following the initiation of axonal FT. It was the purpose of this study to characterize the trafficking of the newly synthesized FT proteins. By using the mammalian optic pathway as a model system (which has been used widely to study axonal transport), the FT proteins were characterized regarding their targets, kinetics, packaging, and intermolecular associations along the transport pathway.

The compartments of adult neurons offers several advantages in the study of protein expression. The translational (ribosomes, mRNA) and sorting/trafficking machinery of the GA are restricted to the somal/dendritic compartments. In contrast, the axon/terminal compartments are believed to be lacking this machinery. Such compartmentalization in adult neurons permits the study of protein expression in cellular compartments separate from the translational/sorting compartments. Microinjection of labeled precursors, such as ^{35}S-methionine, near the vicinity of adult neuronal cell bodies,

such as the mammalian retinal ganglion cells (RGCs), allows the precursors to be incorporated into neuronal proteins resulting in the production of labeled proteins *in vivo*. Some of these labeled proteins are then selectively transported into the axonal compartment. At various time intervals following pulse labeling to allow the movement of FT into the optic pathway, optic nerve/optic tract (ON/OT, respectively) proteins and superior colliculus (SC) (pre-synaptic terminals, primarily) proteins can be studied.

The anatomy of the ocular chamber, itself, provides a further methodological advantage. The RGCs extend their axons through the sclera/choroid somewhat anatomically isolating the RGC cell bodies face from the axon and terminal regions. Thus, when radioisotopes are injected into the vitreous ocular chamber, they remain confined within the eye. The only radioactivity found in the axons and terminal regions should be axonally transported pulse-labeled proteins from the cell bodies of the RGCs.

The first study examined the distribution and kinetics of FT proteins in the rat optic pathway. By radiolabeling the rat RGC proteins *in vivo* and using 2D-SDS-PAGE and fluorography, two-dimensional maps were obtained representing radiolabeled proteins along the optic pathway. From qualitative and quantitative analyses of these two dimensional maps, the relative differences in trafficking of FT to the axon and terminal compartments were evaluated. The results delineated various classes of FT proteins based on their trafficking behavior. In addition, the two-dimensional maps were used to examine the kinetics (turnover) of individual FT proteins.

The second study examined the packaging of FT proteins within the transported organelle (i.e., vesicles). After radiolabeling RGC proteins and allowing fast transport to reach the terminals, synaptosomes from the terminal tissues (SC) were prepared.

Synaptosomes were fractionated to yield integral membrane, peripheral membrane, and soluble vesicular components. One- and two-dimensional fluorographs of each fraction were analyzed to evaluate the membrane/soluble distribution of individual FT proteins.

The final study investigated intermolecular association of SNAP-25 (superprotein) during transport. Labelled FT or slow transported (SCb) proteins were immunoprecipitated with SNAP-25 antibodies and labeled co-immunoprecipitates analyzed by 1D-PAGE/fluorography. Variation in intraocular pulse kinetics (4 hr pulse vs. 12 day pulse), preceding immunoprecipitation (IP) procedures, allowed the differentiation of FT co-immunoprecipitated (CO-IP) proteins from slow transported CO-IP proteins.

In summary, an *in vivo* model system was utilized to study trafficking of individual newly synthesized FT proteins. The polarization of adult neuronal cells allowed the analysis of FT trafficking in cell regions (ON/OT, SC) spatially distinct from the synthesis/packaging compartments (soma). Compartmental analysis of FT proteins was performed to describe the trafficking of individual FT proteins. Further, the distribution of FT proteins comprising the transported organelle was made utilizing synaptosomes fractionation procedures. Synaptosomal fractionation revealed this packaging of FT proteins as constituents of membrane organelles. Finally, the possible intermolecular relationship during transport of the abundant FT protein (SNAP-25) was assessed in CO-IP experiments.

The results of the present studies have provided further insights into the complex mechanisms underlying FT protein trafficking. Six distinct class of proteins were identified according to their differential spatial and temporal localization in the adult rat

optic pathway. The first class of proteins were localized to both compartments (axon and terminal) without showing any major preference to either one. The second class of proteins were either expressed transiently or decreased their expression significantly over a period of time. Increased expression in the OT at 24 hr post intra-ocular injection represented the third class of protein; whereas, delayed appearance with increased expression, as transport time lengthened, characterized the fourth class of proteins. The fifth and six classes of proteins represent those proteins that were preferentially localized in axon and terminal regions, respectively. Evidence of possible prolonged release from the neuronal perikarya was observed in most of the resolved FT proteins. Most FT proteins in the rat optic pathway were conveyed as constituents of integral proteins. Relatively low amounts of soluble proteins were detected. Finally, SNAP-25 was the major ^{35}S-methionine labeled proteins (over 25% of total FT proteins) in the adult rat optic pathway. It appeared to associate with other FT and SCb proteins in the axon and terminal regions. This result suggests that some FT proteins (e.g., SNAP-25) may have elaborated intermolecular relationships during their optic pathway translocation.

CHAPTER II

MATERIALS AND METHODS

A. MATERIALS

1. ANIMALS

Adult male Sprague-Dawley rats (Harlan, Indianapolis, IN) weighing 275 to 300g, were used in all experiments. Care and surgical handling of all rats were in accordance with guidelines specified by the institution's Animal Care and Use Committee and *NIH Guide for the Care and Use of Laboratory Animals*. Copies of approval for these projects can be obtained at the institution's department of Office of Research.

2. RADIOISOTOPES

^{35}S-methionine (1000 Ci/mM), purchased from Dupont (New England Nuclear, Boston, MA), was used in all experiments. All work with radioisotopes was performed, in designated laboratories by certified individuals and in accordance to the guidelines specified by the institution's Radiation Safety Committee. Copies of certificates of approval to use radioisotopes can be obtained at the institution's department of Environmental Health and Safety/Radiation Safety Program office.

3. EQUIPMENT

Eppendorf Centrifuge, model 5415; Beckman Centrifuge, Model J-21C; and Beckman L7 Ultracentrifuge have been used for samples requiring centrifugal forces of $<12Xg$, $<50Xg$, and $>50Xg$, respectively. Quantification of radiolabeled polypeptides was determined using the Omni Media Scanner (XRS) 12cx, Sun Solaris mircrosystem hardware, and the Unix, Bio-Image computer software system. The Beckman LS-7000 Liquid Scintillation Spectrometer was used for acid precipitable counts per minute (CPM) determination of radiolabeled protein transport. Ultrastructural analyses of synaptosomal fractions were performed using the Phillips 301 transmission electron microscope. The Protean II electrophoretic apparatus (BIO-RAD) was used for SDS-PAGE procedures. Gels were dried with the model 583 gel dryer (BIO-RAD).

4. ANTIBODIES

Primary murine monoclonal antibodies, against SNAP-25, were purchased from Chemicon International, Inc. (Temecula, CA). Secondary antibodies of anti-mouse IgG, developed in rabbit using purified mouse IgG as the immunogen, were acquired from Sigma Immuno-Chemicals (St. Louis, MO).

B. METHODS

1. PROTOCOL FOR PREFERENTIAL LOCALIZATION AND KINETICS OF FT PROTEINS STUDY

Three animals per experiment corresponding to three time intervals (4, 24, and 48 hr) were used for this part of the study. The experiment was repeated four more times to substantiate results (figure 1).

Retinal ganglion cell proteins of the left eye were radiolabeled by intraocular injection of ^{35}S-methionine. At 4, 24, and 48 hr post-labeling, animals were sacrificed, and labeled optic pathway components (left retina, left ON, right OT, and right SC) were dissected, and proteins were solubilized in denaturation buffer. Protein radiolabel activity, count per minute (CPM), in optic pathway was assessed by acid precipitable scintillation counting. This provided a quantitative measure regarding the distribution of the FT total protein population in the different compartments of the optic pathway. Denatured tissue proteins were separated and analyzed by 2D-SDS-PAGE for each electrophoretic experiment, and the success of the 2D technique was confirmed by Coomassie blue staining of the gels. The relative 2D gel locations of several abundant proteins (actin, tubulin, etc.) on two dimensional gels are known and detectable by Coomassie-blue (sensitivity to ~ 1μg/spot). Such staining, provided a control check for the 2D separation. Gels were then fluorographed and exposed to x-ray film for various periods of time. Film spots, representing labeled proteins, were examined both visually and by densitometry to evaluate the relative labeling of the various proteins making up the FT proteins in each neuronal compartment. Comparison of the relative labeling of individual proteins between compartments, and evaluation of the relative abundance of

each protein between the different times of post-labeling, were performed.

One potential experimental problem is that optic pathway proteins might be radiolabeled as a result of local synthesis, rather than fast axon transport from RGCs. This could happen if isotopic precursors reached the ON, OT, and/or SC by either tissue diffusion or blood-borne transport and the precursor was subsequently utilized locally to synthesize radiolabeled proteins. This possibility was controlled for in three ways. First, the 2D fluorographs themselves served as diagnostic controls for possible local utilization of precursors. Since actin and tubulins are the major synthesized proteins in tissues, but are not fast-transported proteins, then the presence of these radiolabeled proteins on 2D fluorographs are indicative of local synthesis rather than fast transport. Second, the activity of radiolabeled proteins in the tissues of the primary optic pathway from the non-labeled eye were compared with the activity in the corresponding tissues from the labeled eye. Any local utilization of precursor would be detected as significant labeling in the primary optic pathway tissues from the non-labeled eye. Finally, radiolabeled SC proteins in 2D fluorographs were compared under conditions where the RGC was radiolabeled with conditions where the SC itself was directly radiolabeled labeled. Local labeling would be suspected if the 2D patterns were similar under both labeling conditions.

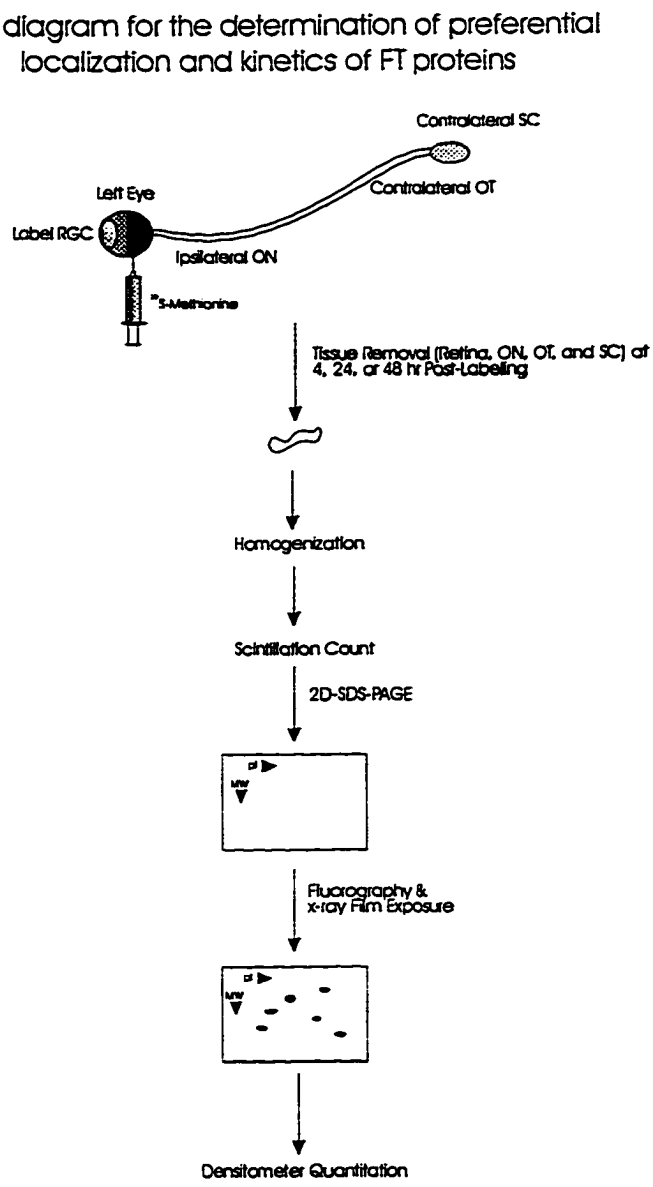

FIGURE 1. Flow diagram for the determination of preferential localization and kinetics of FT proteins. This procedure required four to seven weeks; three to six days, from intraocular injection to fluorography, and up to six weeks for x-ray film exposure.

2. PROTOCOL FOR CHARACTERIZING PROTEIN CONSTITUENTS MAKING UP THE FAST TRANSPORTED VESICLES

RGC proteins of the left eye were radiolabeled with ^{35}S-methionine. At 4 hr post-labeling, animals were sacrificed and synaptosomes were prepared from the contralateral SC. During synaptosomal preparation, the pre-synaptic nerve terminals are torn away from their axons and sealed to form detached particles called synaptosomes (116, 117, 118). Synaptosomes are then separated from other subcellular particles using fractionation procedures. Synaptosomes have been shown to retain the morphological features and biochemical composition of the intact pre-synaptic terminal. Thus, the synaptosomal preparation allows examination of the pre-synaptic FT protein components of the RGC without the interference of possible post-synaptic contamination. Further, fractionation procedures (sodium carbonate, and osmotic lysis methods) have been shown to work well with synaptosomal and microsomal fractions (101, 101).

The synaptosomal fraction was divided into two equal parts to be used in two distinct separation procedures. First, the sodium carbonate (Na_2CO_3) method was used to separate the integral from the peripheral and soluble proteins. Second, the osmotic lysis method was used to separate soluble proteins from the integral and peripheral proteins. The following fractions were obtained from these separation procedures: integral proteins only; peripheral and soluble proteins; soluble proteins only; and integral and peripheral proteins. Following separation, labeled protein activity in each fraction was measured by acid precipitable scintillation counting. Then, 1D- or 2D-SDS-PAGE was performed for each fraction, PAGE gels were fluorographed, and fluorographed gels exposed to x-ray films for various periods of time. Fluorographic spots, representing

labeled proteins, were analyzed to determine the individual proteins that make up the integral, peripheral, and soluble components of the synaptosomal fraction (figures 2 and 3).

3. PROTOCOL FOR IMMUNOPRECIPITATION WITH ANTI SNAP-25

Two animals per experiment were used. In each experiment the first animal was sacrificed 4 hr post-labeling to study the association of SNAP-25 with other FT proteins, and the second animal was sacrificed 12 days post-labeling to evaluate the association of SNAP-25 with slow transported (SCb) proteins (figure 4).

The RGC proteins in the left eye of the rats were radiolabeled with ^{35}S-methionine. At 4 hr and 12 day post-labeling, rats were sacrificed and the components comprising the major axons and terminals of the optic pathway were removed and homogenized with a non-denaturing detergent. The relative activities of labeled proteins in collected compartments (left retina, left ON, right OT, and right SC) were measured by acid precipitable scintillation counting. The tissue of each compartment was divided into two equal volumes, subjected to immunoprecipitation with SNAP-25 monoclonal antibodies, or control antibodies (anti-mouse IgG antisera) and CO-IPs analyzed by 1D-SDS-PAGE. PAGE gels were fluorographed and exposed to x-ray films for various period of time. The 4 hr and 12 day post-labeling experiments revealed co-immunoprecipitation of SNAP-25 with FT and SCb proteins, respectively.

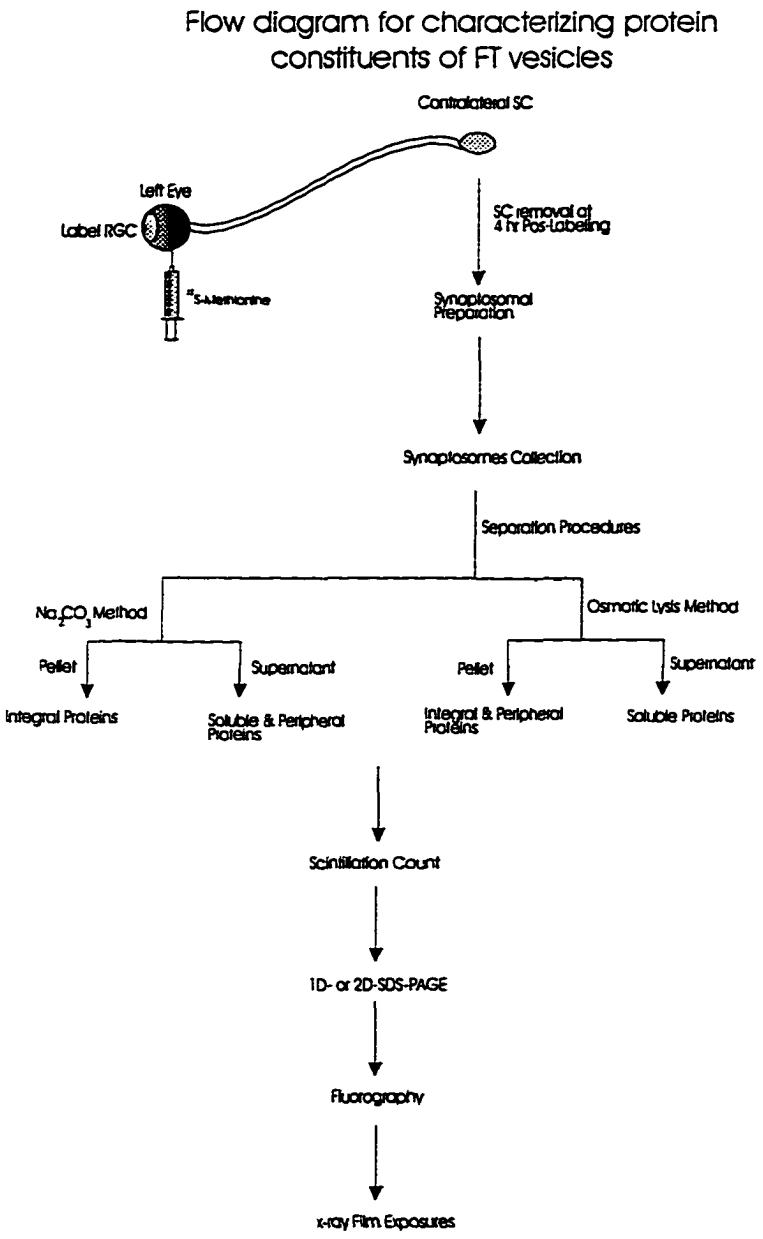

FIGURE 2. Flow diagram for the determination of proteins constituents making up the FT vesicles. The synaptosomal preparation and the separation procedures required three and four hours, respectively.

Further illustration of separation procedures in Figure 2

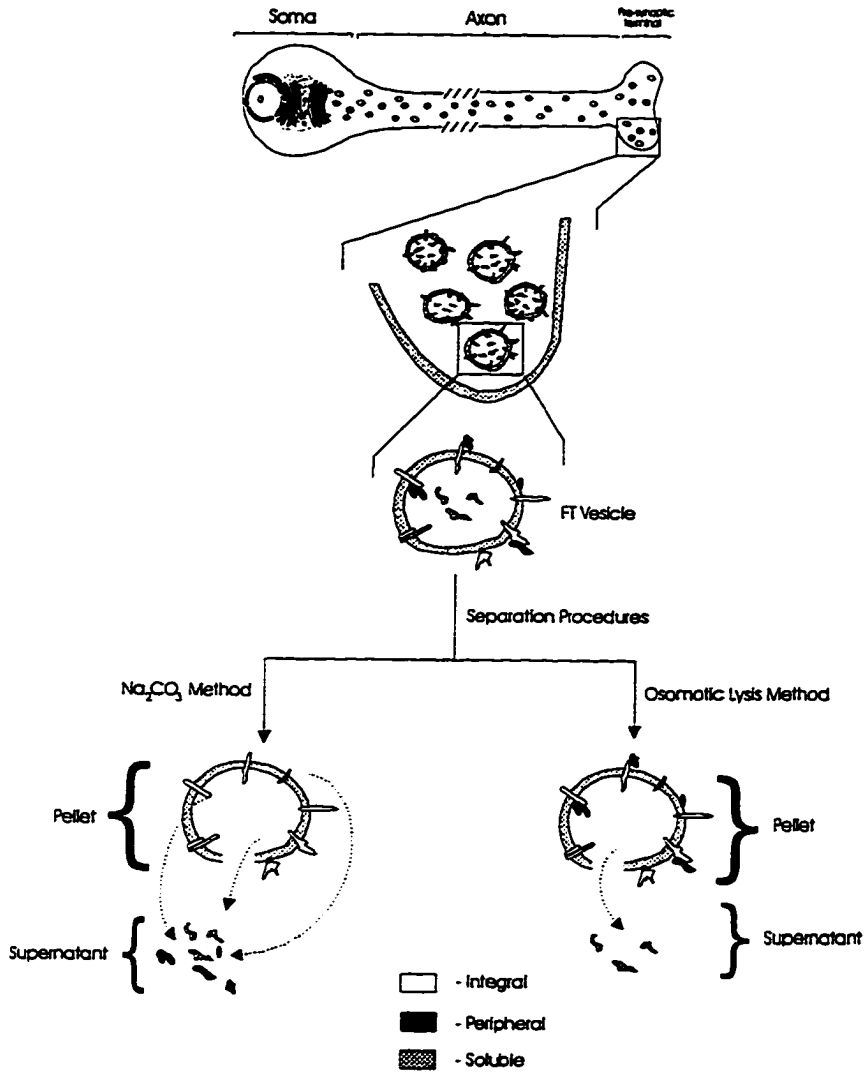

FIGURE 3. Further illustration of separation procedures in figure 2. The FT proteins in the Figure represent all membrane bound integral, peripheral and soluble proteins including cell surface membrane and multivesicular body FT proteins.

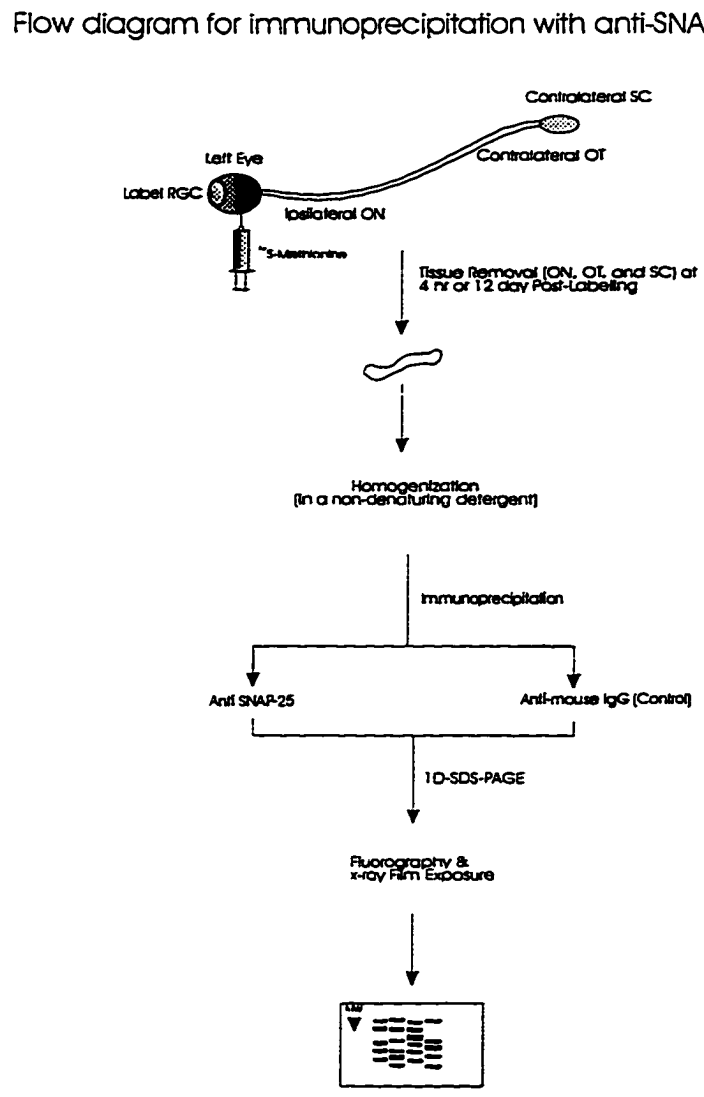

FIGURE 4. Flow diagram of SNAP-25 immunoprecipitation. Immunoprecipitation required two days.

4. PROTOCOL FOR THE DETERMINATION OF ATP DEPENDENCY OF SNAP-25 ASSOCIATION WITH FT AND SCb PROTEINS

To assess whether any SNAP-25 associations were ATP dependent, apyrase (an inhibitor of ATP hydrolysis) was removed from the immunoprecipitation procedure. Instead, ATP (final concentration 1 mM) was added to sample solutions.

5. SPECIFIC METHODS

a. *Radiolabeling RGC proteins* - Adult male Sprague-Dawley rats were used in all experiments. Prior to radioisotope administration, animals were anesthetized with intraperitoneal administration of sodium pentobarbital (35 mg/kg). Then ^{35}S-methionine (approximately 1 to 2 mCi), reduced to 2-3 μl volume under nitrogen, was injected with a Hamilton syringe into the vitreous chamber of the left eye. The needle penetrated the sclera as close to the retina as possible, and the needle tip was placed adjacent to the retina, thereby allowing radioactive labeling of the RGC proteins.

b. *Sample preparation for 2D-SDS-PAGE* - At various post-labeling intervals, animals were sacrificed with lethal injection of sodium pentobarbital. 5 pieces of tissues (left retina, left ON, right OT, and right SC) were removed. Approximately 2-3 mm of the ON proximal to the retina was discarded to minimize the effect of isotope diffusion from the eye into the nerve. Sample preparation was performed as described by O'Farrell (99). Briefly, each tissue or synaptosomal pellet (see below) was homogenized in a glass-on-glass

homogenizer containing 1.0% SDS, 10% ß-mercaptoethanol, and 8 M urea in a total volume of 28 μl. The homogenate was then transferred to a microcentrifuge tube containing 40 μl of lysis buffer (2% NP-40, 2% ampholytes [4-6, 5-7, and 3-10 in a 2:2:1 ratio, respectively], 9.5 M urea, and 5% ß-mercaptoethanol), and 10 μl of lysis supplement (10% NP-40 and 9% ampholytes [4-6, 5-7, 3-10 in a 2:2:1 ratio, respectively]). Final volume of solution was 78 μl. The sample was clarified by centrifugation (8,000Xg, 10 min), and the supernatant was transferred into a clean tube for scintillation counting and 2D-SDS-PAGE analysis.

c. *2D-SDS-PAGE* - Isoelectric focusing (IEF) (first dimension) was performed in cylindrical gels (3 mm diameter by 12 cm long) containing 4% acrylamide, 9 M urea and 2% ampholytes (4-6, 5-7, and 3-10 in a 2:2:1 ratio, respectively). The gels were electrophoresed for 9,000 V-hr (500 V for 16 hr followed 1000 V for 1 hr) in cathode and anode buffers (0.1 M sodium hydroxide, anode; and 1.7 mM phosphoric acid, cathode). Gels were then equilibrated (30 min) in a solution containing 2.3% SDS, 5% ß-mercaptoethanol, 10% glycerol, and 6.2 mM Tris-HCl. For the second dimension, gels were fused with 1% agarose onto stacking and separating gels containing 4.5% and 10% of polyacrylamide, respectively (29.2:0.8 acrylamide:bis-acrylamide ratio), and electrophoresed in a running buffer containing 0.3% tris-HCL, 1.44% glycine, and 0.1% SDS at constant current of 25 mA per gel.

d. *1D-SDS-PAGE* - Tissues for electrophoresis were homogenized in a

glass-on-glass homogenizer containing 75 μl of Laemmli's (103) buffer (10% glycerol, 5% ß-mercaptoethanol, 2.3% SDS, and 0.062 M Tris-HCl (pH 6.8), and 0.001% bromophenol blue). Following homogenization, each sample was heated at 100°C for 5 min and centrifuged at 8,000Xg for 10 min and loaded on a 10% polyacrylamide slab gel. Pre-stained molecular weight markers were loaded to calibrate the molecular weights of the samples. Gels were electrophoresed in a running buffer containing 0.3% Tris-HCl, 1.44% glycine, and 0.1% SDS at constant current of 25 mA. Following electrophoresis, the gels were processed for Coomassie blue staining and fluorography.

e. *Synaptosomal preparation* - All steps were performed at 4°C. Tissue from the right SC was placed in 10 ml sucrose buffer (0.32 M sucrose; 1 mM $MgCl_2$; 150 mM methionine; and 10 mM HEPES, pH 7.4). Each tissue was homogenized in a Teflon-glass homogenizer at 900 rpm for sixteen strokes. Homogenate was centrifuged at 1000Xg for 10 min, and supernatant was collected. The pellet was resuspended with an additional 10 ml of sucrose buffer and re-centrifuged at 1000Xg for 10 min to increase the synaptosomal yield of the sample. This supernatant was added to the first supernatant, and the pellet containing the nuclear pellet was discarded. The supernatant was then centrifuged at 12,100Xg for 20 min, and the crude synaptosome was pelleted. This synaptosome pellet was washed twice with isotonic buffer, HEPES-buffered physiological saline (10 mM HEPES, pH 7.4; 146 mM NaCl; 4 mM KCl; 10 mM dextrose; 0.5 mM sodium pyruvate; and 2 mM $MgCl_2$) and centrifuged at

35,000Xg for 20 min each to obtain a final synaptosomal pellet.

f. *Acid precipitable radioactivity measurement* - Acid precipitable radioactivity was determined by precipitating 1 μl aliquot from each sample in 1 ml of 10% trichloroacetic acid (TCA) and 50 μl of carrier bovine serum albumin (5 mg/l). The precipitate was pelleted by centrifugation (8,000Xg, 10 min) and solubilized in 5 ml of scintillation counting fluid (80% toluene, 9% NCS (Amersham), 4 M ammonium hydroxide, 9% concentrate [10x] of diphenyloxasole/1,4 bis[2-5[-phenyloxazolyl]benzene]). The CPM radioactivity was determined using a liquid scintillation spectrophotometer.

g. *Coomassie blue staining* - Following electrophoresis, gels were stained with 0.05% Coomassie brilliant blue R and 10% acetic acid. The gels were then destained by several washes in 7% acetic acid.

h. *Fluorography* - Fluorography of gels was performed as described by Laskey and Mills (104). Briefly, the gels were first washed twice with dimethyl sulfoxide (DMSO) to remove any water within the gel or vessel. The gels were embedded with a fluor o-diphenyloxasole and vacuum-dried for 2hr at +70°C against cellophane membrane. The dried gels were exposed to Kodak XAR-5 films for various periods of time at -70°C.

i. *Quantification of radiolabeled polypeptides* - The relative labeling of

individual polypeptides on 2D-fluorographs was determined by densitometry. Individual spots corresponding to a radiolabeled polypeptide were scanned using the Omni Media Scanner (XRS) and the Bio-Image computer software and were expressed as *Integrated Intensity* (II). The II (the volume of spot calculated by summing the volume [optical density] of each pixel within the boundaries of the spot [area x height] and then subtracting the background for each pixel of each spot) for each spot was quantified. The final reported value of each spot was the percentage of the total II of all measured spots on a fluorograph (%II = [Spot's II/total Spots II] x 100). To ensure that the measured II was a linear function of the fluorographic exposure, different exposures of the same gel were scanned to verify that the II was proportional to the exposure time.

j. *Local labeling the SC* - To locally label the SC, the rat was anesthetized with sodium pentobarbital, the skull was surgically exposed, and a hole was drilled on the right side of the skull directly above the SC. The exact coordinates of drilling location was determined using a rat brain atlas (100): A-P 7.8 mm Bregma, M-L 3.0 mm lateral to midline, 2.8 mm in depth from surface. The syringe penetrated at a slight angle toward the midline delivering ^{35}S-methionine directly into the SC. One hour after injection, the rat was sacrificed, the SC was removed, and labeled SC proteins analyzed by 2D-SDS-PAGE/fluorography.

k. *Analysis of FT proteins partitioned into integral membrane vs. peripheral membrane/ soluble non-membrane fractions* - All steps were performed at 4°C.

The carbonate method (101) was used for separation. Synaptosomes were resuspended in 400 μl of 100 mM sodium carbonate (pH 11.5) and 400 μl of isotonic buffer and allowed to incubate at 0°C for 30 min. The sodium carbonate opened the closed vesicles, converting them to open membrane sheets. Consequently, peripheral and soluble proteins were released in soluble forms. The solution was centrifuged at 233,000Xg at 4°C for 1 hr. The supernatant, containing the peripheral and soluble proteins, was subjected to acetone precipitation (80% volume). The precipitated proteins were then prepared for 1D- or 2D-SDS-PAGE. The pellet, containing the integral proteins, was first rinsed with distilled water and then prepared for 1D- or 2D-SDS-PAGE.

l. *Analysis of FT proteins partitioned into soluble non-membrane vs. integral/peripheral membrane fractions* - All steps were performed at 4°C. An osmotic-lysis (based on hypotonic Tris buffer) (102) was used for separation. Synaptosomes were resuspended in 400 μl of 1mM Tris (pH 9.0) and allowed to incubate at 0°C for 1 hr. This resulted in hypo-osmotic lysis releasing soluble proteins from synaptosomes. At the end of incubation period, the sample was centrifuged at 105,000Xg for 30 min. The supernatant containing the soluble proteins was subjected to acetone precipitation. These acetone precipitated proteins were prepared for 1D- or 2D-SDS-PAGE. The insoluble fraction, containing the integral/peripheral proteins, was also prepared for 1D- or 2D-SDS-PAGE.

m. *Sample preparation for immunoprecipitation* - All sample preparations for immunoprecipitation were performed at 4°C. Each tissue sample was homogenized in a microcentrifuge tube in a solution containing 0.5 ml of lysis buffer (5 mM $MgCl_2$ and 0.1% triton X-100), ATP hydrolysis inhibitor (apyrase [10 units/ml]), and protease inhibitors (leupeptin [10 μg/ml], pepstatin A [1 μg/ml], and aprotinin [1 μg/ml]). The sample was allowed to rock for 30 min. An equal volume (0.5 ml) of 2X RIPA buffer (1X = 2% sodium deoxycholate, 1% triton X-100, and 0.1% SDS) was then added to each homogenate. The solution was rocked for another 30 min. The sample was centrifuged at 12,000Xg for 5 min. The supernatant was collected for immunoprecipitation and the pellet was discarded.

n. *Sample preparation for immunoprecipitation in the presence of ATP* - All sample preparation for immunoprecipitation was performed at 4°C. Each tissue sample was homogenized in a mirocentrifuge tube in a solution containing 0.5 ml of lysis buffer (5 mM $MgCl_2$ and 0.1% triton X-100), ATP (Sigma) (1 mM final concentration), and protease inhibitors (leupeptin [10 μg/ml], pepstatin A [1 μg/ml], and aprotinin [1 μg/ml]). The sample was allowed to rock for 30 min. An equal volume of (0.5 ml) of 2X RIPA buffer (1X = 2% sodium deoxycholate, 1% triton X-100, and 0.1% SDS) was added to each homogenate. The solution was rocked for another 30 min. The sample was centrifuged at 12,000Xg for 5 min. The supernatant was collected for immunoprecipitation and the pellet was discarded.

o. *Immunoprecipitation (IP)* - All steps for IP were carried out at 4°C. Fifty μl of protein A-agarose beads were added to the sample (supernatant) to clear for non-specific binding, and the solution was allowed to rock for 30 min. The sample was centrifuged at 4,000Xg for 5 min, and the supernatant was collected, and the pellet was discarded. Primary antibody was added to the supernatant and the solution was rocked for another 30 min. In another microcentrifuge tube, 5 μl of secondary antibody was added to 50 μl Protein A-agarose and rocked for 60 min (this secondary antibody procedure was necessary only when the primary antibody had low affinity for binding with the protein A-agarose). After 60 min, 1 ml of 1X RIPA buffer was added to the sample and centrifuged at 3,000Xg for 5 min. The supernatant was discarded and the pellet was washed twice with 1X RIPA to remove any unspecific binding. The sample with the primary antibody was added to protein A-agarose/secondary antibody pellet and rocked overnight. On the following day, antibody/immune complex proteins were pelleted by centrifugation at 12,000Xg for 3 min, and the non-precipitable supernatant was saved for analysis. The pellet was washed four times with RIPA buffer (1 ml/wash) followed by the addition of 75 μl Laemmli's buffer to solubilize the IP proteins. The non-IP precipitable supernatant was subjected to acetone precipitation (80% volume), and the proteins were solubilized by adding 75 μl Laemmli's buffer.

p. *Quantitation of CO-IP proteins* - The IP and non-precipitable samples

were centrifuged at 12,000Xg for 30 min, and the supernatant was transferred to a new mirocentrifuge tube ready for scintillation counting and 1D-SDS-PAGE.

q. *Electron microscopy* - All steps were performed at 4°C. Synaptosomal pellets were fixed for 2 hr with primary fixative (4% para-formaldehyde/0.5% glutaraldehyde in 100 mM cacodylate buffer solution [pH 7.4] and 0.5% NaCl). Pellet was: (1) washed in 100 mM cacodylate buffer and 0.5% NaCl followed by three times (30 min each) wash in the cacodylate buffer solution alone; (2) fixed with 2% osmium tetroxide for 1 hr; (3) washed with propylene oxide; (4) embedded with epoxy (epoxy 812); and (5) sectioned (45-65 nm) with microtome (Reichert Ultracut E ultramicrotome). Sections were placed in 100 mesh copper grids and stained with uranyl acetate and lead citrate before viewing and photographing with a Phillips 301 transmission electron microscope.

r. *Determination of molecular weight of individual proteins* - Molecular weights of individual proteins from two-dimensional fluorographic patterns were determined by the following process: During gel electrophoresis of the second dimension, solutions of rainbow molecular weight marker standards (Amersham) were run adjacent to the samples. Then, by using Bio-Image computer software system, computation of molecular weights were performed to interpolate relative positions of individual proteins to the markers.

s. *Statistical analyses* - Statistical analyses of the optical integrated intensity

of each FT protein were preformed for the data presented in Table 1. Each data set was analyzed by a 2 (compartment: OT vs. SC) by 3 (time: 4, 24, and 48 hours) analysis of variance (ANOVA). In this analysis, compartment was within-subjects factor and time was a between-subjects factor. All of the data sets were unbalanced in that animals did not always have the same number of measurements in OT and SCE for each tiem period. Post-hoc analyses were done using Bonferroni corrected t-test for simple main effects and interaction effects. Statistical differences of $p < 0.05$ were considered significant.

CHAPTER III

RESULTS

A. ROUTING OF FT PROTEINS IN THE OPTIC PATHWAY

Acid-precipitable liquid scintillation counting of the radiolabeled proteins, fast axonally transported in the rat optic pathway, revealed distinct transport trafficking. Figure 5A illustrates the *in vivo* model system that was used to study FT proteins. Four hours following intraocular injection of the left eye with 1 mCi ^{35}S-methionine, tissues containing the axons (ON and OT) and pre-synaptic terminals (LGN and SC) of the RGCs were removed. The activity of radiolabeled proteins in each tissue was measured by acid-precipitable scintillation counting (Figure 5B). The transported results confirmed the known anatomical projections of the rat optic pathway axons and pre-synaptic terminals (120, 121, 124). The distribution of RGC radiolabeled proteins in the optic pathway indicated that the majority of the fast axonally transported proteins were routed from ipsilateral ON to contralateral OT with terminal projections in the contralateral target nuclei, SC and thalamic LGN. A significantly greater amount of radiolabeled FT proteins were found in the contralateral SC relative to the contralateral LGN. Also, LGN is known to contain *en passant* optic pathway axons. Therefore, most further analyses of FT proteins in the terminal compartment were limited to the SC.

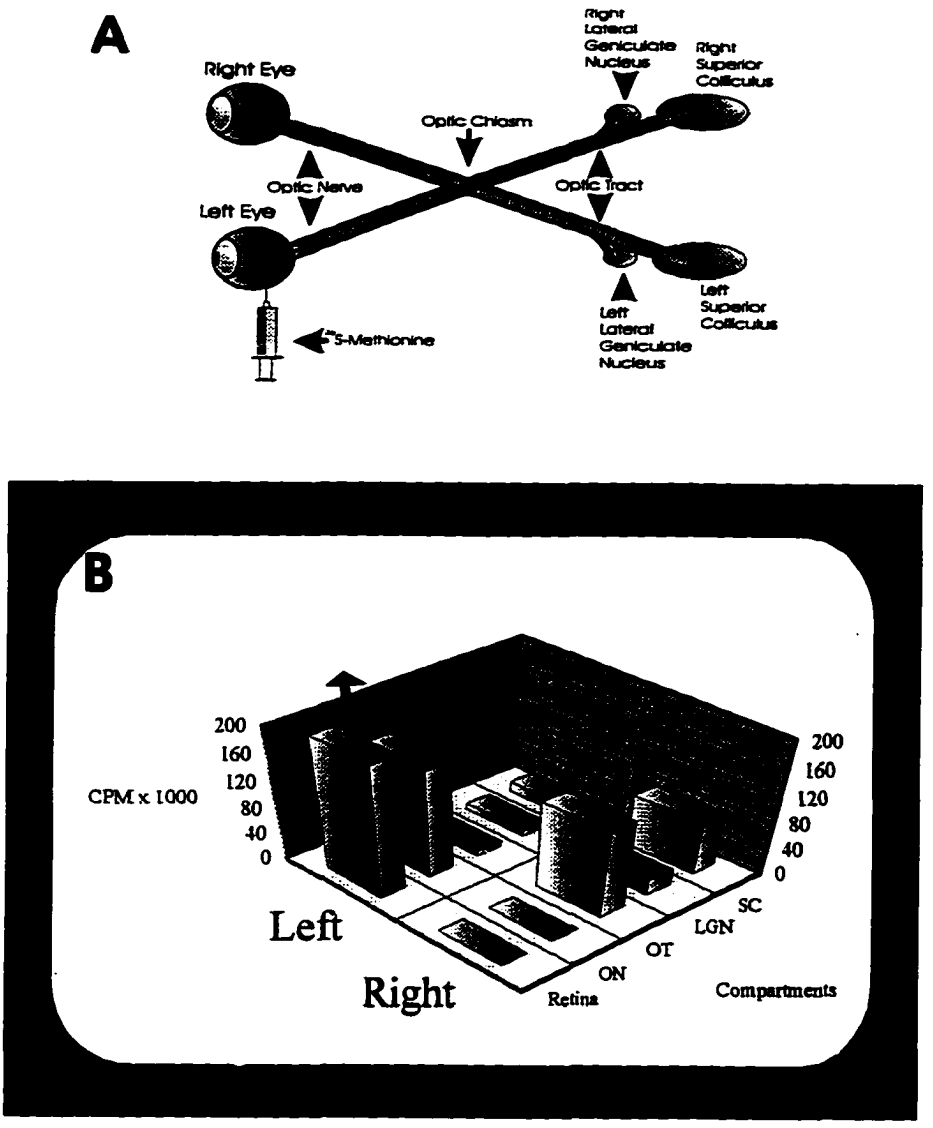

FIGURE 5. Experimental paradigm to examine axonally transported FT proteins. (A) the rat optic pathway - *in vivo* injection of ^{35}S-methionine into the vitreous chamber of the left eye. (B) Acid-precipitable (CPM), four hours post-injection, in the different compartments of the optic pathway. Abbreviations: CPM, count per minute; ON, optic nerve; OT, optic tract; LGN, lateral geniculate nucleus; SC, superior colliculus. Arrow in B indicates CPM significantly higer that 200,000.

B. A SELECTIVE SUBSET OF RGC PROTEINS ARE FAST TRANSPORTED IN THE AXON

Radioisotopic pulse labeling, combined with 2D-SDS-PAGE analyses, revealed a distinct subset of RGC proteins rapidly transported in the axon. In the adult Sprague-Dawley rat, radiolabeled FT RGC proteins reached the pre-synaptic terminals (SC and LGN) within 4hr following intraocular injection of radioisotope. The 2D-SDS-PAGE fluorographic patterns in Figure 6B and 6C represent the ^{35}S-methionine-labeled proteins of the OT and retina, respectively, 4hr post intra-ocular injection (PIL). As shown in Figure 6, the FT proteins (6B) did not represent the most abundantly synthesized proteins by the retina (6C). Among the most abundant radiolabeled proteins seen in the retina, and not in the optic pathway, were cytoskeletal subunits - actin and the tubulins. These subunits are known to be conveyed by slow axonal transport at less than 5 mm/day and therefore, would not have entered the ON from the retina for at least another 4 or 5 hr (20, 21, 22, 23). If these subunits were radiolabeled in 2D fluorographs taken from optic pathway tissues (OT, ON, SC, LGN) after four hours PIL, then diffusion and anomalous local utilization of label would have been suspected. The 2D fluorographic patterns in the present study consistently demonstrated the absence of anomalous local labeling by this criterion.

In order to assess whether radiolabeled SC proteins in the intraocular pulse paradigm represented transported RGC proteins or locally-synthesized SC proteins, SC fluorographs were compared following a 4 hr PIL with SC fluorographs following direct SC microinjection. Figure 7A diagrammatically illustrates the method used to obtain the

2D pattern shown in Figure 7C. SC fluorographs following PIL (Figure 7B) were distinctly different from SC fluorographs following direct SC microinjection (Figure 7C). The most abundantly synthesized proteins in the SC appeared to resemble that of the retina shown in Figure 6C.

The fast transported 25 kDa synaptosomal associated protein (SNAP 25) was abundantly labeled (Figures 6B and 7B) in both compartments (OT, SC) at 4 hr PIL. Indeed, this protein has been described in many studies as the major methionine-labeled protein among the FT proteins (62, 93, 110). Although, its prominence was apparent in the axon and terminal regions following a 4 hr intraocular pulse, it was not the most abundantly synthesized protein in the retina (Figure 6C). Further characterization of this protein is described later.

C. KINETICS OF RETINAL PROTEIN SYNTHESIS AND FAST AXONAL TRANSPORT IN THE OPTIC PATHWAY

Other studies have shown that following intraocular injection, ^{35}S-methionine does not remain available for incorporation into RGC proteins after ~0-4 hr PIL (122). These results were supported in the present study by comparing FT fluorographic patterns obtained at 24 hr PIL by following a 4 hr intraocular label with a 4 hr intraocular label subsequently chased with excess (> 100x) unlabeled methionine. In both conditions, identical 2D-FT pathway were obtained (data not shown). The unlabeled methionine chase appeared to have no influence in reducing the amount of labeled FT proteins suggesting that very little or no incorporation of the radioisotope

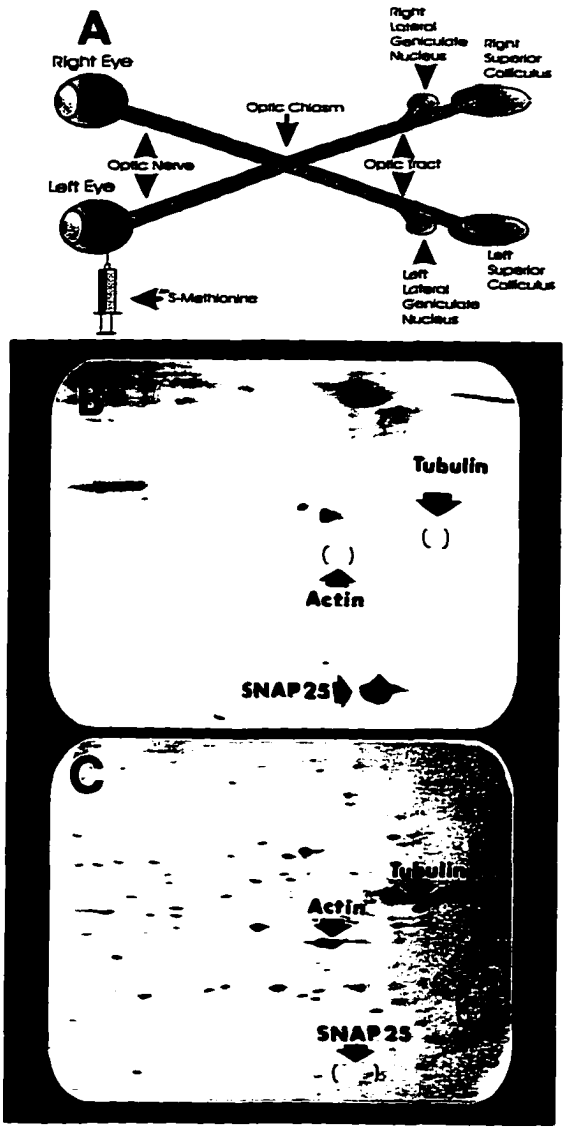

FIGURE 6. Comparison between retina synthesized and fast axonally transported proteins. (A) the rat optic pathway - *in vivo* injection of ^{35}S-methionine into the vitreous chamber of the left eye. (B) 2D fluorograph of radiolabeled FT proteins in the right optic tract. (C) 2D fluorograph of radiolabeled proteins synthesized in the retina.

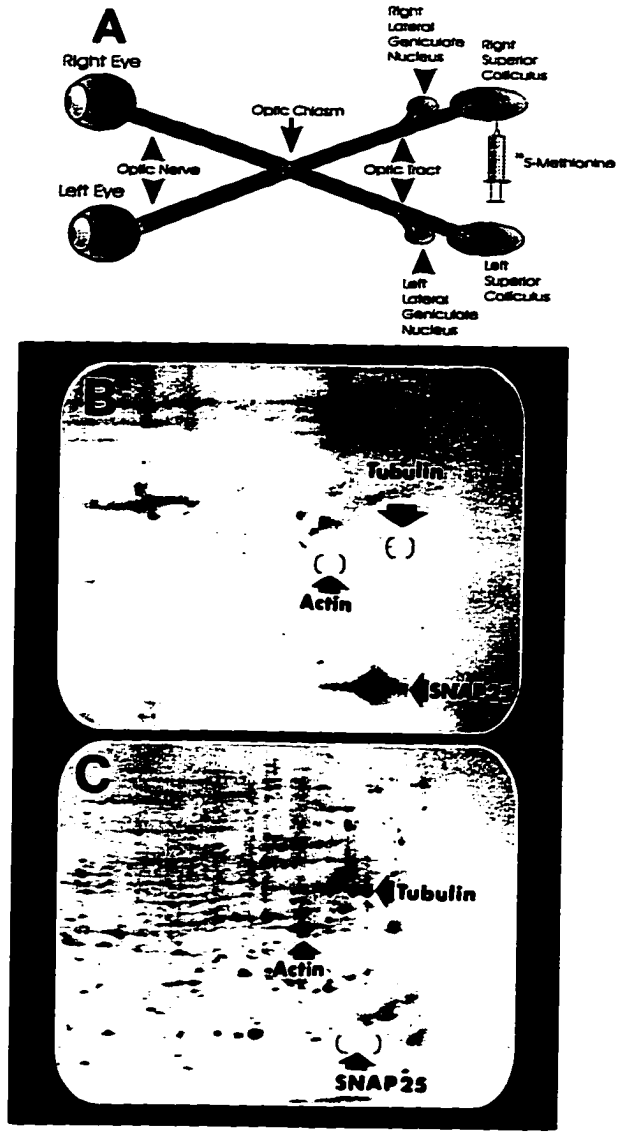

FIGURE 7. Comparison between locally synthesized SC proteins and FT proteins. (A) the rat optic pathway - *in vivo* injection of ^{35}S-methionine into the right SC. (B) 2D fluorograph of radiolabeled FT proteins in the right SC (obtained from RGC labeling experiment). (C) 2D fluorograph resulting from direct labeling of the SC - activity of locally synthesized proteins.

occurred after 4 hr. Despite this observation, labeled FT proteins were seen in the nerve and SC in great abundance even after 48 hr PIL. Figure 8 displays the acid-precipitable CPM of FT proteins at 4, 24, and 48 hr PIL. At 4 hr PIL, most of the radiolabeled FT proteins appeared to be in the ON; while relatively less radiolabeled FT proteins had reached the SC. FT proteins were most abundant at 24 hr both in the OT and SC, as previously reported by Garner and Mahler (61). The acid-precipitable ON CPM, at both 24 and 48 hr PIL, was mostly influenced by the slow transported proteins (SCb) entering ON. Therefore, statistical analyses excluded the 24 and 48 hr ON data.

D. QUALITATIVE AND QUANTITATIVE ANALYSES OF INDIVIDUAL FT PROTEINS

Among >90 resolved FT proteins, twenty were selected for extensive analyses. These FT proteins were chosen for further study based on their abundance and consistent gel migration behavior. Figure 9 displays samples of two-dimensional fluorographic patterns of these proteins in the OT at 4 (A), 24 (B), and 48 (C) hr PIL. A map of the abundant proteins is shown in Figure 9D. Approximate protein molecular weights were determined by interpolation of molecular weight marker standards that were used during gel electrophoresis of the second dimension.

Visual analyses of the fluorographs revealed several consistent patterns in FT protein behavior. The vast majority of the radiolabeled FT proteins were visually detectable in all the compartments at each time point analyzed. Some of the acidic high molecular weight proteins (e.g., 89 and 131) appeared to turn over rapidly. Their

abundance was apparent at 4 hr PIL in all compartments (ON, OT, SC), but at 24 hr PIL, some of these proteins appeared to have moved to the terminal (SC) and disappeared from the nerve region. At 48 hr PIL, most of these proteins were virtually undetectable in any of the compartments. In contrast, some FT proteins (e.g., 61 and 69) displayed a delayed FT appearance in the compartments. Most of these FT proteins became resolvable in the compartments only at the 24 hr time point and their relative activity appeared to increase at 48 hr in each compartment. Still other FT proteins (e.g., 17, 18.5, and 19) seemed to disappear from the OT at 24 hr but persisted in the SC even at 48 hr. Finally, one FT protein (i.e., 22) showed a unique feature unlike the other nineteen labeled FT proteins. This protein was expressed solely in nerve compartments (ON, OT) and was not detected in SC at any PIL time point.

Further characterization of each newly synthesized FT protein was performed by densitometric quantification of 2D fluorographs at various x-ray film exposures. Spots in the 2D fluorographs were evaluated by their optical integrated intensity (II). Since x-ray film exposure time varies linearly with the amount of radioactivity in a spot only up to a certain density, a control study was performed to ensure that the measured II of each spot was a linear function of fluorographic exposure. As shown in Figure 10, three film exposures (10, 15, and 50 days) of the same gel were scanned by densitometer. Five spots from each exposure time were randomly selected to verify that their measured optical II was proportional to their exposure time. The figure shows table of regression statistics and plots of the regression lines with 95% confidence interval for the mean of the optical II. Since the amount of radioactivity in the control gel was typical of the experiments in the present study, it was concluded that linearity of fluorographic

exposures was within acceptable parameters.

Following verification of fluorographic linearity, fluorographic spots were scanned and quantitative analyses were subsequently performed. Table 1 shows raw data of the 20 proteins analyzed and their respective measured values at the three time points (4, 24, and 48 hr PIL) in the different compartments of the system. The table is a summary of what is presented in the following 20 figures. Figures 11 to 30 present a graphic and fluorographic delineation of the spatial and temporal disposition, as well as the corresponding level of relative activity, of individual newly synthesized FT proteins.

E. CLASSIFICATION OF QUANTIFIED FT PROTEINS

The spatial and temporal kinetics of the analyzed FT proteins showed variations between the 20 proteins. However, six minimum classes were defined by which transport behavior of the 20 proteins could be completely described.

CLASS 1

The first class of FT proteins demonstrated relatively little or no preferential localization behavior in any of the compartments at the three time points analyzed. The relative amount of radiolabeling of protein 28 (Figure 11) did not change significantly over time, within and between compartments. Proteins 25 (Figure 12), 57 (Figure 13), 59b (Figure 14), 64 (Figure 15), 69 (Figure 16), 194 (Figure 17) and 206 (Figure 18) showed some statistically significant compartmental differences in their relative labeling activity at some of the time points analyzed.

Class 2

The second class of FT proteins displayed transient activity or showed gradual decreased activity with greater PIL in all compartments. The relative activity of proteins 59a (Figure 19), 89 (Figure 20), and 131 (Figure 21) was apparent at 4 hr PIL. At 24 hr PIL, however, their relative activity either decreased significantly (proteins 59a and 89) or was not detected at all (protein 131). At 48 hr PIL none of these proteins were detected in any of the compartments.

Class 3

The third class of FT proteins displayed significant increases in their relative activity of radiolabeling at 24 hr PIL. The OT activity of protein 149 was significantly greater at 24 hr PIL than the respective OT activity at 4 hr or 48 hr PIL (Figure 22). This protein did not show compartmental preference at any other time points.

Class 4

The fourth class of FT proteins displayed a gradual appearance, with increased activity, as transport time lengthened. At 4 hr PIL, protein 56 (Figure 23) displayed nearly basal level activity in all compartments. However, at 24 and 48 hr, its activity significantly increased. Similar characteristic were seen in proteins 61 and 67 (Figure 24 and 25 respectively) where activities were undetectable at 4 hr PIL but increased at 24 and 48 hr PIL in both compartments.

Class 5

The fifth class of FT proteins appeared to be preferentially localized at the pre-synaptic terminal of the SC at 24 and 48 hr PIL. At 4 hr PIL these proteins were significantly more abundant in nerve regions than terminal regions. At 24 and 48 hr PIL, however, they were not detected in nerve regions. Instead, they appeared to have moved to the SC where three of these proteins, 18.5 (Figure 26), 19 (Figure 27) and 19.5 (Figure 28) displayed significantly increased labeling at 24 hr PIL while protein 17 (Figure 29) showed significantly increased SC activity only at 48 hr PIL.

Class 6

The sixth class of protein (n=1) was never detected in the SC over the three time points. Protein 22 (Figure 30), not only seemed to be localized in the OT, but its relative activity in this compartment increased with greater PIL.

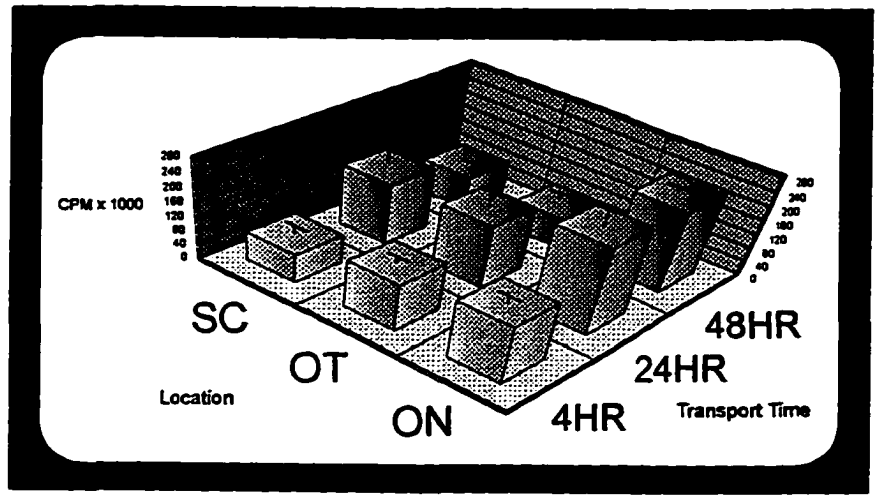

FIGURE 8. Acid-precipitable CPM of FT RGC proteins in tissues containing the major axons and terminals of the optic pathway 4, 24, and 48 hr following ^{35}S-methionine injection into the vitreous chamber of the left eye. Counts were taken from the ipsilateral ON, contralateral OT and SC. Each bar represents mean ± SEM from at least three experiments.

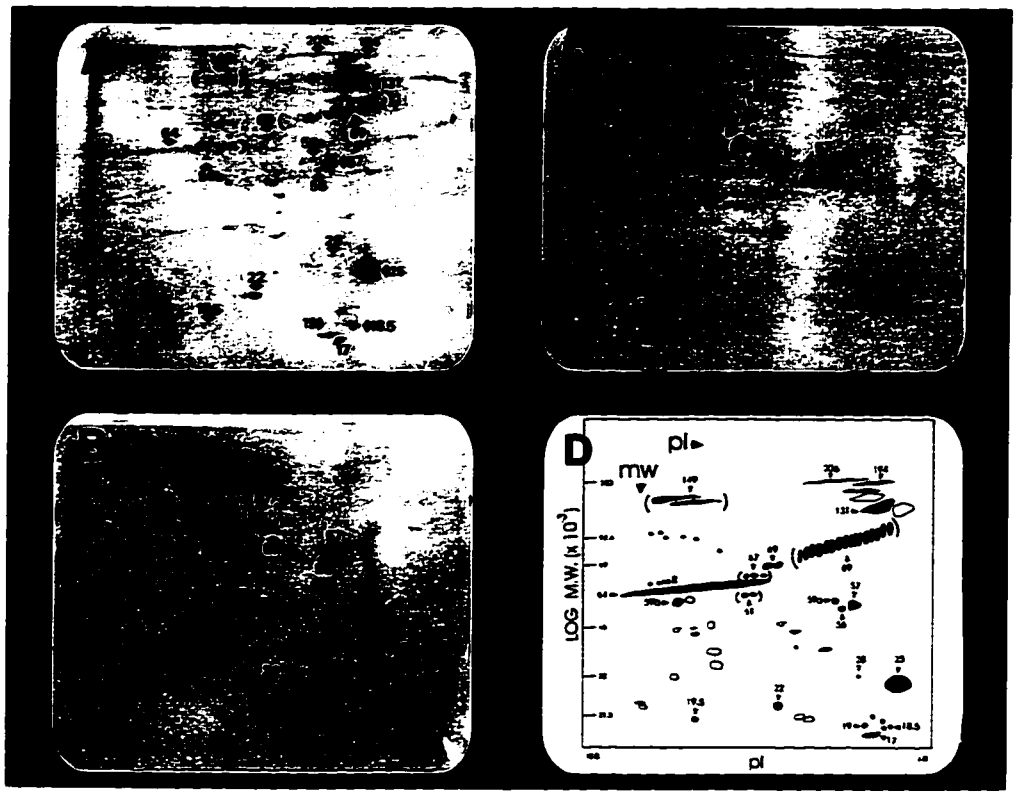

FIGURE 9. 2D-SDS-PAGE fluorographic patterns of radiolabeled FT proteins in the OT at 4 (A), 24 (B), and 48 (C) hr PIL. Spots that were investigated are identified by their molecular weights (M.W. $x10^{-3}$). (D) Diagrammatic representation of 2D pattern of the individually characterized FT proteins. Abbreviations: mw, molecular weight; pI, isoelectric point.

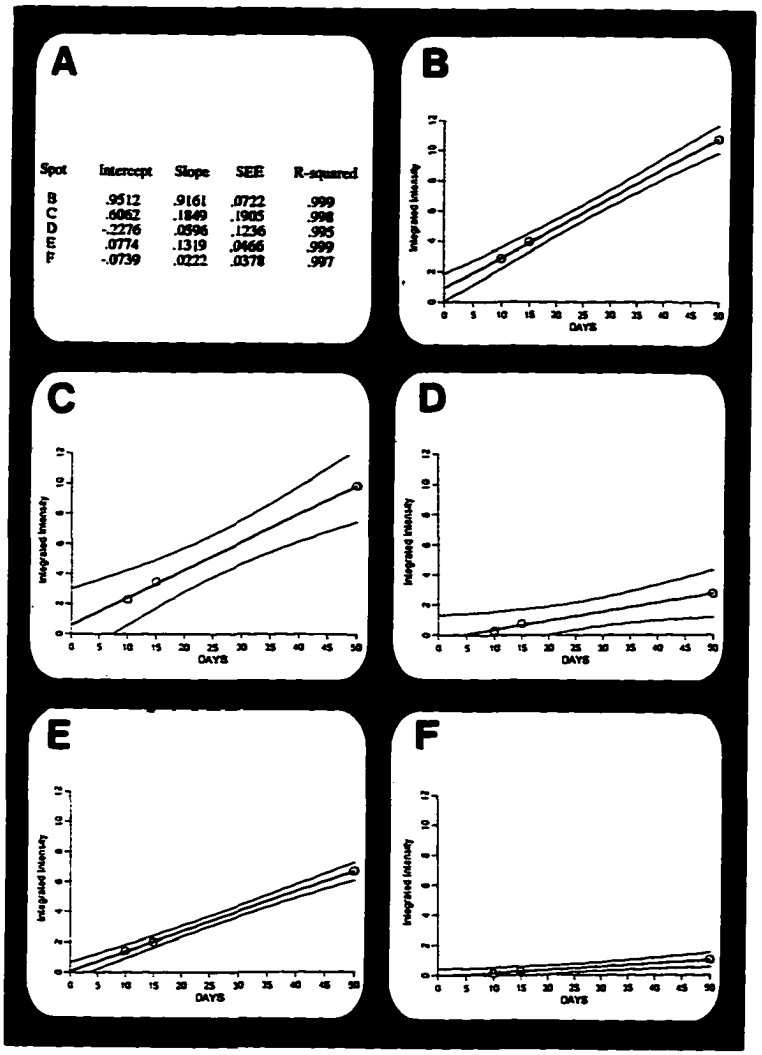

FIGURE 10. Control study to verify linearity of fluorographic exposure. Five individual spots were randomly selected for quantification at three different exposures (10, 15, and 50 days) of the same gel. (A) Table of the linear regression values of the five spots of optical integrated intensity. (B), (C), (D), (E), and (F) Plots of the regression lines and a 95% confidence interval (curved lines) for the mean of the predicted value of integrated intensity. SEE is the standard error of estimated, the error variance of the regression.

TABLE 1.

Raw data obtained from densitometric analyses of 2D fluorographs.

	4hr									24hr						48hr					
	ON			OT			SC			OT			SC			OT			SC		
M.W.	%II	±SEM	n	%II	±SEM	n	%II	±SEM	n	%II	±SEM	n	%II	±SEM	n	%II	±SEM	n	%II	±SEM	n
17	2.21	0.030	2	2.01	0.214	2	0.94	0.030	2	<.01	—	2	0.10	0.058	2	<.01	—	2	2.00	0.204	2
18.5	1.12	0.015	2	1.06	0.118	2	0.17	0.021	2	<.01	—	2	0.80	0.323	2	<.01	—	2	0.43	0.042	2
19	0.57	0.185	2	0.45	0.325	2	0.45	0.001	2	<.01	—	3	1.58	0.377	3	<.01	—	3	0.71	0.057	3
19.5	0.42	0.008	2	0.85	0.049	2	0.39	0.049	2	0.26	0.072	3	1.00	0.325	2	0.16	0.020	2	0.21	0.020	2
22	2.81	0.472	2	0.91	0.243	3	<.01	—	2	4.19	1.093	4	<.01	—	3	6.92	2.417	3	<.01	—	4
25	27.3	7.430	3	32.2	8.481	3	32.1	0.603	2	36.2	2.100	4	27.7	6.790	4	31.6	7.009	3	15.6	1.820	2
28	0.48	0.061	2	0.47	0.083	2	0.24	0.043	2	0.20	0.039	3	0.51	0.337	3	0.35	0.195	3	0.35	0.034	2
56	1.95	0.501	2	0.17	0.044	2	0.14	0.079	2	2.26	0.482	4	2.49	1.241	4	4.35	1.139	3	6.19	1.769	2
57	5.27	1.378	2	5.19	1.871	2	2.35	0.414	2	1.68	0.234	4	2.55	1.180	4	1.17	0.326	3	1.62	0.988	2
59a	1.46	0.570	2	1.22	0.247	2	1.08	0.359	2	<.01	—	2	<.01	—	2	<.01	—	2	<.01	—	2
59b	0.55	0.279	2	0.46	0.091	3	0.53	0.017	2	0.27	0.049	3	0.45	0.145	3	0.29	0.148	2	0.73	0.062	2
61	<.01	—	3	<.01	—	3	<.01	—	2	0.71	0.077	3	0.27	0.057	3	0.74	0.160	2	1.10	0.030	2
64	7.65	0.427	3	7.03	0.890	3	6.48	0.523	2	6.89	1.816	3	9.79	0.405	3	5.25	0.221	2	8.86	0.858	2
67	<.01	—	4	<.01	—	4	<.01	—	2	0.74	0.132	4	1.20	0.377	4	1.55	0.401	3	1.25	0.213	2
69	0.25	0.033	2	0.16	0.033	2	0.58	0.144	2	0.71	0.022	2	0.51	0.109	3	0.58	0.055	2	0.84	0.143	2
89	1.01	0.039	2	3.05	0.634	2	3.22	1.144	2	0.50	0.016	2	0.44	0.188	3	<.01	—	2	<.01	—	3
131	6.57	3.258	2	9.73	0.061	2	13.2	0.674	2	1.63	0.120	2	2.89	0.867	3	<.01	—	2	<.01	—	3
149	4.14	0.085	2	2.33	0.078	2	3.45	2.411	2	14.7	0.986	3	3.21	1.041	4	3.11	1.178	3	2.47	0.294	2
194	1.12	0.410	2	2.34	0.337	3	1.69	0.981	2	0.76	0.249	3	1.37	0.145	3	1.30	0.252	2	2.44	0.146	2
206	1.83	0.371	2	3.11	0.592	3	1.59	1.310	2	<.01	—	3	2.47	0.839	4	1.42	1.216	3	0.52	0.050	2

Fluorographs from tissue samples of ON, OT, and SC at 4 hr, and tissue samples of OT and SC at 24 and 48 hr were analyzed. Proteins were numbered according to their molecular weights (M.W. $x10^{-3}$). Quantitative measurement of each spot (representing a protein) is based on the percent optical integrated intensity (%II) of all spots found on the fluorograph. Standard error of mean (SEM) and number of replicates analyzed (n) are also presented.

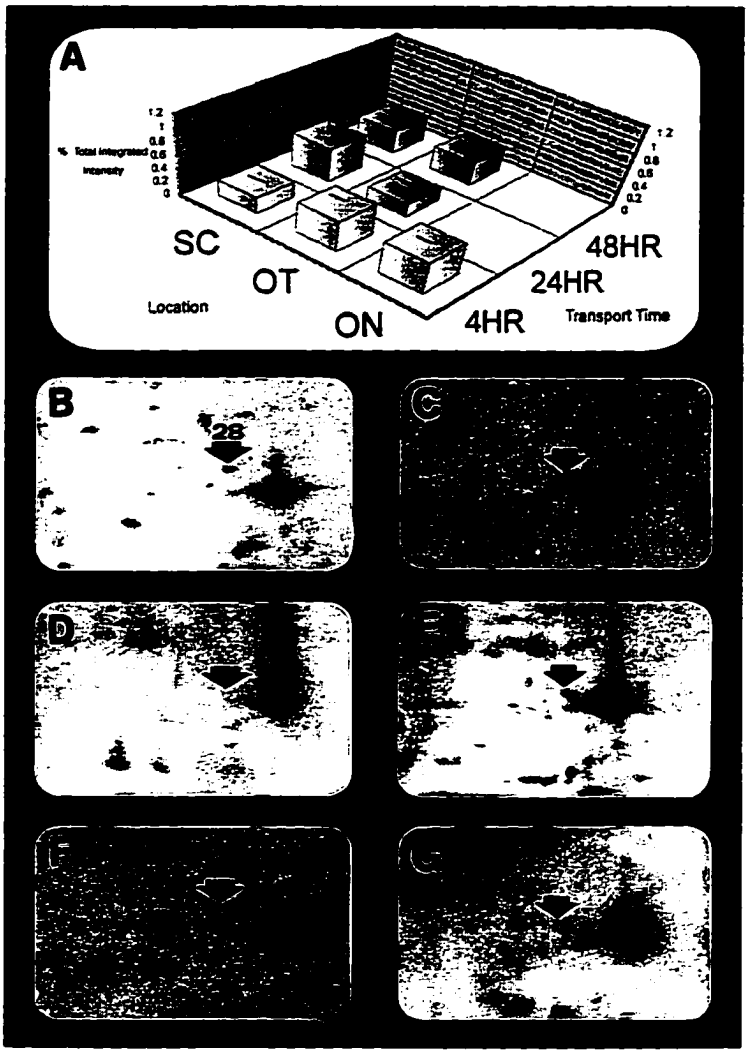

FIGURE 11. Non-preferential of compartmental and temporal localization of the FT protein 28. (A) Mean ± SEM of the protein in compartments ON, OT, and SC at 4, 24, and 48 hr PIL. No significant differences between compartments or time ($p > 0.22$ for all). Fluorographic representation of the protein in OT (B) and SC (C) at 4hr, OT (D) and SC (E) at 24 hr, and OT (F) and SC (G) at 48 hr PIL.

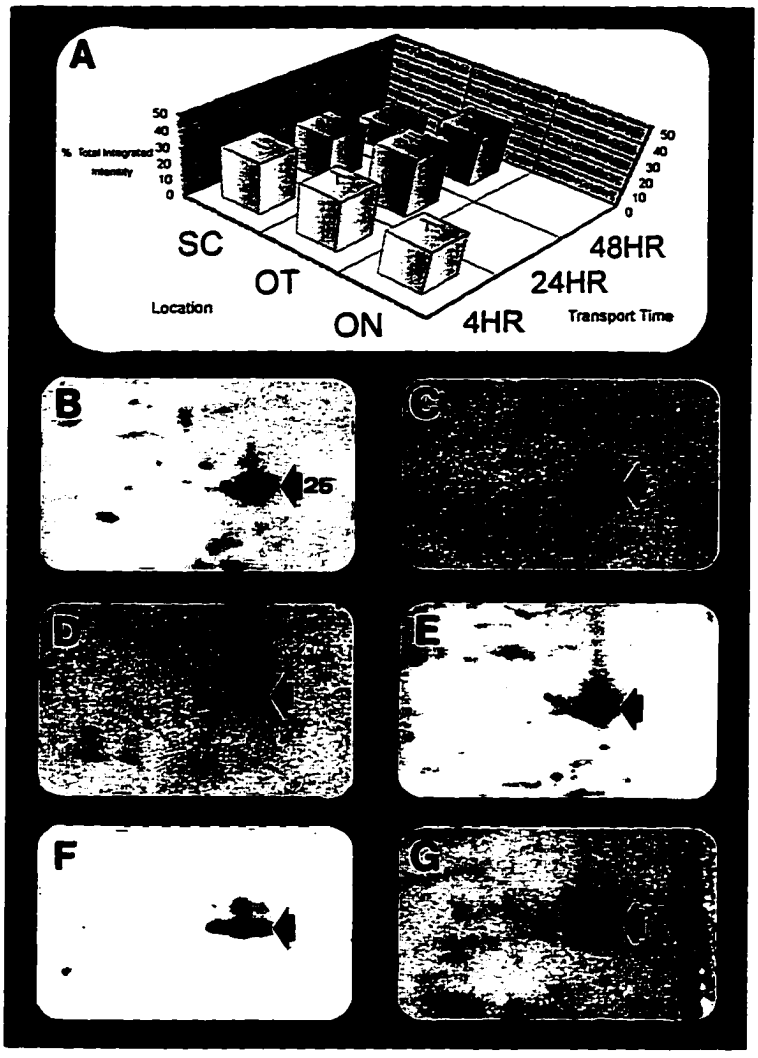

FIGURE 12. Compartmental and temporal localization of the FT protein 25. (A) Mean ± SEM display of the protein in compartments ON, OT, and SC at 4, 24, and 48 hr PIL. Relative activity in SC at 48 hr was significantly less than that at 4 and 24 hr in SC, and 4, 24, 48 hr in OT($p < 0.05$ for all comparisons). No other significant differences between compartments or time ($p > 0.16$ for all). Fluorographic representation of the protein in OT (B) and SC (C) at 4hr, OT (D) and SC (E) at 24 hr, and OT (F) and SC (G) at 48 hr PIL.

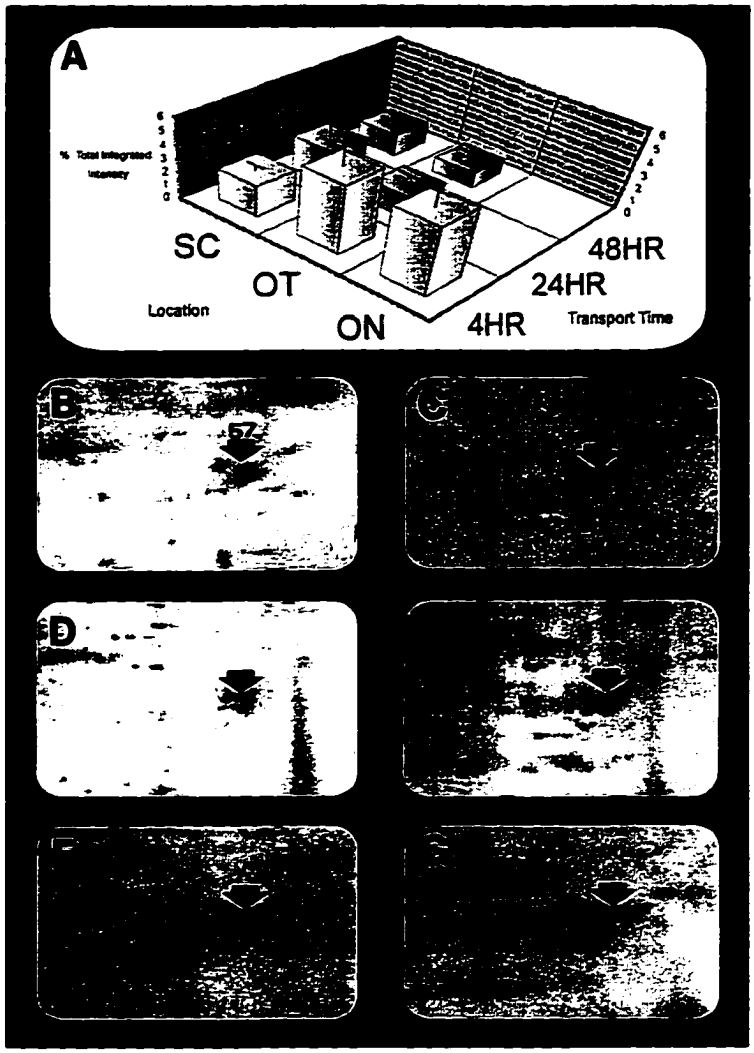

FIGURE 13. Compartmental and temporal localization of the FT protein 57. (A) Mean ± SEM of the protein in compartments ON, OT, and SC at 4, 24, and 48 hr PIL. Relative activity in OT at 4 hr was significantly greater than that at 24 and 48 hr in OT and SC ($p < 0.5$). No other significant differences between compartments or time ($p > 0.6$ for all). Fluorographic representation of the protein in OT (B) and SC (C) at 4hr, OT (D) and SC (E) at 24 hr, and OT (F) and SC (G) at 48 hr PIL.

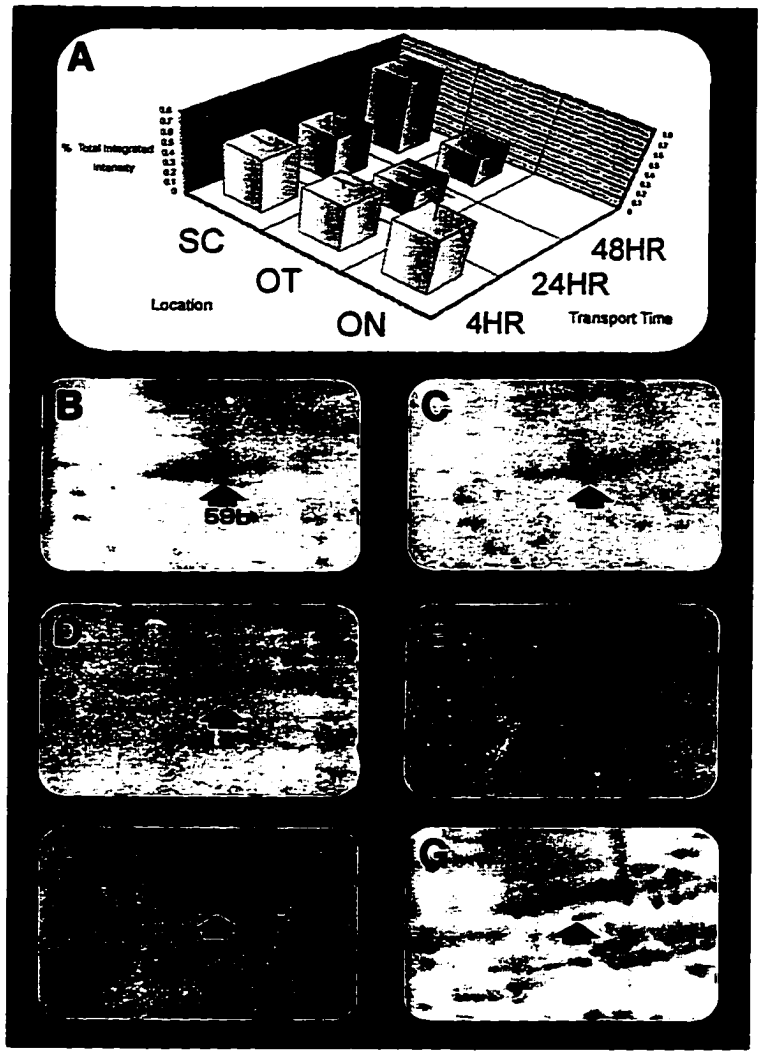

FIGURE 14. Compartmental and temporal localization of the FT protein 59b. (A) Mean ± SEM of the protein in compartments ON, OT, and SC at 4, 24, and 48 hr PIL. Relative activity in SC at 48 hr was significantly greater that at 24 hr and 48 hr in OT ($p < 0.05$). No significant differences between compartments or time at any other time ($p > 0.06$ for all). Fluorographic representation of the protein in OT (B) and SC (C) at 4hr, OT (D) and SC (E) at 24 hr, and OT (F) and SC (G) at 48 hr PIL.

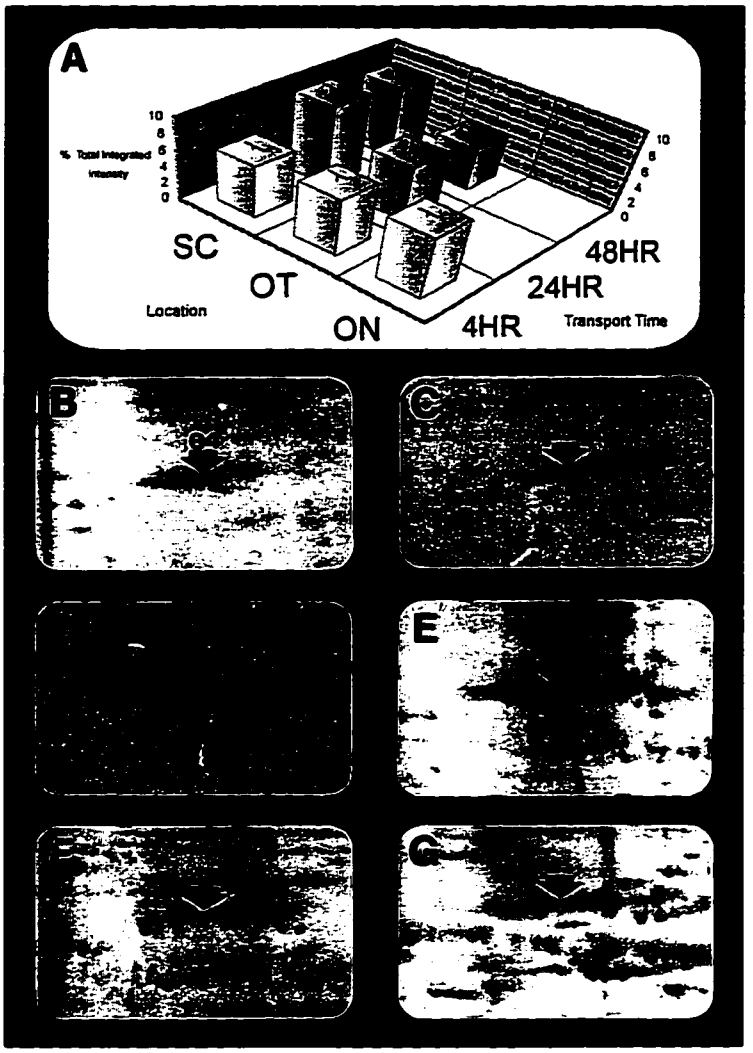

FIGURE 15. Compartmental localization of the FT protein 64. (A) Mean ± SEM of the protein in compartments ON, OT, and SC at 4, 24, and 48 hr PIL. Relative activity in SC was significantly greater than that in OT at 24 and 48 hr ($p < 0.05$ for both). Fluorographic representation of the protein in OT (B) and SC (C) at 4hr, OT (D) and SC (E) at 24 hr, and OT (F) and SC (G) at 48 hr PIL.

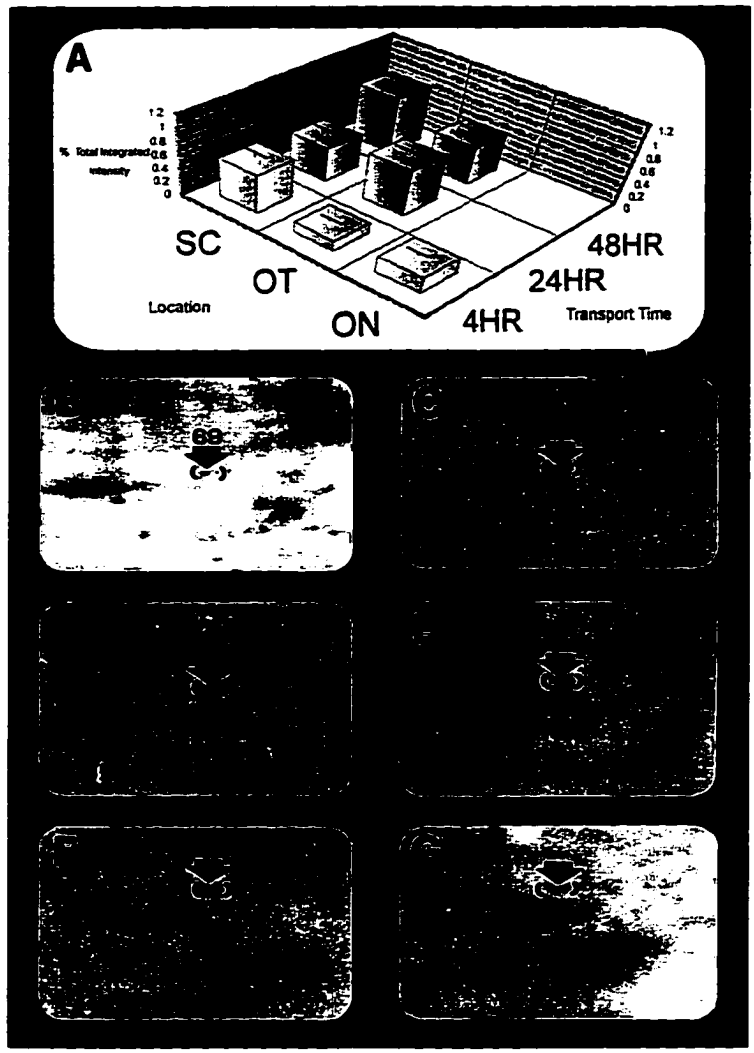

FIGURE 16. Temporal preferential localization of the FT protein 69. (A) Mean ± SEM of the protein in compartment, ON, OT, and SC at 4, 24, and 48 hr PIL. Relative activity in OT at 24 hr was significantly greater than that at 4 hr ($p < .05$), but not at 24 or 48 hr; and in SC activity at 4, 24 and 48 hr did not differ significantly ($p > 0.05$ for both comparisons). Fluorographic representation of the protein in OT (B) and SC (C) at 4hr, OT (D) and SC (E) at 24 hr, and OT (F) and SC (G) at 48 hr PIL.

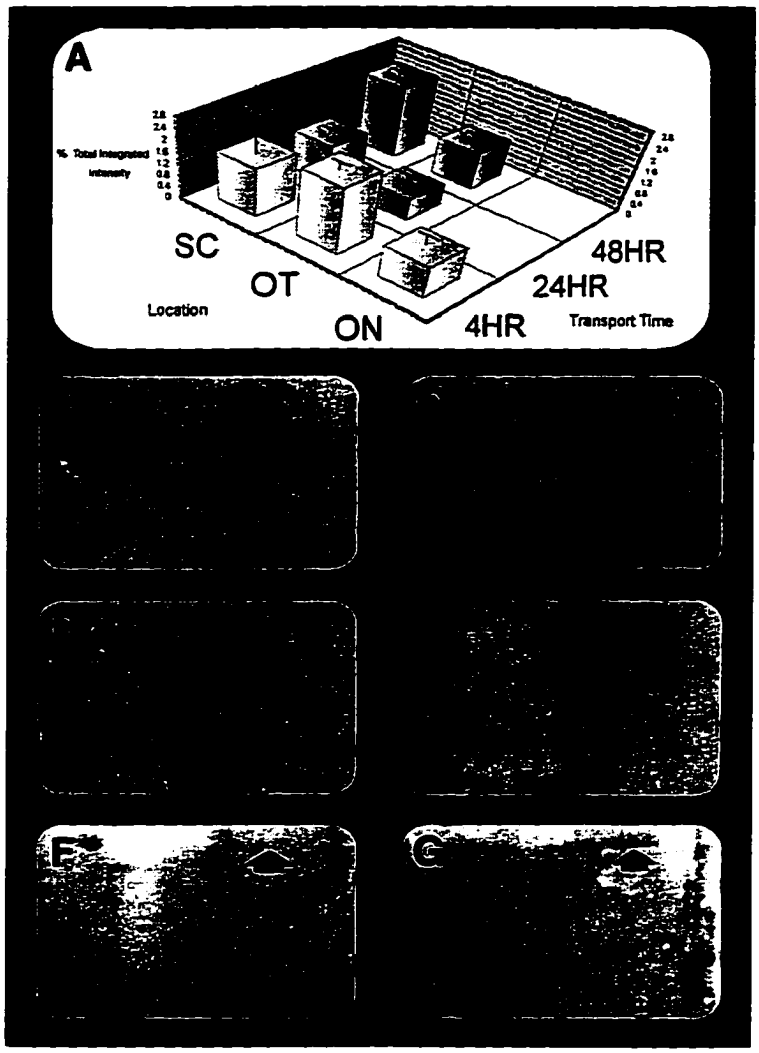

FIGURE 17. Compartmental and temporal localization of the FT protein 194. (A) Mean ± SEM of the protein in compartments ON, OT, and SC at 4, 24, and 48 hr PIL. Relative activity in OT at 24 hr was significantly less than that at 4 hr in OT and at 48 hr in SC ($p < 0.05$). No other significant differences between compartments or time ($p > 0.19$ for all). Fluorographic representation of the protein in OT (B) and SC (C) at 4hr, OT (D) and SC (E) at 24 hr, and OT (F) and SC (G) at 48 hr PIL.

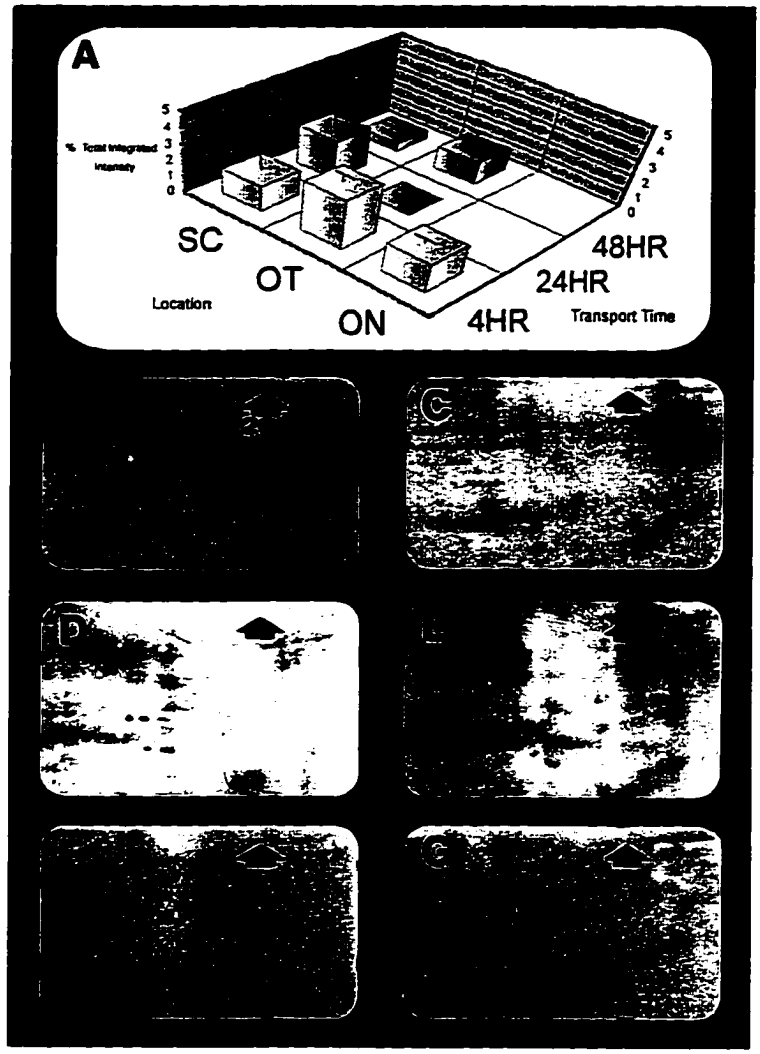

FIGURE 18. Compartmental and temporal localization of the FT protein 206. (A) Mean ± SEM of the protein in compartments ON, OT, and SC at 4, 24, and 48 hr PIL. Relative activity in OT at 24 hr was significantly less than that at 4 or 48 hr in all compartments ($p < 0.05$). Relative activity in SC at 48 hr was significantly less than that at 24 hr in SC and at 4 in OT ($p < 0.05$). Fluorographic representation of the protein in OT (B) and SC (C) at 4hr, OT (D) and SC (E) at 24 hr, and OT (F) and SC (G) at 48 hr PIL.

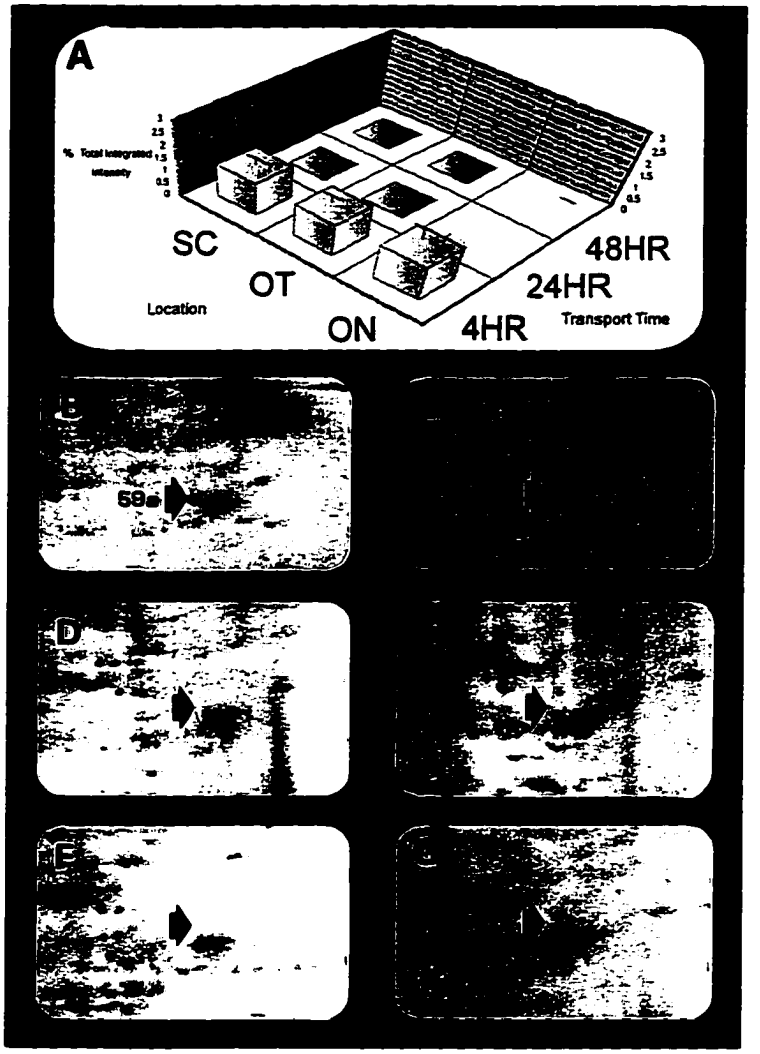

FIGURE 19. Temporal localization of the FT protein 59a. (A) Mean ± SEM of the protein in compartments ON, OT, and SC at 4, 24, and 48 hr PIL. Significantly greater activity was observed at 4 hr than at 24 and 48 hr ($p < 0.03$ for both comparisons). Fluorographic representation of the protein in OT (B) and SC (C) at 4hr, OT (D) and SC (E) at 24 hr, and OT (F) and SC (G) at 48 hr PIL.

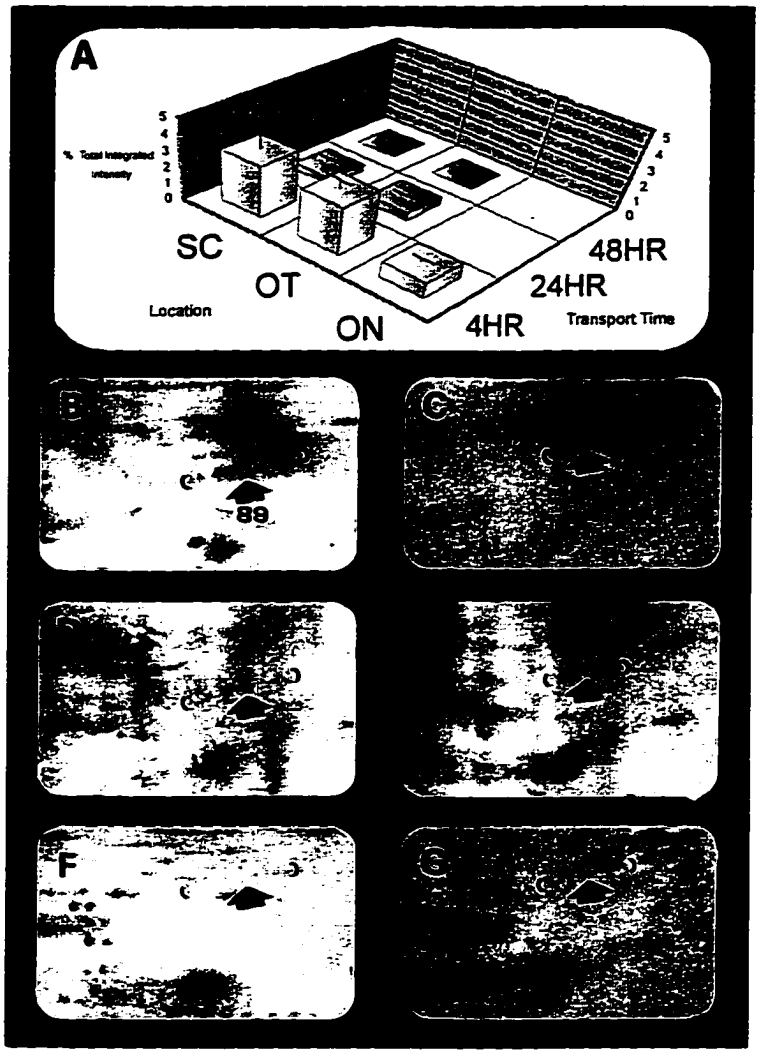

FIGURE 20. Temporal localization of the FT protein 89. (A) Mean ± SEM of the protein in compartments ON, OT, and SC at 4, 24, and 48 hr PIL. Significantly greater activity at 4 hr than at 24 and 48 hr ($p < 0.05$ for both comparisons). Fluorographic representation of the protein in OT (B) and SC (C) at 4hr, OT (D) and SC (E) at 24 hr, and OT (F) and SC (G) at 48 hr PIL.

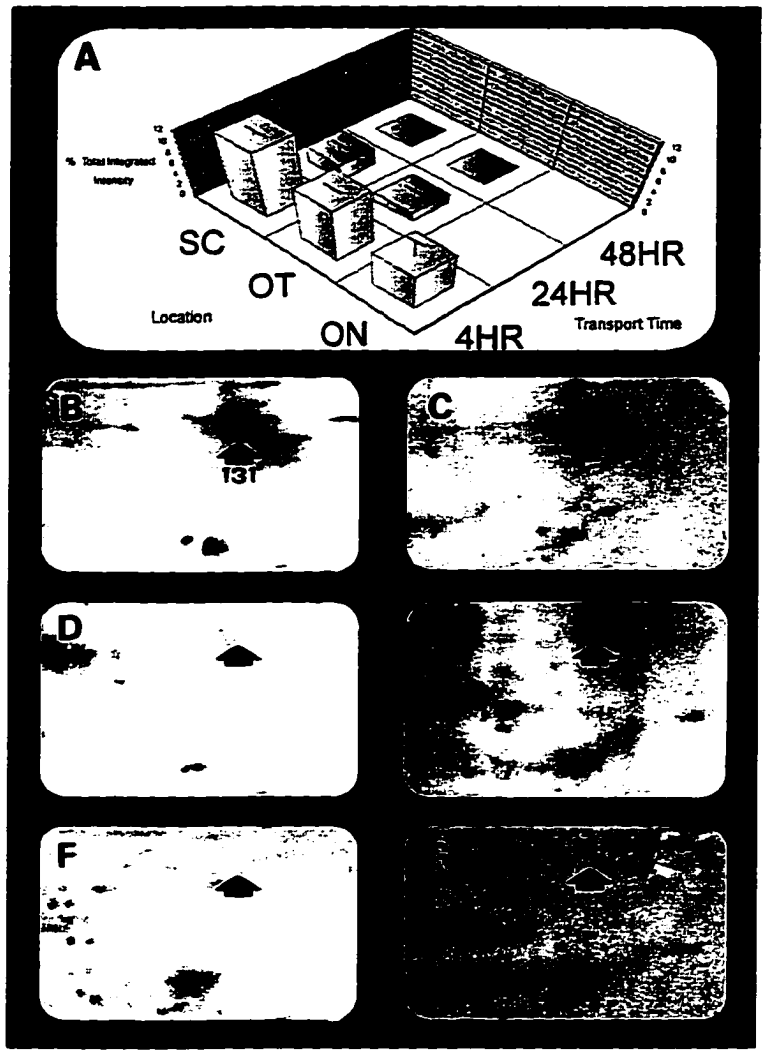

FIGURE 21. Temporal localization of the FT protein 131. (A) Mean ± SEM of the protei in compartments ON, OT, and SC at 4, 24, and 48 hr PIL. Significantly greater activity at 4 hr than at 24 and 48 hr ($p < 0.001$ for both comparisons). Fluorographic representation of the protein in OT (B) and SC (C) at 4hr, OT (D) and SC (E) at 24 hr, and OT (F) and SC (G) at 48 hr PIL.

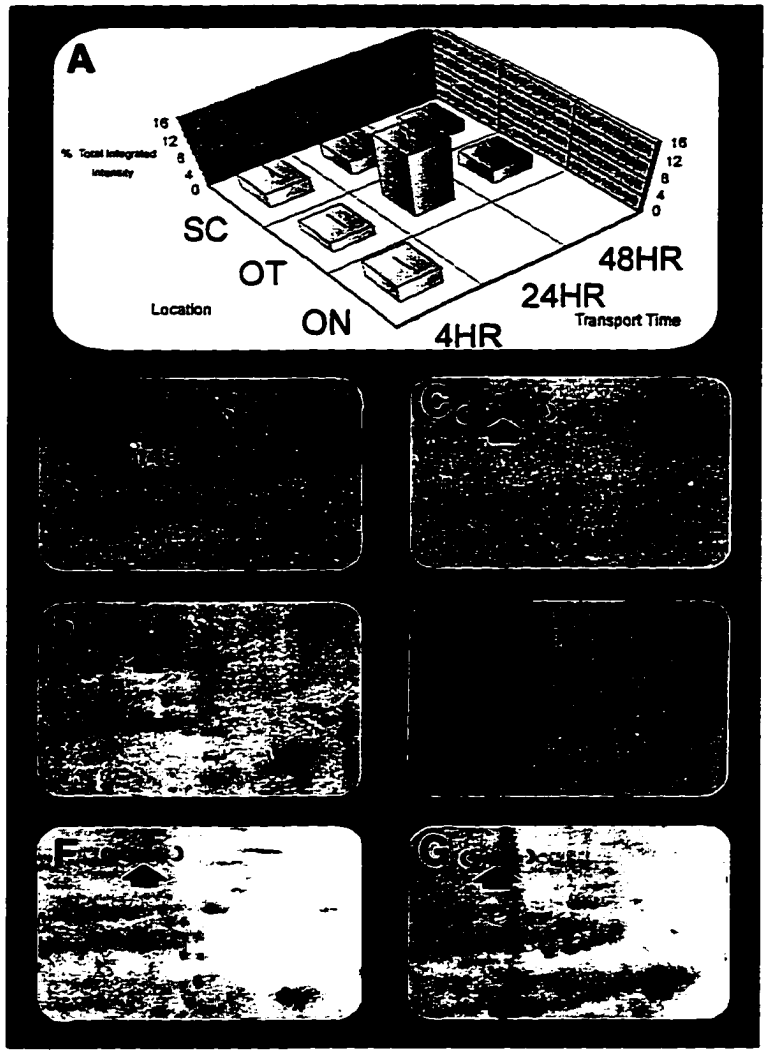

FIGURE 22. Compartmental and temporal localization of FT protein 149. (A) Mean ± SEM of the protein in compartments ON, OT, and SC at 4, 24, and 48 hr PIL. Activity in OT was significantly greater than in SC at 24 hr ($p < 0.001$), but activities in OT and SC did not differ significantly at 4 or 48 hr. In OT, the amount at 24 hr was significantly greater than at 4 and at 48 hr ($p < 0.001$ for both comparisons) Fluorographic representation of the protein in OT (B) and SC (C) at 4hr, OT (D) and SC (E) at 24 hr, and OT (F) and SC (G) at 48 hr PIL.

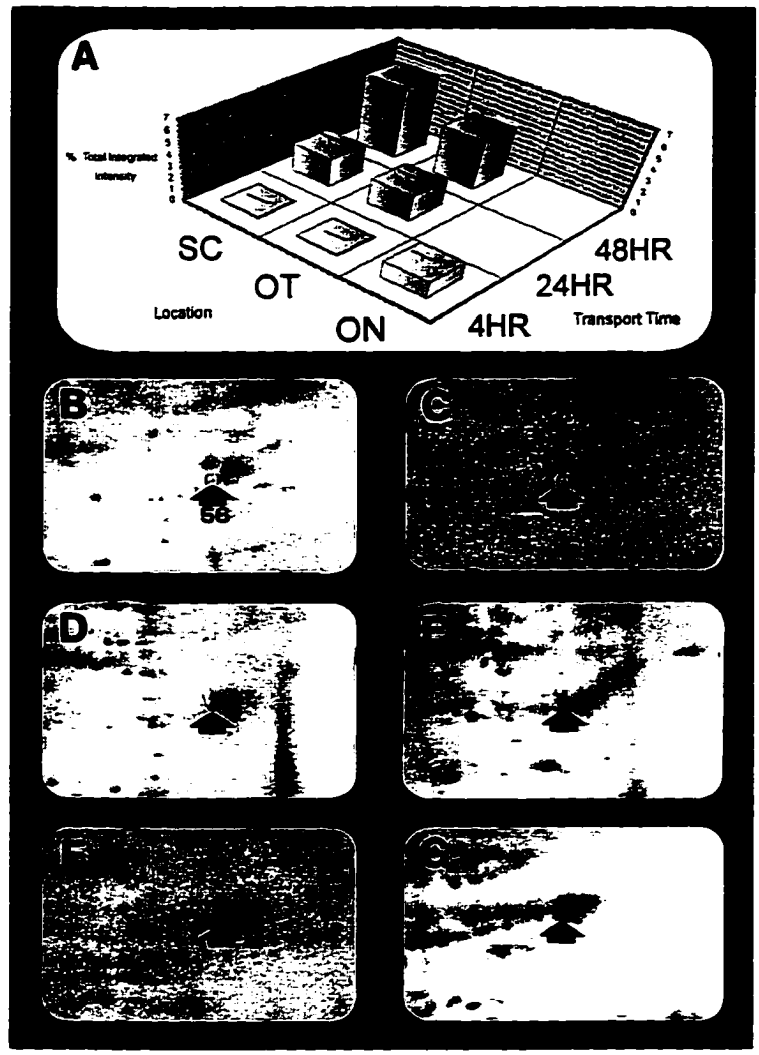

FIGURE 23. Increased activity of the FT protein 56 with longer PIL. (A) Mean ± SEM of the protein in compartments ON, OT, and SC at 4, 24, and 48 hr PIL. Activities in OT and SC at 48 hr was significantly greater than at 4 and 24 hr ($p < 0.05$ for both comparisons). Fluorographic representation of the protein in OT (B) and SC (C) at 4hr, OT (D) and SC (E) at 24 hr, and OT (F) and SC (G) at 48 hr PIL.

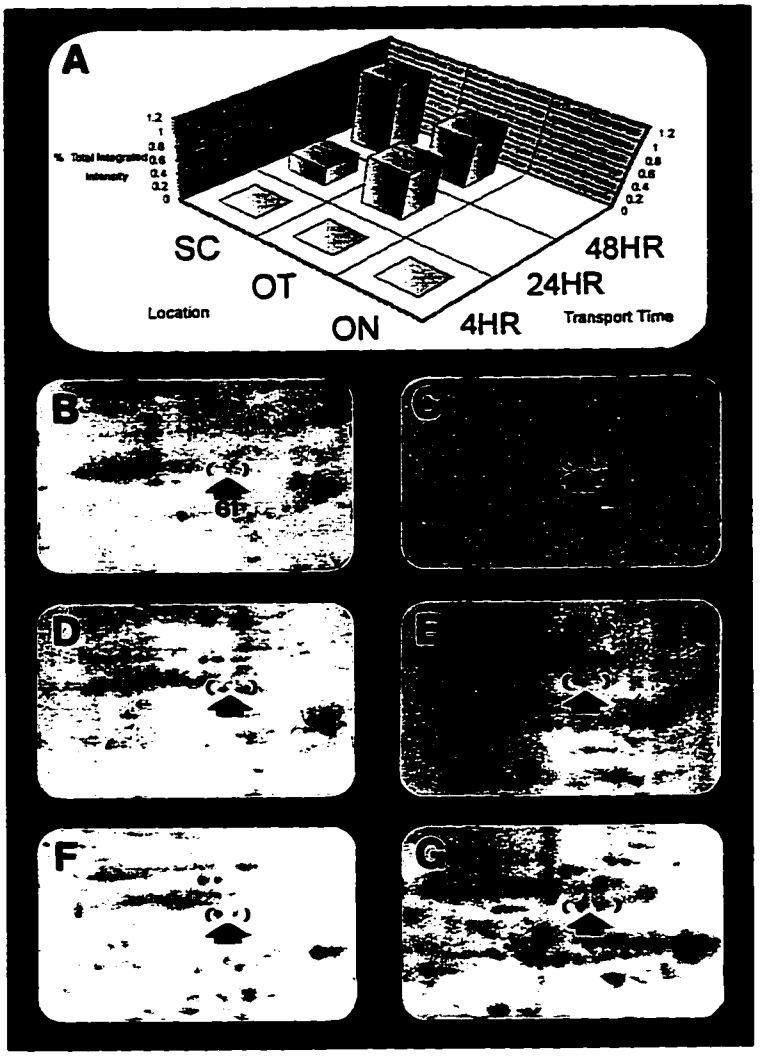

FIGURE 24. Increased activity of the FT protein 61 with longer PIL. (A) Mean ± SEM of the protein in compartments ON, OT, and SC at 4, 24, and 48 hr PIL. Activities in OT at 24 and 48 hr was significantly greater than at 4 hr ($p < 0.01$ for both comparisons). Activities in SC at 24 and 48 hr was significantly greater than at 4 hr ($p < 0.05$ for both comparisons). Fluorographic representation of the protein in OT (B) and SC (C) at 4hr, OT (D) and SC (E) at 24 hr, and OT (F) and SC (G) at 48 hr PIL.

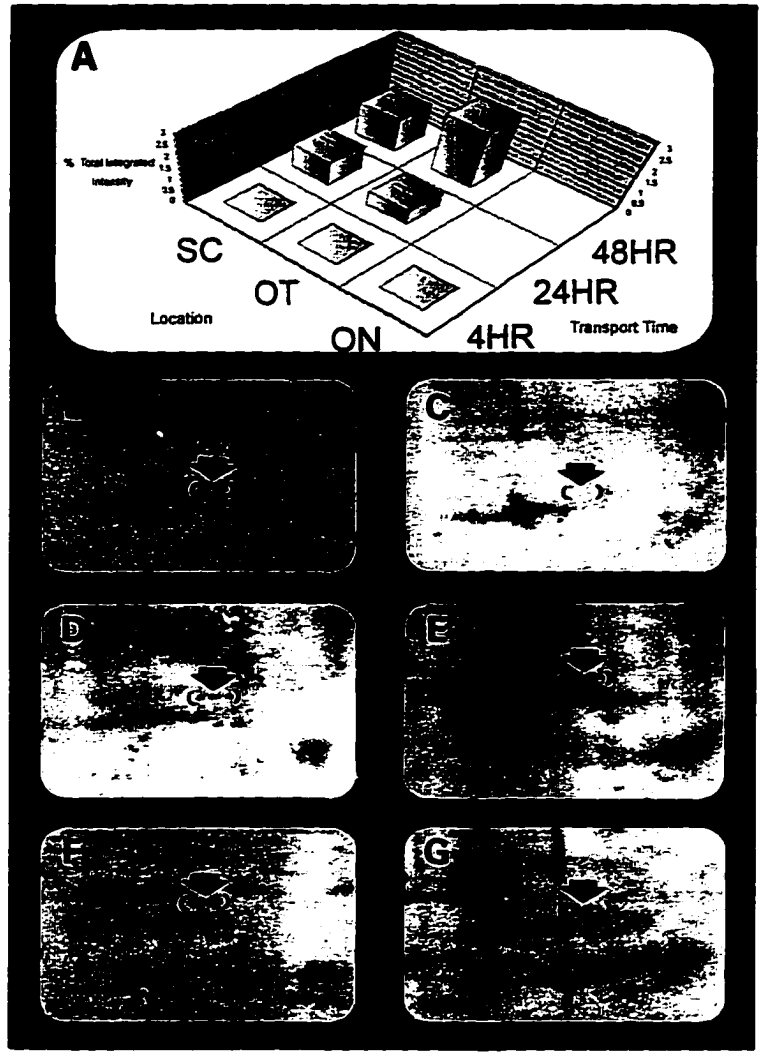

FIGURE 25. Increased activity of the FT protein 67 with longer PIL. (A) Mean ± SEM of the protein in compartments ON, OT, and SC at 4, 24, and 48 hr PIL. Activities in OT at 24 and 48 hr was significantly greater than at 4 hr ($p < 0.05$ for both comparisons). Activities in SC at 24 and 48 hr was significantly greater than at 4 hr ($p < 0.05$ for both comparisons). Fluorographic representation of the protein in OT (B) and SC (C) at 4hr, OT (D) and SC (E) at 24 hr, and OT (F) and SC (G) at 48 hr PIL.

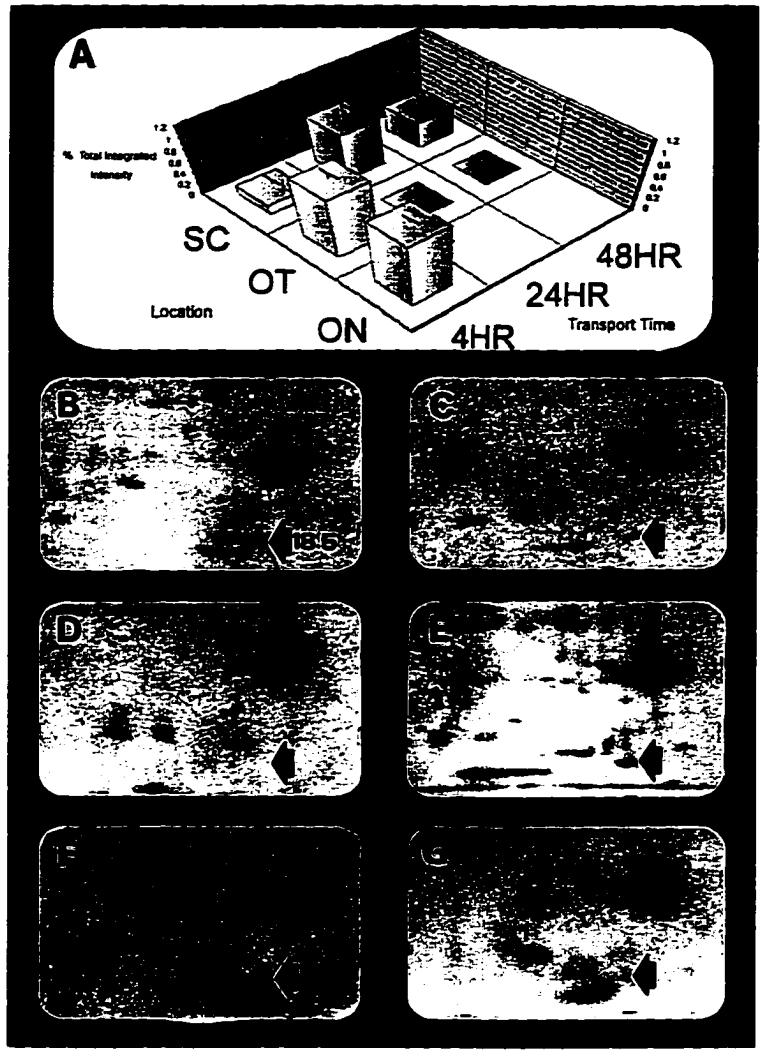

FIGURE 26. Preferential localization of the FT protein 18.5 in the SC at 24 and 48 hr PIL. (A) Mean ± SEM of the protein in compartments ON, OT, and SC at 4, 24, and 48 hr PIL. Activities in SC at 24 and 48 hr was significantly greater than at 4 hr ($p < 0.05$ for both comparisons). Fluorographic representation of the protein in OT (B) and SC (C) at 4hr, OT (D) and SC (E) at 24 hr, and OT (F) and SC (G) at 48 hr PIL.

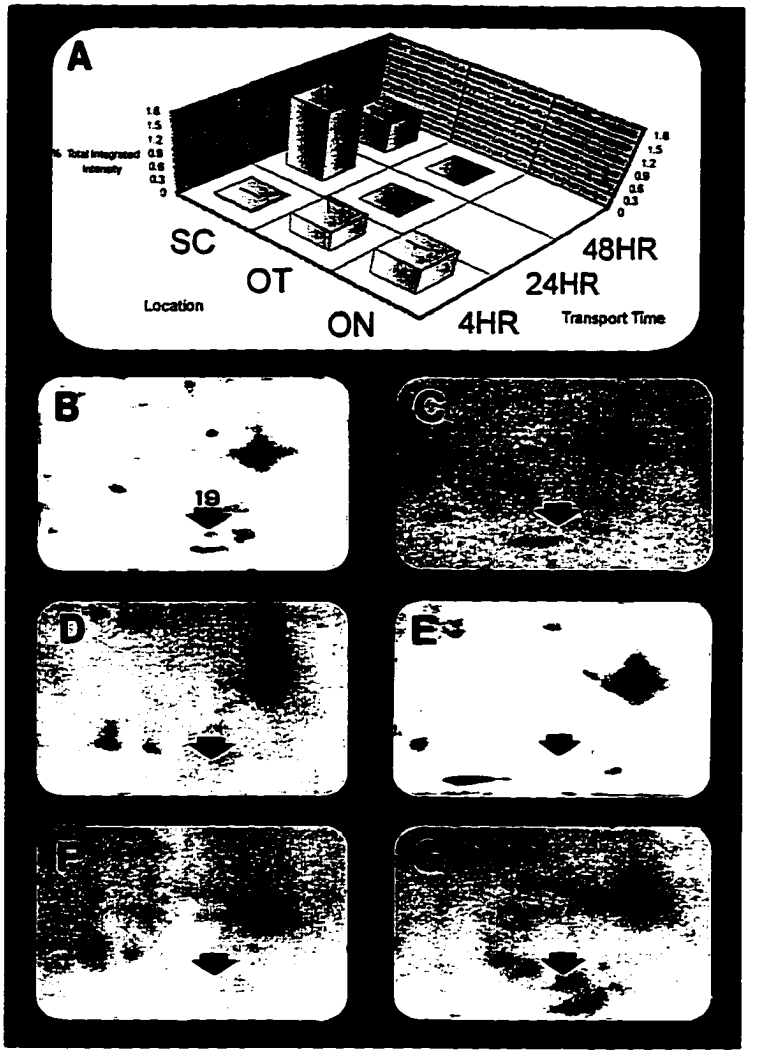

FIGURE 27. Preferential localization of the FT protein 19 in the SC at 24 and 48 hr PIL. (A) Graphic display of the protein in compartments ON, OT, and SC at 4, 24, and 48 hr PIL. Activities in SC at 24 was significantly greater than at 4 or 48 hr ($p < 0.05$ for both comparisons). Fluorographic representation of the protein in OT (B) and SC (C) at 4hr, OT (D) and SC (E) at 24 hr, and OT (F) and SC (G) at 48 hr PIL.

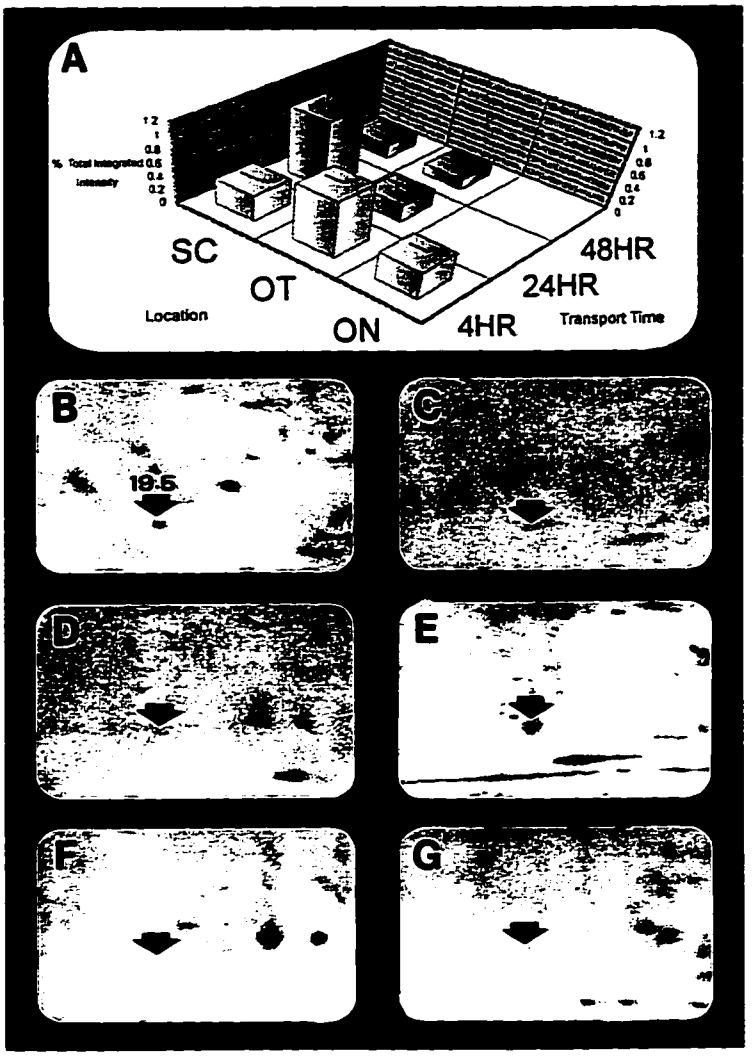

FIGURE 28. Compartmental and temporal localization of the FT protein 19.5. (A) Mean ± SEM of the protein in compartments ON, OT, and SC at 4, 24, and 48 hr PIL. Activity in SC was significantly greater than in OT at 24 hr ($p < 0.05$), but not at 48 hr. The amount in OT at 4 hr was significantly greater than at 24 and 48 hr ($p < 0.05$ for both comparisons). Fluorographic representation of the protein in OT (B) and SC (C) at 4hr, OT (D) and SC (E) at 24 hr, and OT (F) and SC (G) at 48 hr PIL.

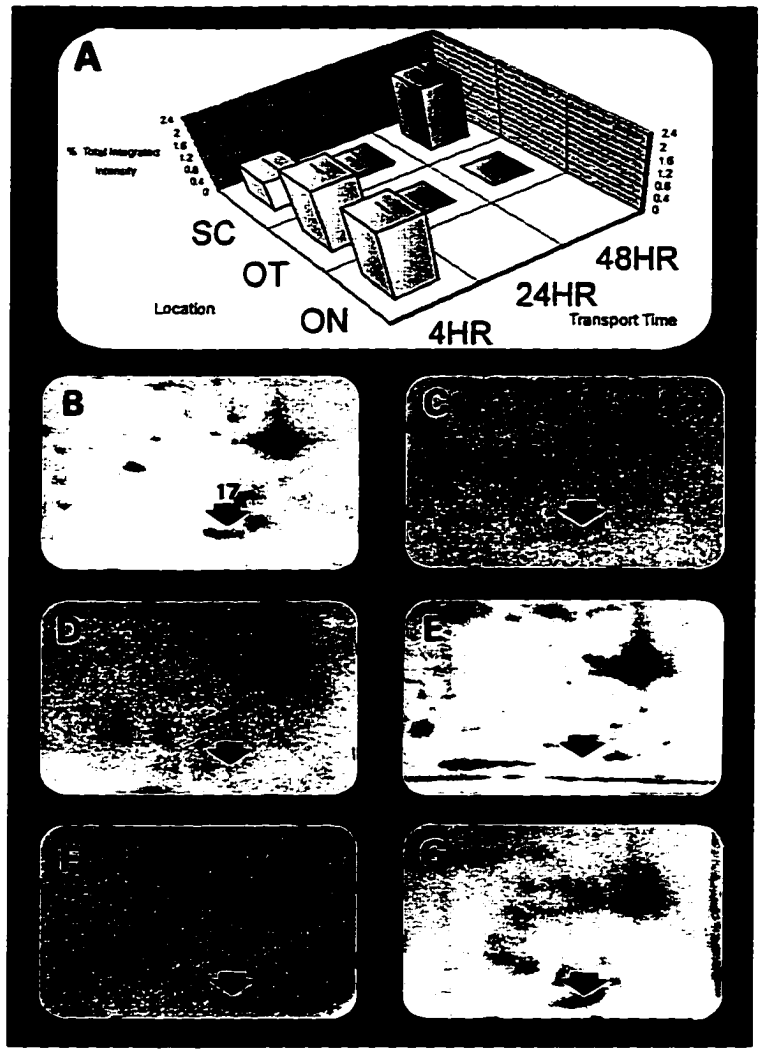

FIGURE 29. Preferential localization of the FT protein 17 in the SC at 24 and 48 hr PIL. (A) Mean ± SEM of the protein in compartments ON, OT, and SC at 4, 24, and 48 hr PIL. Activities in SC at 48 hr was significantly greater than at 4 or 24 hr ($p < 0.01$ for both comparisons). Activities in OT at 4 hr was significantly greater than in SC ($p < 0.01$). Fluorographic representation of the protein in OT (B) and SC (C) at 4hr, OT (D) and SC (E) at 24 hr, and OT (F) and SC (G) at 48 hr PIL.

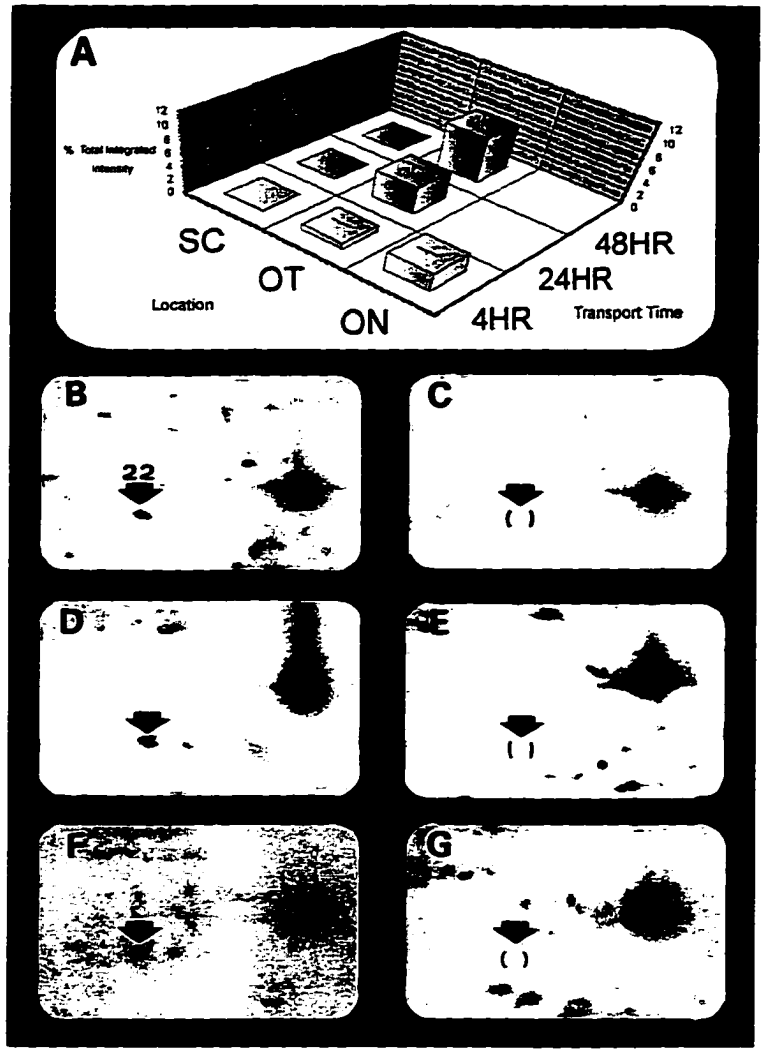

FIGURE 30. Preferential localization of the FT protein 22 in the OT. (A) Mean ± SEM of the protein in compartments ON, OT, and SC at 4, 24, and 48 hr PIL. Activities in OT at 48 hr was significantly greater than at 4 or 24 hr ($p < 0.01$ for both comparisons). Fluorographic representation of the protein in OT (B) and SC (C) at 4hr, OT (D) and SC (E) at 24 hr, and OT (F) and SC (G) at 48 hr PIL.

F. FT PROTEIN ASSOCIATION WITH THE TRANSLOCATED VESICULAR ORGANELLES

The purpose of the next set of experiments was to evaluate the vesicular distribution of FT proteins, particularly, the FT protein organization in the translocated membrane vesicles. In order to examine this organization, synaptosomes were prepared from SC at 4 hr PIL. Confirmation of synaptosomal integrity was made by electron microscopy. Electron micrographs revealed intact pinched-off terminal membranous bodies (synaptosomes) containing visible ultrastructural components (Figure 31). Structures identified in the EM included: small clear vesicles, mitochondria, multivesicular bodies, membranous cisternae, synapses, and relatively dense cytoplasmic matrix, as previously reported by Wittaker *et al.* (118). The majority of vesicles in the synaptosomes appeared as small clear organelles with diameters in the range of 30 - 50 nm in agreement with the size described by Hodge and Adelman (123).

In the present study, some of the SC synaptosomes contained radiolabeled FT proteins of the RGC presynaptic terminals. Each of two fractionation procedures (described in Material and Methods) was used to delineate the type of association (soluble, integral membrane, peripheral membrane) that FT proteins made with the transport vesicles. Figure 32 displays the acid-precipitable CPMs contained in radiolabeled FT proteins following fractionation: (1) the Na_2CO_3 method (which separates integral membrane proteins from soluble/peripheral membrane proteins) and (2) osmotic lysis method (which separates soluble proteins from integral/peripheral membrane proteins). The results demonstrated that the vast majority of resolved FT proteins were

conveyed as integral membrane proteins, while only a few resolved FT proteins were transported as soluble or peripheral membrane proteins.

Analyses of individual radiolabeled FT proteins by 2D-SDS-PAGE fluorography confirmed the acid-precipitable CPM results. Figure 33 shows two-dimensional fluorographic patterns of FT proteins fractionated with the membranes by Na_2CO_3 extraction (Figure 33A) and peripheral plus integral membranes by hypotonic osmotic lysis (Figure 33B). For both fractionation procedures the 2D fluorographs of the radiolabeled FT proteins were similar. However, more detailed analysis revealed two proteins (57 and 59a) that were not detectable in the integral membrane fraction (Figure 33C) but were detected in the peripheral plus integral membrane fraction (Figure 33D). This result suggests that FT proteins 57 and 59a could be peripheral membrane proteins and/or vesicle-soluble proteins.

The hypotonic osmotic lysis fractionation results provided direct experimental support that the FT proteins 57 and 59a are, at least partially, vesicle-soluble species. Figure 34 shows two-dimensional fluorographic patterns of the FT proteins fractionating with the peripheral/integral membranes (Figure 34A) and the FT proteins fractionating as vesicle-soluble species (Figure 34B). This results showed that FT proteins 57 and 59a co-purified with the vesicle soluble fraction.

The radiolabeled FT proteins in the soluble/peripheral membrane of the Na_2CO_3 fraction were undetectable in either 2D or 1D fluorographs (Figure 35). One reason for the absence of vesicle-soluble FT proteins 57 and 59a in the soluble fraction using Na_2CO_3 extraction could be the harsher conditions (e.g., pH 11.5) employed, relative to the osmotic lysis fractionation.

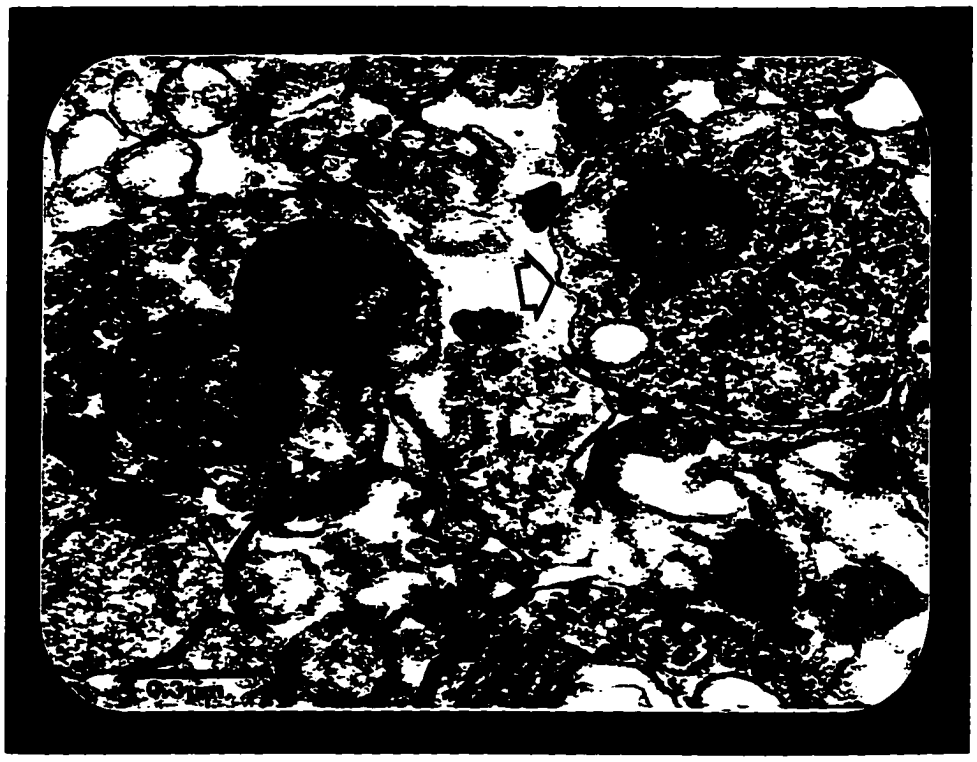

FIGURE 31. Electron micrograph of rat SC synaptosomal fractions revealed intact synaptosomes (large open arrows) and synapses (arrowhead). Internal structures (e.g., small clear vesicle (small open arrows), mitochondrion (large arrow), multivesicular body (arrow head), and dense cytoplasmic matrix) have remained intact and localized within the synaptosomes. X68,000

A

	Na_2CO_3			Osmotic lysis			
	CPMx1000	±SEM x1000	n		CPMx1000	±SEMx1000	n
Integral	41.86	13.69	4	Soluble	1.147	1.986	3
Soluble/Peripheral	2.569	1.147	4	Integral/Peripheral	20.576	35.638	3

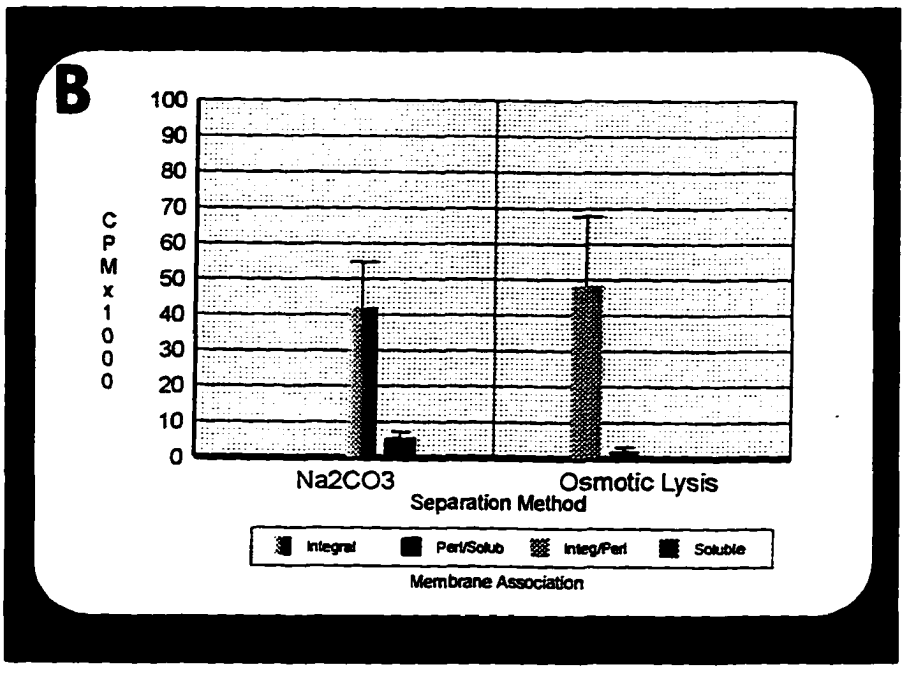

FIGURE 32. Acid-precipitable CPMs of peripheral and soluble FT proteins from SC synaptosomes. (A) Results of Na_2CO_3 and osmotic lysis methods. (B) Mean ± SEM of result A. Abbreviations: CPM, count per minute; SEM, standard error of mean; n, number of replicates

FIGURE 33. Composition of FT proteins in fractionated SC synaptosomes . (A) 2D fluorograph of Na_2CO_3 fraction containing FT integral membrane proteins. (B) 2D fluorograph of osmotic lysis fraction containing integral and peripheral proteins. (C) and (D) are magnified version of (A) and (B) respectively.

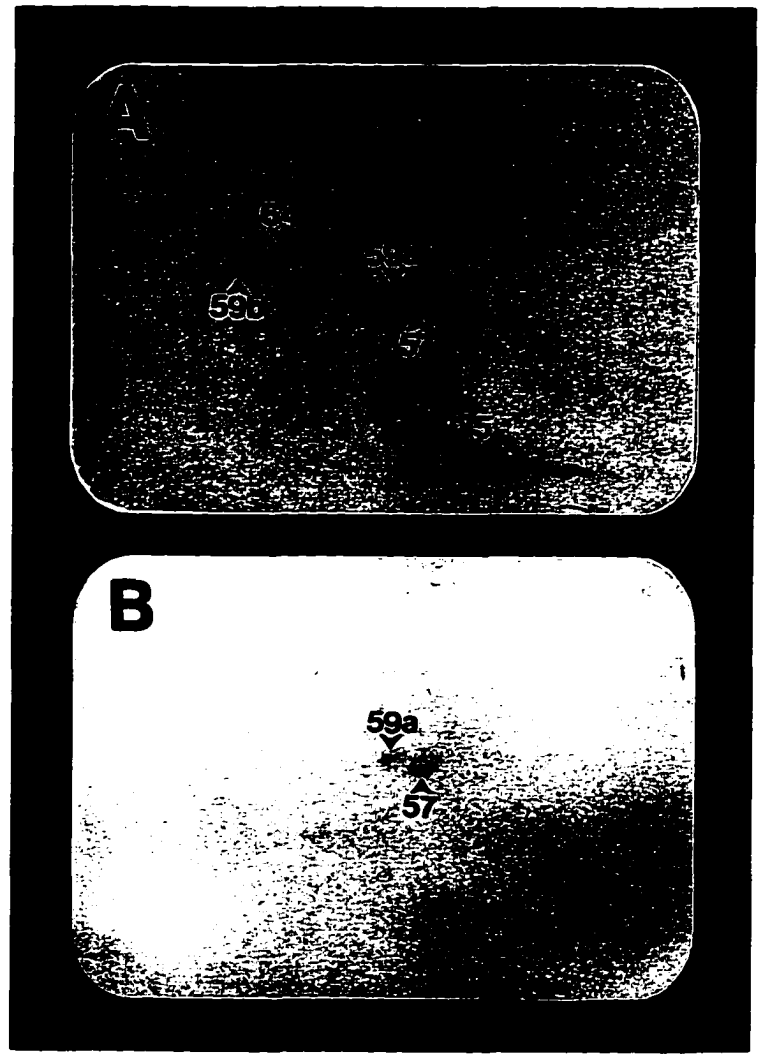

FIGURE 34. Composition of FT proteins in fractionated SC synaptosomes. (A) 2D fluorograph of osmotic lysis fraction containing integral membrane and peripheral membrane proteins. (B) 2D Fluorograph of osmotic lysis fraction containing aqueous-soluble proteins.

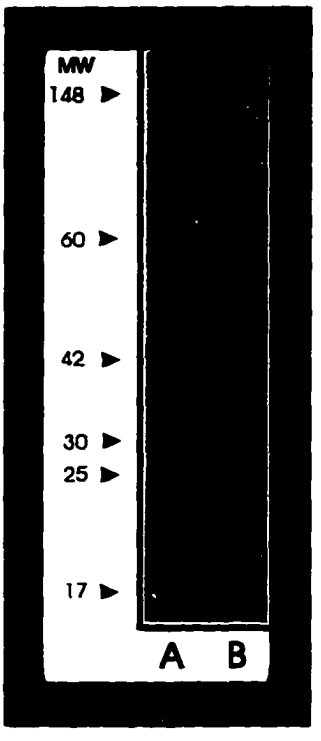

FIGURE 35. Composition of FT proteins in fractionated SC synaptosomes. 1D fluorograph of integral (A) and soluble + peripheral (B) synaptosomal FT proteins obtained from fractions of Na_2CO_3 method.

G. ANTIBODIES TO THE MAJOR FT PROTEIN (SNAP-25) CAN CO-IMMUNOPRECIPITATE SUBSETS OF BOTH FAST AND SLOW TRANSPORTED PROTEINS

In order to assess whether the most heavily labeled FT protein (i.e., SNAP-25) might have intermolecular relationships with other proteins in axons and/or pre-synaptic terminals, radiolabeled proteins from tissues containing nerve segments (ON and OT) and pre-synaptic terminals (SC) were immunoprecipitated with SNAP 25 antibodies at 4 hr and 12 d PIL. Immunoprecipitation (IP) studies at 4 hr PIL allowed assessment of a SNAP-25 relationship with other FT proteins while IP studies at 12 d PIL allowed evaluation of a SNAP-25 relationship with slow transported (SCb) proteins. Results showed that significant amounts (i.e., acid-precipitable CPM) of FT and SCb proteins were co-immunoprecipitated (CO-IP) with SNAP-25 antibodies. Table 2 shows that as much as 3% of the total radiolabeled SCb proteins and up to 6% of the total radiolabeled FT proteins were CO-IP. One-dimensional SDS-PAGE fluorographs of SNAP-25 CO-IP radiolabeled FT and SCb proteins are shown in Figures 36 and 37, respectively. Such results revealed several radiolabeled FT and SCb proteins were CO-IP with SNAP-25 in both nerve and SC compartments.

Comparisons between compartments (nerve vs. terminal) of CO-IP proteins with SNAP-25 revealed quantitative but not qualitative differences. Examination of the radiolabeled FT CO-IP proteins (Figure 36) showed proteins with relatively low molecular weight (M_r < 30 kDa). Among these proteins, the putative CO-IP radiolabeled SNAP-25 was seen at M_r ~25 kDa in both compartments. While other

CO-IP proteins of M_r ~18 kDa and ~8 kDa were detected in both compartments, protein(s) of M_r 16 kDa was observed only in nerve segments.

The radiolabeled SCb CO-IP proteins (Figure 37), on the other hand, showed predominantly higher molecular weights than that of FT radiolabeled CO-IP proteins. Their molecular weights ranged from ~18 kDa to ~55 kDa. Here also, differential quantitative expression of CO-IP proteins was observed. CO-IP proteins with M_rs ~25 kDa, ~44 kDa, and ~55 kDa were seen in both compartments; whereas, proteins with M_rs of ~33 kDa and ~53 kDa were observed in only nerve segments and protein(s) of M_r of ~18 kDa was detected only in the SC.

Previous studies have only reported a SNAP-25 association with a small set of pre-synaptic terminal proteins (79, 80, 87). The above results, however, might suggest possible relationship of SNAP-25 with other FT and SCb proteins in both axons and pre-synaptic terminals.

Additional studies were performed to investigate if the relationships between SNAP-25 and a subset of FT and SCb proteins were ATP-dependent. To address this question, IP were performed in the presence of exogenous ATP, without apyrase (an inhibitor of ATP). Figures 38 and 39 show the one-dimensional fluorographic results of FT and SCb CO-IP by SNAP-25 antibodies, respectively. Results showed that the CO-IP patterns of FT and SCb proteins were similar whether ATP was inhibited (Figures 38-1 and 39-1) or ATP was available (Figures 38-3 and 39-3). These results provide evidence that the relationships of SNAP-25 with FT and SCb proteins may not be dependent on ATP.

TABLE 2.

Mean acid-precipitable CPM of slow transported (SCb) and FT proteins CO-IP with SNAP-25 antibodies.

	Slow Transported (SCb) Proteins CPM x 1000							Fast Transported Proteins CPM x 1000						
	Total	±SEM	CI	±SEM	%CI	±SEM	n	Total	±SEM	CI	±SEM	%CI	±SEM	n
Nerve	2,276	37.8	19.8	0.47	0.7	0.13	5	205	66.2	9.0	2.3	5.1	1.5	5
SC	175	134	2.96	1.37	3.0	1.6	3	178	25.9	10.2	3.5	6.1	3.0	3
Control	149	19.1	0.57	0.57	0.3	0.2	2	143	24.7	0.64	0.28	0.4	0.01	2

Nerve represents both ON + OT segments. The percentage of proteins that were CO-IP with SNAP-25 (%CI) was obtained by dividing CPM of CO-IP proteins by the Total CPM of radiolabeled proteins. CPM, counts per minute; SEM, standard error of mean; n, number of replicates; CI, co-immunoprecipitates.

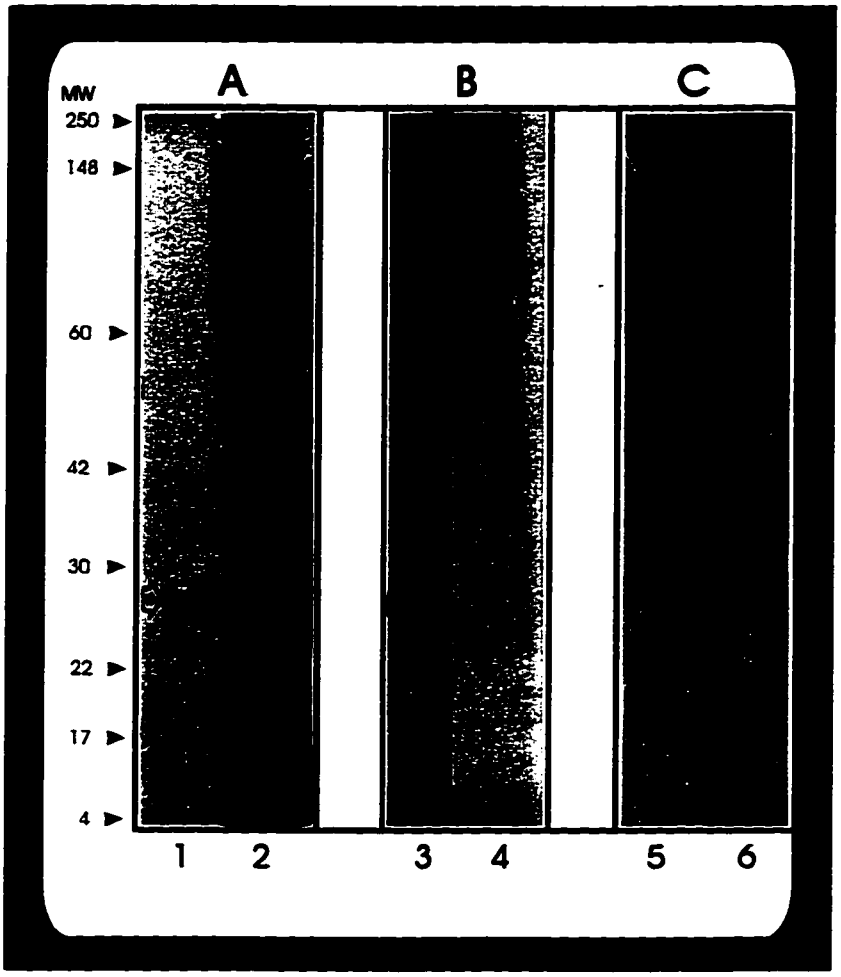

FIGURE 36. 1D fluorographic profiles of radiolabeled FT proteins CO-IP from nerve (A), and SC (B) with SNAP-25 antibodies; nerve proteins (C) IP with control anti-mouse IgG antisera. Lanes 1, 3, and 5 CO-IP proteins; lanes 2, 4, and 6 supernatant of IP. Small solid arrowheads indicate the position of CO-IP proteins (Large open arrowhead, indicates the position of SNAP-25 [M_r = 25 kDa]). Solid arrowheads show the positions and M_r (kDa) of molecular weight standards.

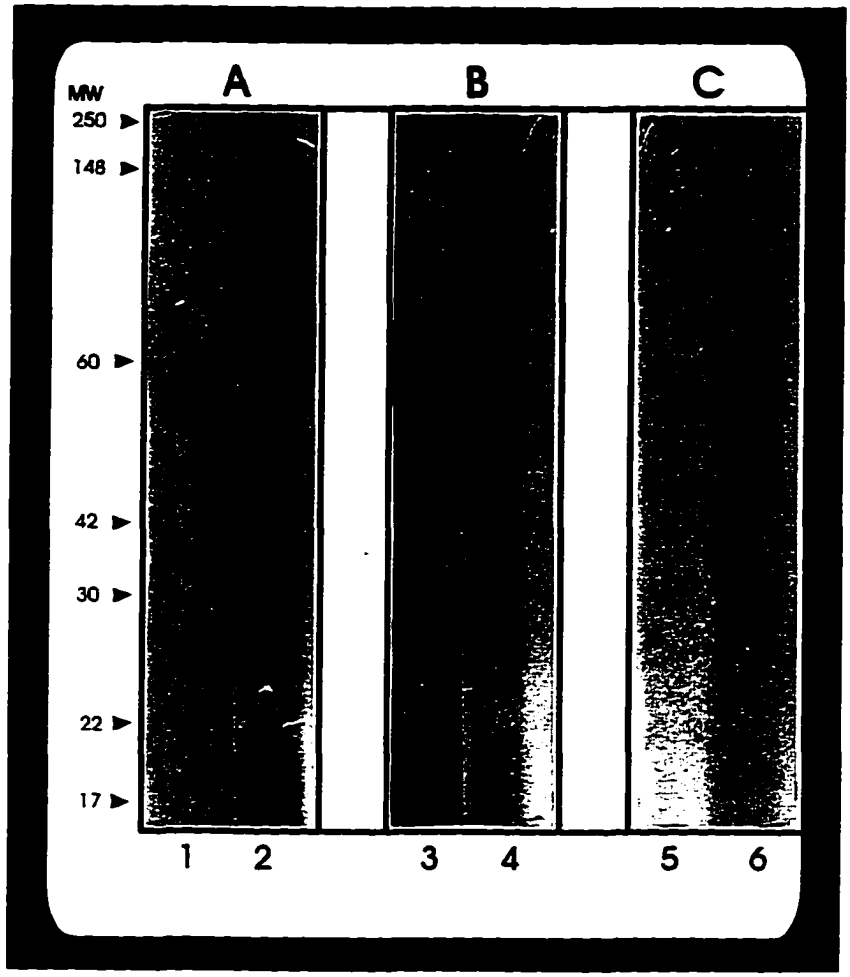

FIGURE 37. 1D fluorographic profiles of radiolabeled slow tranported (SCb) proteins CO-IP from nerve (A) and SC (B) with SNAP-25 antibodies; nerve proteins (C) IP with control anti-mouse IgG antisera. Lanes 1, 3, and 5 CO-IP proteins; lanes 2, 4, and 6 supernatant of IP. Small solid arrowheads indicate the position of CO-IP proteins (Large open arrowhead, indicates the position of SNAP-25 [M_r = 25 kDa]). Solid arrowheads show the positions and M_r (kDa) of molecular weight standards.

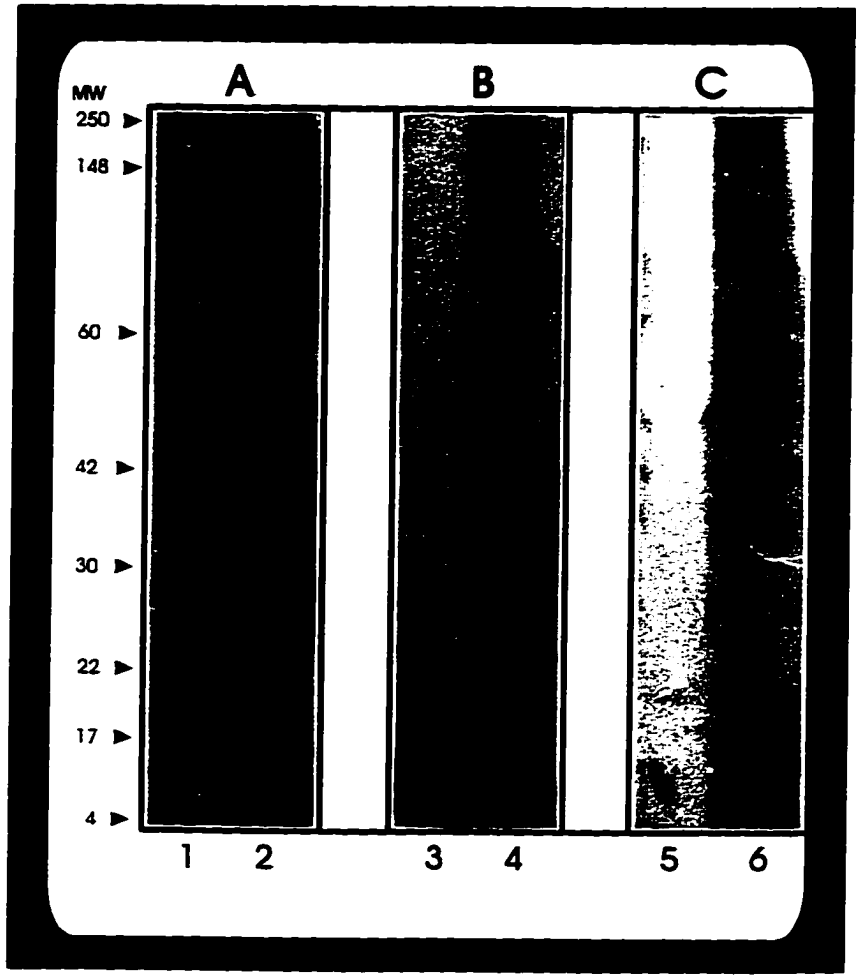

FIGURE 38. 1D-PAGE fluorographic IP profiles of radiolabeled FT nerve (ON + OT) proteins IP with SNAP-25 antibodies in the absence (A) and presence (B) of ATP; nerve proteins IP in the presence of ATP (C) with control anti-mouse IgG antisera. Lanes 1, 3, and 5, CO-IP proteins; lanes 2, 4, and 6, supernatant of IP. Small solid arrowheads indicate the position of CO-IP proteins (large open arrowhead, indicates the position of SNAP-25 [M_r = 25 kDa]). Solid arrowheads show the positions and M_r (kDa) of molecular weight standards.

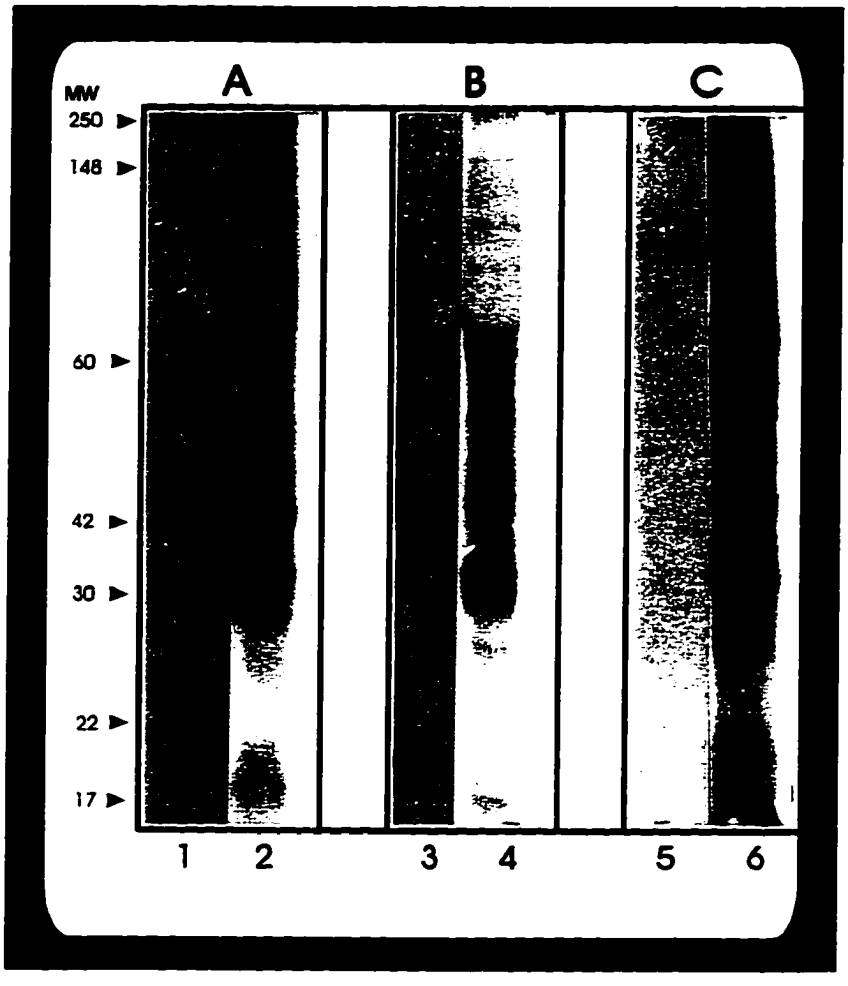

FIGURE 39. 1D-PAGE fluorographic profiles of radiolabeled SCb nerve (ON + OT) proteins of IP with SNAP-25 antibodies in the absence (A) and presence (B) of ATP; nerve proteins IP in the presence of ATP (C) with control anti-mouse IgG antisera. Lanes 1, 3, and 5, CO-IP proteins; lanes 2, 4, and 6, supernatant of IP. Small arrowheads indicate the position of CO-IP proteins. Larger arrowheads show the positions and M_r (kDa) of molecular weight standards.

CHAPTER IV

CONCLUSIONS AND DISCUSSION

In order to gain further insights into the trafficking of the mammalian anterograde fast axonally transported proteins, the most abundant methionine-containing FT proteins of the adult Sprague-Dawley rat optic pathway were identified and characterized. The results presented in this study lead to several conclusions which are discussed below.

A. CONTRALATERAL PROJECTIONS OF THE RAT OPTIC PATHWAY

The majority of rat optic pathway axons have contralateral projections. Observation of the acid-precipitable distribution of radiolabeled FT rat optic pathway proteins 4 hr PIL indicated that the majority of FT proteins were axonally routed from the ipsilateral ON to the contralateral OT, SC, and LGN. These results suggested that the majority of RGC axons cross-over from the ipsilateral ON to the contralateral OT and project to contralateral subcortical nuclei of SC and LGN, as previously reported by Paxinos (120), Jeffery *et al.* (121), and Dreher *et al.* (124). Based on previous work, 90% of the 120,000 axons comprising the rat optic nerve are projected contralaterally past the optic chiasm (129, 130, 131, 132, 133). Further obeservation have also shown that the majority of axons are projected to the SC while relatively fewer axons branch to supply the LGN as previously described by Linden and Perry (128) and Sefton (131). Earlier, it was described how the compartmentalized structure of the RGCs can be an ideal model system for studying protein transport (see Introduction, Part B). The 90%

contralateral projection RGC axons, described here, provided an added advantage by directing the bulk of radiolabeled RGC proteins to fewer compartments, thus, increasing the amount of radiolabel activities found in each compartment. This high protein activity had allowed the resolution and analysis of individual FT proteins.

B. HETEROGENEITY OF THE FAST AXONAL TRANSPORT PROTEIN POPULATION

Results from 2D-SDS-PAGE fluorographs and acid-precipitable CPMs showed a heterogenous population of proteins being conveyed by fast axonal transport. Twenty of the >90 resolved newly synthesized radiolabeled FT proteins in the 2D fluorographs were subjected to qualitative and quantitative analyses. They were subsequently categorized into six distinct classes according to their localization in the different compartments (OT and SC) as well as their kinematic variations within and between compartments over time. 2D fluorographs revealed their distinct transport behavior. class 1 proteins exhibited little or no preference to any of the compartments at the three time points analyzed. They mostly appeared to be evenly distributed between compartments and did not change significantly over the three time points analyzed. Their locations in 2D fluorographs did not show any unusual distribution patterns. Class 2 were transient proteins with molecular weights > 55 kDA and showed a decline in their activity, or complete disappearance over time, but did not exhibit preferential localization in any of the compartments. In contrast, the activity of class 3 proteins increased at 24 hr PIL in the optic tract. Delayed appearance was observed in the class 4 proteins in

which at 4 hr PIL they were either in small amounts or virtually undetectable; but, they were clearly apparent at 24 and 48 hr PIL in all compartments. The last two classes of proteins showed preferential localization to one of the compartments. Class 5 proteins were localized preferentially in the SC, while class 6 protein was only observed in axonal regions. Most class 5 proteins were low molecular weight (M_r < 20 kDa) acidic proteins. Figure 40 summarizes the position of each of the 20 proteins as they appeared in 2D fluorographs. Table 3 summerizes the characteristics and special features of the six classes of proteins.

Previous studies have reported that a significant proportion of FT proteins may be deposited along the axon (67, 68, 125, 140). In addition to proteins, lipids (58, 141), biogenic amines (e.g., serotonin [142], norepinephrine [143]), and peptides (e.g., substance P [126]), may also be deposited within the axon. In the present study, however, only one (protein 22) of the 20 analyzed proteins appeared to be deposited exclusively in the axon. However, it is possible that, among the resolved proteins in the 2D fluorographs, other axon-deposited proteins may exist. For example, among the six FT classes, classes 1, 2, 3, and 4 proteins were present in either compartment suggesting the possibility that, perhaps, some of these proteins were destined for both compartments, as previously described (126). Additional studies are required to discriminate proteins that are laid down in the axons from those that are destined to the terminals.

Another common characteristic observed among FT classes 1, 3, 4, 5 and 6 is that the labelled FT activity persisted in all compartments at 24 and 48 hr PIL. Some of the FT protein activity could be explained by slow turn-over time and, therefore, the activity may have persisted over a period of time. This could be true for some FT

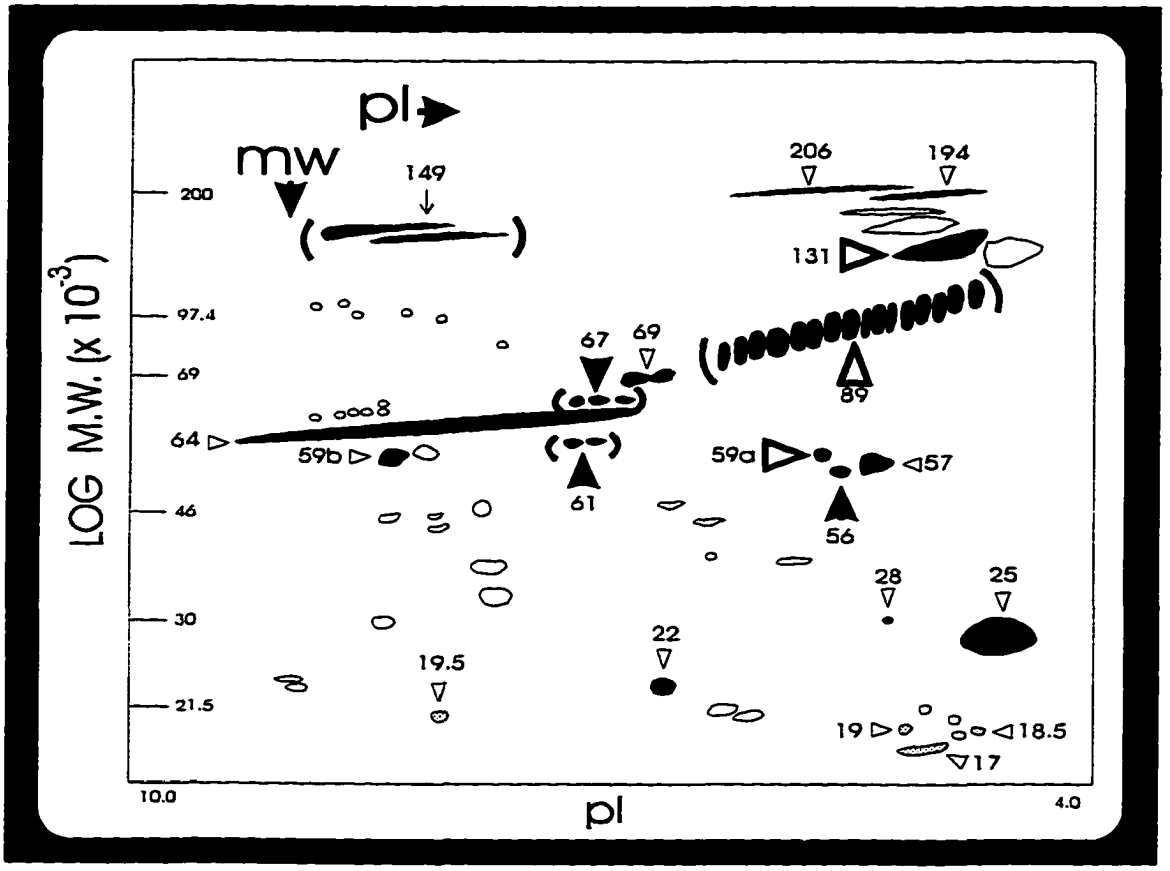

FIGURE 40. Diagrammatic 2D map of labeled FT proteins summarizing the fluorographic positions of the six FT protein classes. Class 1 proteins (solid spots with small arrowheads), class 2 (large open arrowheads), class 3 (arrow), class 4 (large solid arrowhead), class 5 (light grey spots), class 6 (dark gray spot). abbreviations: M.W.(mw), molecular weight; pI, isoelectric point.

Table 3.

Classes of FT proteins.

Class	Name	Characteristics	Special Features
1	25, 28, 57, 59b 64, 69, 194, 206	Found in both axon and terminal	——
2	59a, 89, 131	Displayed transient behavior	Mostly High MW
3	149	Abundance increased at 24 hr in OT	High MW basic
4	56, 61, 67	Displayed delayed behavior	——
5	17, 18.5, 19, 19.5	Preferentially destined to terminal	Mostly low MW acidic
6	22	Preferentially deposited in axon	——

Summary of the characterized FT proteins.

proteins, such as classes 1 and 5. However, the activity observed in other FT proteins, such as class 4 proteins, could not be explained solely by slow turn-over time. The relative abundance of these FT proteins increased from 4 to 48 hr PIL even though CPM result of the total FT population did not show a similar increase. The CPM result of the total FT population was highest at 24 hr PIL in both OT and SC compartments. This result agrees with previous findings reported by Garner and Mahler (61), whereby the abundance of newly synthesized FT proteins in the guinea pig SC peaked by 24 hr PIL. One explanation for such results could be the possibility that newly synthesized FT proteins continue to be released from the neuronal perikarya, even after the cessation of radioisotopic incorporation. The continuous release of FT proteins from the GA or a labeled storage pool, combined with different turnover kinetics, could yield increased, decreased, or steady-state levels of individual FT proteins. Therefore, the outcome of prolonged release of slowly turning-over proteins would be increased leveles of these proteins in axon and/or terminal regions for a period of time. Further, FT proteins that showed delayed release, such as class 4 proteins, suggest that these proteins could have been retained in the cell body before their release to the axon. Consistent with this view are reports that the somatic release of some synapsin I-like protein (62) and other unidentified FT proteins to axon and terminal regions in rabbit RGCs is delayed (71).

The imputed continuous release of labeled FT proteins would suggest that some FT proteins may enter a somal storage pool(s), from which they are slowly released, but fast-transported once they enter the axon, as previously suggested, but not characterized, by Berry (60) and Hammerschlag *et al.* (66). As illustrated in Figure 41, this suggested storage pool(s) may include proteins that show delayed release, such as class 4 proteins,

or prolonged release, such as class 1, 3, 5, and 6 proteins. Thus, at least three populations of FT organelles may be released from the soma into the axon. First, organelles that are initially routed from trans-Golgi into a storage pool and then released into the axon at a later time (delayed release). Second, organelles that are, in part, directly routed to a storage pool for delayed release and, in part, released immediately into the axon (prolonged release). Third, organelles that are immediately released into the axon without entering a storage pool (direct release). Among these organelles, there may exist a subpopulation of organelles that are destined to the axon, terminal, or both compartments of the neuron. Further studies are required to definitively determine the existence of such a somal pool and whether all FT proteins pass through the pool. Nevertheless, the existence of a somal pool would suggest a novel mechanism by which the amount and type of FT proteins entering the axon can be regulated independently of protein synthesis.

Since the existence of a somal storage pool is still speculative, other possiblities to explain continuous release may relay upon the mechanism of protein synthesis and sorting in the RER and TGN. Subcellular fractionation and electron microscopic autoradiograph (134, 171, 172) studies have revealed that in the first few minutes after exposure to radioisotope amino acids, radioactive proteins are associated with the RER. Within 10 minutes the proteins appear in the cis regions of the GA, and after an hour, most of the radioactivity is localized in vesicular organelles. Some radioactive proteins remain in RER/GA and have been detected at > 6 hours post-radiolabeling. As described earlier (see introduction) some of these proteins contain retention signals to remain as membrnae-bound or soluble luminal constituents of RER and GA. However,

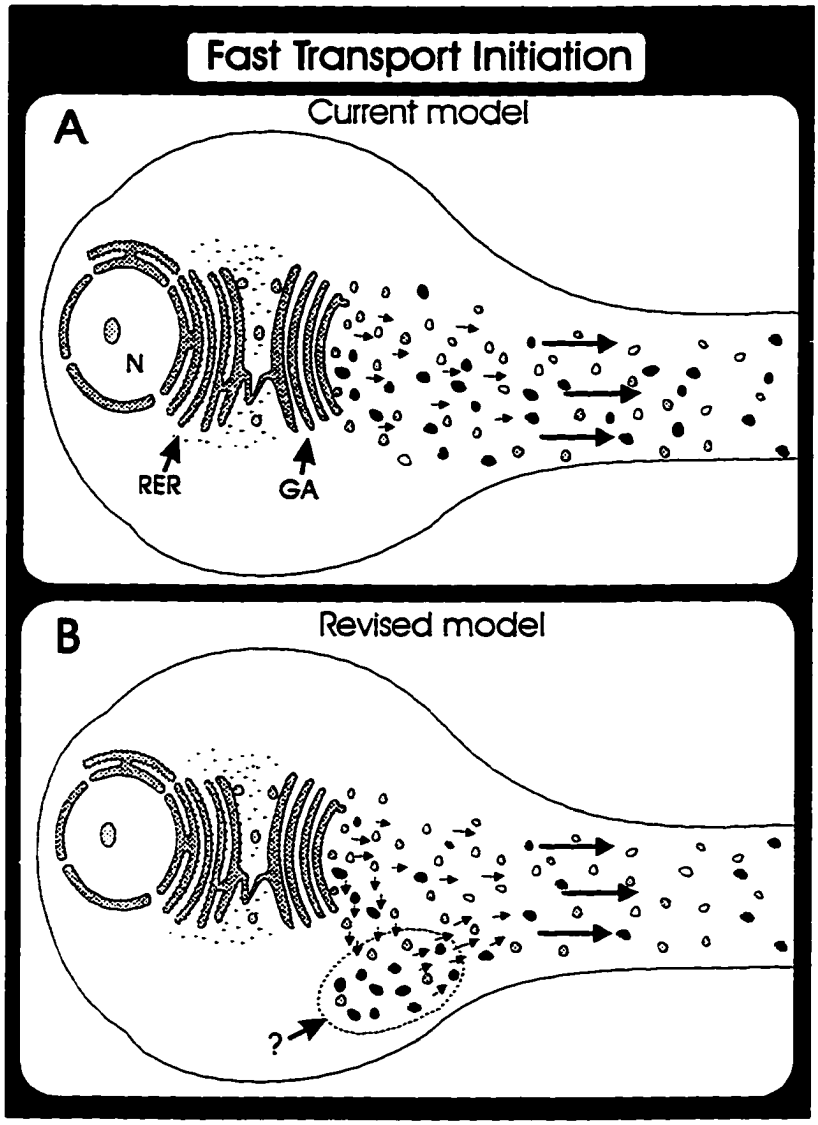

FIGURE 41. Models of FT initiation. (A) Current model of FT initiation - a direct translocation of FT vesicle from trans-Golgi into axon. (B) Proposed model based on results of the present study: (1) some FT vesicles, from the trans Golgi may go directly into the axon (open, light gray, and dark gray vesicles); (2) a second FT vesicle population, in addition to directly entering the axon, may enter storage pool(s) for slow release (light gray, and dark gray vesicles); (3) a third FT vesicle population may enter the storage pool directly with subsequent delayed release to the axon (solid vesicles). (?) indicates an uncharacterized storage pool.

there may exist some proteins that are retained temporaryly and then released from the GA at a later time. One hypothesis suggests that there is a selective retention of FT proteins in the RER/GA (13, 175, 176). The mechanisms by which this selective transient retention take place are yet to be elucidated. Nevertheless, such transient retention of protein in the RER/GA would provide similar effects as the somatic storage pool. Thus, the RER and GA may possess additional functions in the regulation of selective retention and release of some FT proteins.

Despite this latter possiblility of RER and GA protein storage, the existence of somal storage pool remains valid since studies have shown continueous release of some proteins from the soma to the axon after the ditruption of RER and GA events by pharmacological agents. Monensin, a Na^+ ionophore which interrupts intracellular traffic through the GA (36, 173); Co^{2+}, an antagonist of Ca^{2+}-mediated events (vesicle transfer from RER to GA and release of vesicles at the trans-GA) (60, 63, 173), brefeldin A, which disrupts the cis- and medial-GA (105), Fenfluramine, which affects phopholipid biosynthesis (19, 109), and cycloheximide, which inhibits proteins synthesis (174); are some of the agents that have been utilized to demonstrate continuous release of some FT proteins even after the disruption of RER/GA processes.

The transient presence of class 2 proteins may be the result of one of two possibilities. One possibility is that, soon after synthesis, these proteins could be quickly cleared from the neuronal perikarya to their axon and terminal compartments and rapidly (within 24 hr) degraded. A second possibility is that some of these proteins are diffusible FT proteins that are removed following exocytosis. This latter possibility is supported by evidence in the present study indicating that protein 59a of class 2 proteins was found

among the soluble proteins of the FT organelles destined for secretion. The other two transiently expressed proteins, proteins 89 and 131, were represented in the 2D fluorographs as multiple spots, each having a similar molecular weight but different isoelectric point. This type of appearance has been known to be a characteristic of glycoproteins in which variation in the number of sugar residues present on a given protein can slightly shift the isoelectric points (22). Most of these glycoproteins are also known to have molecular weights greater than 35 kDa (56).

The expression of class 5 proteins in the SC, but not in OT, at 24 and 48 hr PIL suggests that these low molecular weight (<20 kDa) acidic proteins were destined to terminal regions of the neuron. The 2D fluorograph positions of these proteins highly resemble that of the terminally destined FT proteins that contain sulfated tyrosine residues reported by Stone *et al.* (69, 77) and Huttner (127).

In contrast, the class 6 FT protein (protein 22) was found to be selectively labelled in nerve compartments suggesting axonal deposition of this protein. Protein 22 was the only one of the >90 resolved proteins that consistently displayed preferential localization in the axon. Radiolabeled FT protein 22 in SC was not significantly detected on 2D fluorographs at any time point. Morin *et al.* (71) have reported that the FT glucose transporters are preferentially destined to the axolemma. However, these glucose transporter subunits have molecular weights >45 kDa and, therefore, are unlikely to be protein 22 candidates. Other known axonally transported proteins, with similar molecular weights as protein 22, include the GTP-binding rab 3 proteins and the 23 kDa growth associated protein (GAP 23). Additional studies are necessary to further identify and evaluate protein 22.

Although the six classes of protein that were analyzed were regarded as anterogradely transported proteins, we can not exclude the possibility that any of the proteins could be retrogradely transported proteins. Reports have shown that some terminal proteins, known to have been moving anterogradely at some initial time, move retrogradely at a later time (167, 168, 169). Other retrogradely transported FT proteins may be transported as components of lysosomal, pinocytic, and endocytic vesicles. These retrogradely transported FT proteins may also undergo structural changes due to proteolytic events. Similarities and differences between newly synthesized anterograde and retrograde FT proteins at different time of post-labeling have been shown in one-dimensional electrophoretic studies by Bisby (155). However, further studies are required to elucidate differences between anterograde and retrograde FT proteins in two-dimensional fluorographic patterns.

C. FT PROTEIN COMPOSITION OF THE TRANSPORT ORGANELLES

Two- and one-dimensional fluorographic analysis of fractionated SC synaptosomal proteins was used to determine the vesicular packaging of FT proteins. The relationship of newly synthesized FT proteins with the translocated membrane organelles was examined by isolating synaptosomal fractions of pre-synaptic terminals of the SC. Previous light and electron microscopic autoradiographic studies have demonstrated that the majority of axonally transported radiolabeled materials delivered to the terminals remain within the pre-synaptic neuron (136, 137, 138, 139). Thus the majority of radiolabeled FT proteins are contained within the synaptosomal fractions. However, the

2D fluorographic patterns of the present study resolved only the major labeled FT protein.

Ultrastructural studies revealed the presence of predominantly small clear type vesicles in the SC synaptosomes. Dense-cored vesicles, which are known to carry secretory granules (30), were rarely seen. Small clear vesicles are known to be associated with secretory neurotransmitters such as γ-aminobutyric acid (GABA) and acetylcholine (31, 31).

In support of the ultrastructural evidence for predominantly small clear vesicles in SC synaptosomes, 1D and 2D fluorographs revealed that the majority of radiolabeled FT proteins were found as integral membrane, and not as secretory constituents, of synaptosomal fractions. The fluorographic results delineated only two FT proteins, proteins 57 and 59a, as vesicle-soluble radiolabeled proteins. However, it is possible that other soluble labeled FT proteins could have been lost during the rigorous fractionation processes. The two resolved soluble proteins could also have an additional peripheral membrane association with the vesicles, although this was not directly demonstrated.

The two imputed vesicle-soluble proteins belong to classes 1 and 2 of the newly synthesized FT proteins. The activity of the class 2 FT proteins decline precipitously in the pathway compartments from 4 to 24 hrs PIL. Given the apparent vesicular soluble characteristics of these proteins, one possible explanation for their rapid decline in specific activity, relative to other FT proteins, could be loss or turnover following vesicle exocytosis. In summary, the results of this second study suggest that the bulk of the major radiolabeled FT proteins are conveyed as integral membrane constituents of FT organelles, while very few species are transported as secretory or peripheral membrane

proteins.

D. SNAP-25: IMPLICATION OF POSSIBLE ASSOCIATIONS WITH FT AND SCb PROTEINS

The acid-precipitable CPM results showed SNAP-25 to be the most highly ^{35}S-methionine-labeled (>25% of the total FT labeling) FT protein. SNAP-25's prodigious incorporation of ^{35}S-methionine and its distinctive electrophoretic mobilities have been described in several mammalian neural systems including: the RGCs of rabbits (90, 91, 92, 145, 145), guinea pigs (146, 147), rats (93, 148, 149), and hamsters (150); the geniculocortical neurons of rats (151); spinal ganglion neurons of guinea pigs (152); auditory neurons of guinea pigs (152); nigrostriatal neurons of rats (151); vagus nerve of rabbits (153) and guinea pigs (154); hypoglossal nerve of rabbits (153); ventral horn motor neurons of rats (155); dorsal root ganglion cells of rats (156, 157) and hippocampal neurons of mice (158). Its abundance has been indicated in both axons and terminal regions (91, 93, 145, 151). In the present study, results showed that SNAP-25 was a class 1 FT protein with a similar distribution in axons and pre-synaptic terminal compartments.

Previous fractionation studies have attributed a role for SNAP-25 in vesicular docking and fusion at pre-synaptic terminals. This role is believed to be mediated by SNAP-25's association and interaction with syntaxin, v-SNARES, NSF, and the cytosolic SNAP family (see introduction). The results of the present study provided evidence that SNAP-25 was differentially associated with FT and SCb proteins both in the axon and

terminal regions. FT proteins CO-IP with SNAP-25 in the axon were similar to FT proteins CO-IP in the pre-synaptic terminal region. Among the four resolved FT proteins that CO-IP with SNAP 25, the putative SNAP-25 band was observed along with another CO-IP protein band which displayed a molecular weight (M_r ~18 kDa) similar to synaptobrevin (159). However, the other CO-IP protein bands displayed molecular weights (M_rs ~8 kDa and ~16 kDa) unlike other known SNAP-25 associated proteins. The t-SNARE protein, syntaxin (36 kDa) (160), the v-SNARE protein synaptotagmin (65 kDa) (161), the small GTP binding protein, rab 3A protein (23 kDa) (162, 163), or the N-ethylmaleimide (NEM)-sensitive factor (NSF) (76 kDa) (80, 164), which are all believed to be associated with SNAP-25, were not detected.

Several reasons could account for the inability to detect these proteins. First, the amino acid composition of some of these proteins may not bear enough methionine residues to allow fluorographic detection. Second, some of the aforementioned proteins might not be fast transported. Third, since neurotransmission at pre-synaptic terminals may involve transient interactions between proteins, FT protein association with SNAP-25 at the pre-synaptic terminals may be a function of neural activity. Fourth, binding of antibody to SNAP-25 during IP may have produced conformational changes which release some of the associated proteins. Finally, the antibody may have recognized a SNAP-25 epitope that was already occupied by another SNAP-25 associated protein such as syntaxin. Since the site that the antibody binds to SNAP-25 protein was already taken, CO-IP of syntaxin with the SNAP-25 antibody might not be facilitated.

The results of SCb proteins CO-IP with SNAP-25 revealed compartment-specific

SCb associations with SNAP-25. One-D fluorographs revealed that, while some of the CO-IP SCb proteins in axons displayed similarities with those CO-IP SCb proteins in terminals, others did not. Apparent differences were noticed between two of the five resolved proteins (M_rs ~33 kDa and ~53 kDa) in axons and one of the four resolved proteins (M_r ~18) in terminals. No studies have reported an association of SNAP-25 with SCb proteins or other slow transported proteins. However, a family of cytosolic proteins known as NSF attachment proteins (SNAPs), which may be conveyed by slow transport, are believed to have indirect associations with SNAP-25 at pre-synaptic terminals (165). The α-SNAP (35 kDa), ß-SNAP (36 kDa), γ-SNAP (39 kDa) and NSF complex are known to play a major role in the mechanism of synaptic vesicle fusion (80, 166). The type of association, direct or indirect, of SNAP-25 with either FT or SCb proteins is not known.

Further results showed the association of SNAP-25 with the subsets of FT and SCb proteins was ATP-independent. The presence of exogenous ATP during IP did not effect the CO-IP results.

The current model of transport envisions SNAP-25 as a terminally-bound protein conveyed as a component of FT vesicles (Figure 42). The axonal distribution of SNAP-25, observed in previous studies, was interpreted as terminally-bound species in transit. As a t-SNARE protein, SNAP-25 becomes incorporated into the cell surface membrane at the terminal. The result of the present study suggest that some SNAP-25 may be delivered to axolemma rather than the pre-synaptic terminal. Thus, in this model, SNAP-25 may be deposited in the axon. Stationary SNAP-25 might then interact with FT and SCb proteins in its role as a t-SNARE. Alternatively, SNAP-25 may

interact with other FT and SCb proteins during its axonal transport and at pre-synaptic terminals (Figure 43). However, the association of SNAP-25 with terminal SCb proteins may be different from those of axonal SCb proteins. The results of the present study suggest that SNAP-25's associations with other proteins may be more extensive than previously realized.

E. CONTINUED STUDIES

It was observed that the majority of the resolved FT proteins appeared to be targeted to both axon and terminal regions. Whether the presence of these proteins in axons was a result of their prolonged release from the neuronal perikarya or a result of protein deposition is not known. Investigation is underway to differentiate those FT proteins that are deposited in axons from those that are destined to pre-synaptic terminals. The strategy for such studies is to dissociate the RGC soma from the nerve and terminal regions by an ON cut thereby preventing continuous flow of protein from the cell body to the axon. At various times PIL, the axons of the RGCs will be cut *in vivo* at the optic nerve and transport will be allowed to continue for sometime so that terminally bound FT proteins in the cut nerve distal to the cell body will reach their destinations (144, 169, 170). Since, in the distal nerve no more FT proteins are coming from the cell body FT proteins destined for pre-synaptic terminals will be cleared from the nerve at the rate of fast transport. Electrophoretic evaluation of the label kinetics in the distal region will allow a better differentiation of FT proteins deposited in axons and FT proteins destined for terminals.

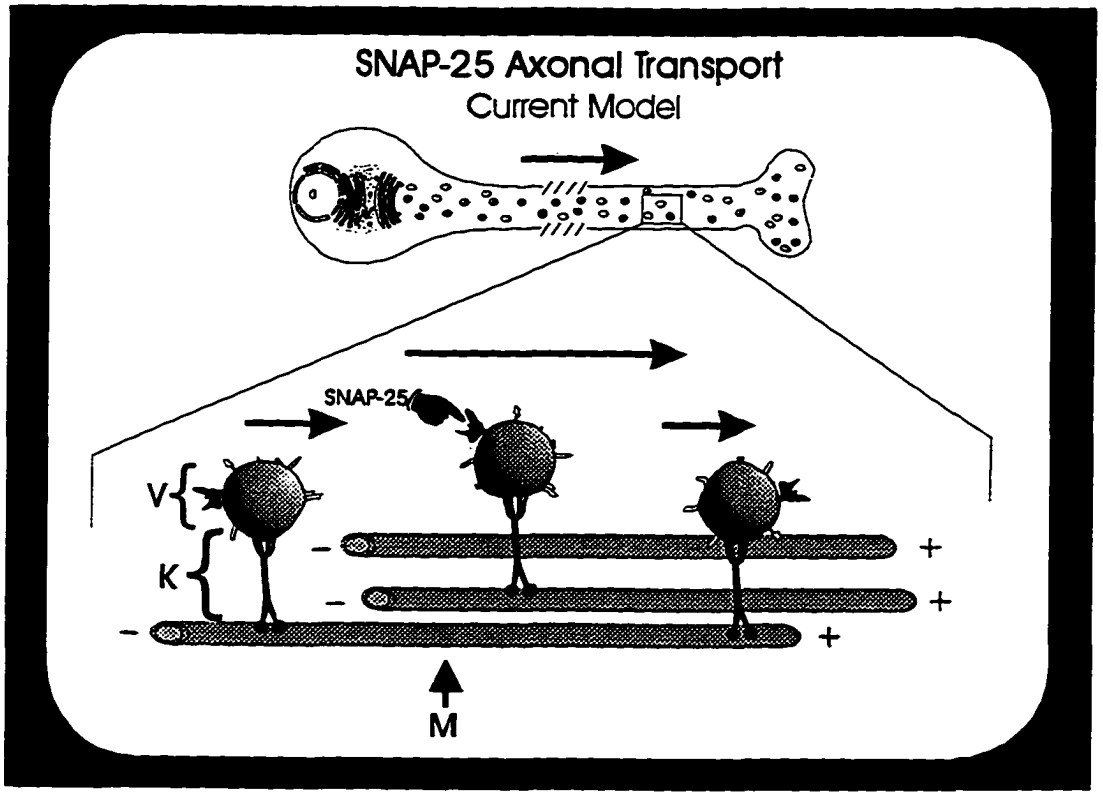

FIGURE 42. Current model of SNAP-25 transport. SNAP-25 is transported on the outside of vesicles, anchored to the vesicular membrane by palmitoyl side chains attached to four tandem cysteine residues. Vesicles (V) are conveyed by the motor protein kinesin (K) on slower moving microtubules (M). Vesicles containing SNAP-25 are delivered to pre-synaptic terminal.

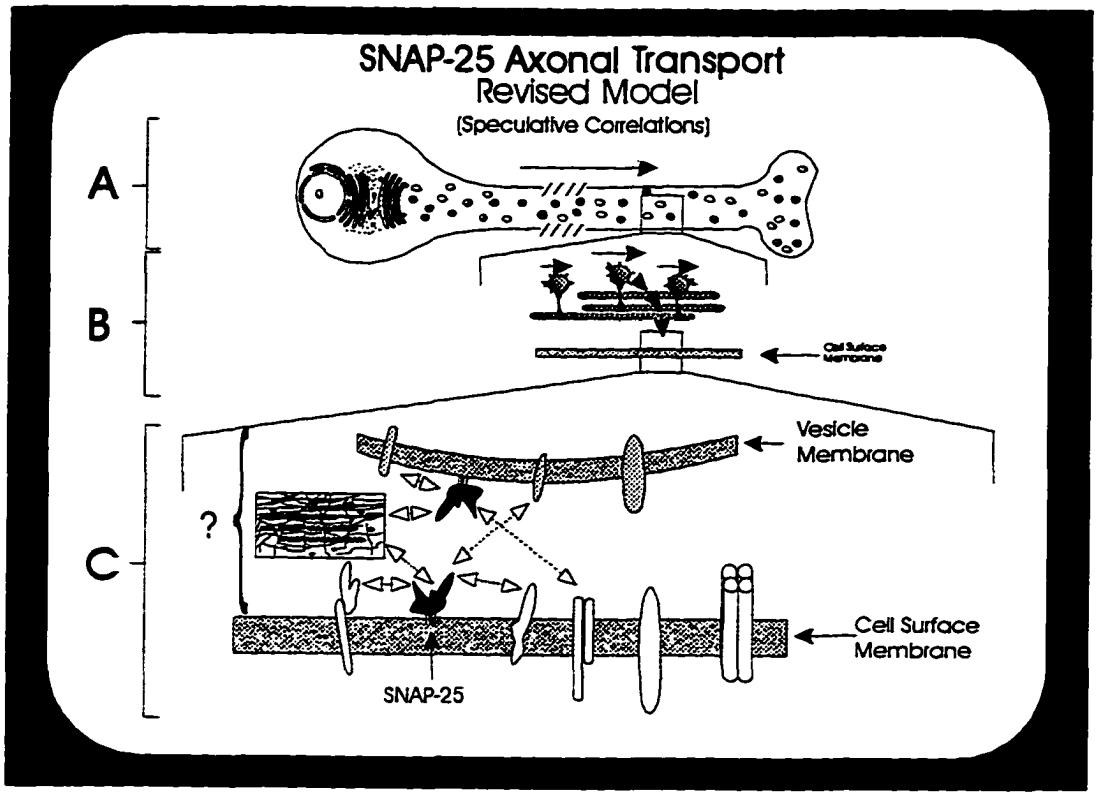

FIGURE 43. Revised model of SNAP-25 transport. During axonal transport (A), some of the vesicles containing SNAP-25 may be dropped off in the axon for incorporation into the axolemma (B). There, they may associate with other FT vesicle, proteins, or cell surface membrane proteins, or cytosolic (SCb) proteins (rectangular image) (C). Also, vesicle bound SNAP-25 may associate with the cytosolic (SCb) or other FT proteins during transit (C). Similar events may exist in the pre-synaptic terminal.

CHAPTER V

SUMMARY

The objective of this study was to understand further the trafficking of the fast axonally transported proteins. By using the mammalian optic pathway as a model system , the fast transported (FT) proteins were characterized in order to illustrate further their transport initiation, packaging, kinetics, compartmentation, and intermolecular associations along the transport pathway. The specific aims of this study were to: (1) determine the compartmental distribution and kinetics of FT proteins; (2) characterize the organization of FT proteins in the membranous transport vectors; and (3) investigate intermolecular associations of the fast transported 25 kDa synaptosomal-associated protein (SNAP-25) during transport.

1. To address the first aim, the retinal ganglion cell (RGC) proteins of the adult rat were radiolabeled, *in vivo*, by intraocular injection of ^{35}S-methionine in the vitreous chamber of the eye. Tissues comprising the major axons and terminals of the optic pathway were removed at different times post-labeling. By using 2D-SDS-PAGE and fluorography, two-dimensional maps were obtained representing radiolabeled proteins along the optic pathway. From quantitative and qualitative analyses of these 2D maps, the following questions were addressed: (a) what is the relative abundance of proteins in one compartment vs. another (i.e., do any of the FT-proteins exhibit preferential localization in the axon or the terminal?); and (b) what are the kinetics (turn-over, increased/decreased activity as transport time increases) of individual FT proteins in the optic pathway?

2. To address the second aim, RGCs were radiolabeled and FT proteins were allowed to reach the pre-synaptic terminals in the superior colliculus (SC). The synaptosomal fractions from the SC were prepared and FT proteins partitioned into integral, peripheral, and soluble components. From 1D and 2D fluorographic analyses of the FT protein partitioning, the packaging of FT proteins as constituents of membranous organelles was elucidated.

3. To accomplish the third aim, RGCs were radiolabeled and nerve (optic nerve, optic tract), and terminal (SC) tissues of the otpic pathway were removed four hours and twelve days PIL. Tissue homogenates were immunoprecipitated with SNAP-25 antibodies and electrophoretically analyzed. Co-immunoprecipitated proteins from four hours and twelve days PIL allowed the determination of SNAP-25 association with other FT proteins and slow transported (SCb) proteins, respectively.

Localization behavior of twenty individual FT proteins in tissues containing the major axons and terminals of the optic system were determined. Spatial and temporal examination of these proteins revealed six classes of FT proteins which displayed distinctive trafficking behavior: class 1 proteins (n=7) were found in both compartments (axon and terminal) with little or no differences in their specific activity; class 2 proteins (n=4) showed transient activity or gradual decrease over a period of time (48 hrs) in all compartments; class 3 proteins (n=1) showed increased activity in the optic tract at 24 hr PIL; class 4 proteins (n=3) displayed a delayed appearance, with increased activity as transport time extended; class 5 proteins (n=4) demonstrated preferential localization to pre-synaptic terminal regions; and a class 6 protein (n=1) was preferentially localized in the axon region. These kinetics in class 5 and 6 FT proteins would be expected of FT

proteins which bear signals for specific localization. The delayed appearance of class 4 proteins may reflect a delayed release of these proteins from the neuronal perikarya. The increased activity, with greater post-labeling time observed in classes 4, 5, and 6 proteins, may indicate prolonged release of these proteins from a fast transport storage pool in the neuronal perikarya.

The majority of FT proteins were found to be conveyed as integral membrane constituents of transported organelles while two FT proteins were transported as soluble components of the organelles. Further analysis appeared to indicate that one of the soluble proteins could be destined for secretion.

Two-dimensional electrophoretic analyses revealed that SNAP-25 was the major ^{35}S-methionine-labeled FT protein in the adult rat optic pathway. Immunoprecipitation studies results provided evidence that SNAP-25 may have associations with other FT and SCb proteins in axon and terminal regions. While differential association of SNAP-25 with SCb proteins between axon and terminal regions was observed, its association with FT proteins in these regions seemed to be similar. These results suggest that SNAP-25 may have significant intermolecular association both in the axon and at pre-synaptic terminals.

In summary, the FT proteins in the regions containing the major axonal and terminal components of the rat optic pathway displayed heterogenous transport initiation, kinetics, compartmentation, and intermolecular association. Since axons lack sorting organelles (e.g., Golgi), these results indicate that neurons may have evolved complex mechanisms for differential delivery of FT proteins from the perikarya.

LIST OF ABBREVIATIONS

1D	One dimensional
2D	Two dimensional
CI	Co-immunoprecipitates
CO-IP	CO-immunoprecipitated
Ci	Curie
FT	Fast transported
GA	Golgi apparatus
GAP	Growth associated protein
IEF	Isoelectric focusing
II	Integrated Intensity
IP	Immunoprecipitation
LGN	Lateral geniculate nucleus
NIH	National Institute of Health
NSF	N-ethylmaleimide-sensitive factor
ON	Optic nerve
OT	Optic tract
PIL	Post intra-ocular labeling
RER	Rough endoplasmic reticulum
RGC	Retinal ganglion cell
RT	Retrograde transport
SC	Superior colliculus
SCa	Slow component a
SCb	Slow component b
SD	Standard deviation
SDS-PAGE	Sodium dodecyl sulfate polyacrylamide gel electrophoresis
SNAP	Soluble NSF attachment protein
SNAP-25	Synaptosomal associated protein of 25 kDa
SNARE	Synaptic vesicle receptor
TCA	Tricarboxylic acid
TGN	Trans-Golgi network
kDa	Kilo Dalton
pI	Isoelectric point
t-SNARE	Target SNARE
v-SNARE	Vesicle SNARE

LIST OF REFERENCES

1. Kandel, R. E., J. H. Schwartz, and T. M. Jessel. 1991. Nerve cells and behavior. In Principals of Neuroscience. Elsevier, New York. 18-25.

2. Martinez, P. F. A. 1982. Neuroanatomy: Development and structure of the central nervous system. Saunders. Philadelphia.

3. Valee, R. B., and G. S. Bloom. 1991. Mechanism of fast and slow axonal transport. *Annu. Rev. Neurosci.* **14**:59-92.

4. Moore, H-P. H, L. Orci, and G. F. Oster. 1988. Biogenesis of secretory vesicles. In Protein Transfer and Organelle Biogenesis. Academic Press, San Diago. 521-561.

5. Shwartz, A. L. 1990. Cell biology of intracellular protein trafficking. *Annu. Rev. Immunol.* **8**:195-229.

6. Munro, S., and H. R. B. Pelham. 1987. A C-terminal signal prevents secretions of luminal ER proteins. *Cell.* **48**:899-907.

7. Teichberg, S., and E. Holtzman. 1973. Axonal agranular reticulum and synaptic vesicles in culture embryonic chick sympathetic neurons. *J. Cell Biol.* **57**:88-108.

8. Moore, D. J., T. W. Keenan, and C. M. Huang. 1974. Membrane flow and differentiation: Origin of Golgi apparatus from endoplasmic reticulum. *Adv. Cytopharm.* **2**:107-125.

9. Lindsey, J. D., and M. H. Ellison. 1983. The varicose tubule: A direct connection between rough endoplasmic reticulum and the Golgi apparatus. *J. Cell. Biol.* **97**:304a

10. Hirschberg, C. B., and M. D. Snider. 1987. Topography of glycosylation in the rough endoplasmic reticulum and Golgi apparatus. *Ann. Rev. Biochem.* **56**:63-87.

11. Kandel, R. E., J. H. Schwartz, and T. M. Jessel. 1991. Synthesis and trafficking of neuronal proteins. In Principals of Neuroscience. Elsevier, New York. 49-65.

12. Tartkoff, A., and P. Vassalli. 1978. Comparative studies of intracellular transport of secretory proteins. *J. Cell Biol.* **79**:694-707.

13. Burgess, L., and R. Kelly. 1987. Constitutive and regulated secretion of proteins. *Annu. Rev. Cell Biol.* **3**:243-294.

14. Vale, R. D., T. S. Reese, and M. P. Sheetz. 1985. Identification of a novel force-generating protein, kinesin, involved in microtubule-based motility. *Cell.* **42**:39-50.

15. Vale, R. 1987. Intracellular transport using microtubule-based motors. *Annu. Rev. Cell. Biol.* **3**:317-378.

16. Valee, R. B., and G. S. Boom. 1991. Mechanism of fast and slow axonal transport. *Annu. Rev. Neurosci.* **14**:59-92.

17. Noda, Y., R. Sato-Yoshitake, S. Kondo, M. Nangaku, and N. Hirokawa. 1995. KIF2 is a new microtubule-based anterograde motor that transport membranous organelles distinct from those carried by kinesin heavy chain or KIF3A/B. *J. Cell Biol.* **129**:157-167.

18. Okada, Y., H. Yamazaki, Y. Sekine-Aizawa, and N. Hirokawa. 1995. The neuron-specific kinesin superfamily protein KIF1A is a unique monomeric motor for anterograde axonal transport of synaptic vesicle precursors. *Cell.* **81**:769-780.

19. Hammerschlag, R. 1983. How do neuronal proteins know where they are going? Speculations on the role of molecular address markers. *Dev. Neurosci.* **6**:2-17.

20. Grafstein, B., and D. S. Forman. 1980. Intracellular transport in neurons. *Physiol. Rev.* **60**:1167-1282.

21. Lasek, R. J., J. A. Garner, and S. T. Brady. 1984. Axonal transport of cytoplasmic matrix. *J. Cell. Biol.* **99**:212-221.

22. Hoffman, P. N., and R. J. Lasek. 1975. The slow component of axonal transport: identification of major structural polypeptides and their generality among mammalian neuron. *J. Cell Biol.* **66**:351-366.

23. Brady, S. T., and R. J. Lasek. 1981. Nerve specific enolase and creatine phosphokinase in axonal transport: soluble proteins and the axoplasmic matrix. *Cell.* **23**:515-523.

24. Ellisman, M. H., and J. D. Lindsey. 1983. The axoplasmic reticulum within myelinated axons is not transported rapidly. *J. Neurocytol.* **12**:393-411.

25. Smith, R. S. 1980. The short term accumulation of axonally transported organelles in the region of localized lesion of single myelinated axons. *J. Neurocytol.* **9**:39-65.

26. Tsukita, S., and H. Ishikawa. 1980. The movement of membranous organelles in axons. Electron microscopic identification of anterogradely and retrogradely transported organelles. *J. Cell Biol.* **84**:513-530.

27. Smith, R. S., and R. E. Snyder. 1992. Relationships between the rapid axonal

transport of newly synthesized proteins and membranous organelles. *Mol. Neurobiol.* **6**:285-300.

28. Kelly, R. B., and E. Grote. 1993. Protein targeting in the neuron. *Annu. Rev. Neurosci.* **16**:95-127.

29. Chwo, R. H., and L. Von Rudin. 1992. Delay in vesicle fusion revealed by electrochemical monitoring of single secretory events in adrenal chromaffin cells. *Nature.* **356**:60-63.

30. De Camilli, P., and R. Jahn. 1990. Pathways to regulated exocytosis in neurons. *Annu. Rev. Physiol.* **52**:625-645.

31. Kelly, R. B., and E. Grote. 1993. Protein targeting in the neuron. *Annu. Rev. Neurosci.* **16**:95-127.

32. Thureson-Klein, A. K., and R. L. Klein. 1990. Exocytosis from neuronal large dense-cored vesicles. *Int. Rev. Cyto.* **121**:1215-1227.

33. Droz, B., and H. L. Koeng. 1970. Localization of proteins metabolism in neurons. In Lajtha, Protein metabolism of the nervous system. Plenum press, New York. 93-108.

34. Grafstein, B., and D. S. Forman. 1980. Intracellular transport in neurons. *Physiol. Rev.* **60**:1167-1283.

35. Hammerschlag, R., and G. C. Stone. 1982. Membrane delivery by fast axonal transport. *Trends Neurosci.* **5**:12-15.

36. Hammerschlag, R., G. C. Stone, F. A. Bolen, J. D. Lindsey, and M. H. Ellisman. 1982. Evidence that all newly synthesized proteins destined for fast transport pass through the Golgi apparatus. *J. Cell. Biol.* **93**:568-575.

37. Sabatini, D. D., G. Kreibich, T. Morimoto, and M. Adesnik. 1982. Mechanisms for the incorporation of protein in membrane and organelles. *J. Cell Biol.* **92**:1-22.

38. Blobel, G. 1982. Regulation of intracellular protein trafficking. *Harvey Lect.* **76**:125-147.

39. Devillers-Thiery, A., T. Kindt, G. Scheele, and G. Blodel. 1975. Homology in amino terminal sequence of precursors to pancreatic secretory proteins. *Proc. Natl. Acd. Sci. U. S. A.* **72**:5016-5020.

40. Kemper, B., J. F. Habener, R. C. Mulligan, J. T. Potts, and A. Rich. 1974. Preparathyroid hormone: a direct translation product of parathyroid messenger RNA. *Proc. Natl. Acd. Sci. U. S. A.* **71**:3731-3735.

41. Milstein, C., G. G. Brownlee, T. M. Harrison, and M. B. Mathews. 1972. A possible precursor of immunoglobulin light chains. *Nature New Biol.* **239**:117-120.

42. Swan, D., H. Aviv, and P. Leder. 1972. Purification and properties of biologically active messenger RNA for a myeloma light chain. *Proc. Natl. Acd. Sci. U. S. A.* **69**:1967-1971.

43. Blobel, G. 1980. Intracellular protein topogenesis. *Proc. Natl. Acd. Sci. U. S. A.* **77**:1496-1500.

44. Tomita, M., and V. T. Marchesi. 1975. Amino-acids sequences and oligosaccharide attachment sites of human erythrocyte glycophorin. *Proc. Natl. Acd. Sci. U. S. A.* **72**:2964-2968.

45. Lingappa, V. R., J. R. Lingappa, R. Prasad, K. E. Ebner, and G. Blobel. 1978. Coupled cell-free synthesis, segregation, and core glycosylation of secretory protein. *Proc. Natl. Acd. Sci. U. S. A.* **75**:2338-2342.

46. Fleischer, B. 1981. Orientation of glycoprotein galactosyl-transferase and sialyl-transferase enzymes in vesicles derived from rat liver Golgi apparatus. *J. Cell Biol.* **89**:246-255.

47. Hirano, H., B. Parkhouse, G. L. Nicolson, S. Lennox, and S. J. Singer. 1972. Distribution of saccharide residues on membrane fragments form a myeloma-cell homogenate: its implication for membrane biogenesis. *Proc. Natl. Acd. Sci. U. S. A.* **69**:2945-2949.

48. Tartakoff, A., and P. Vassalli. 1979. Plasma cell immunoglobulin M molecules. Their biosynthesis, assembly and intracellular transport. *J. Cell Biol.* **83**:284-299.

49. Tartakoff, A., and P. Vassalli. 1978. Comparative studies of intracellular transport of secretory proteins. *J. Cell Biol.* **79**:694-707.

50. Townsend, L. E., and J. A. Benjamins. 1983. Effects of monensin on posttranslation processing of myelin proteins. *J. Neurochem.* **40**:1333-1339.

51. Allen, R. D., J. Metuzals, I. Tasaki, S. T. Brady, and S. P. Gilbert. 1982. Fast axonal transport in squid giant axon. *Science.* **218**:1127-1129.

52. Brady, S. T., R. J. Lasek, and R. D. Allen. 1982. Fast axonal transport in extruded axoplasm from squid giant axon. *Science.* **218**:1129-1131.

53. Fahim, M. A., R. J. Lasek, S. T. Brady, and A. J. Hodge. 1985. AVEC-DIC and electron microscopic analyses of axonally transported particles in cold-blocked squid giant axons. *J. Neurocytol.* **14**:689-704.

54. Olden, K., J. B. Parent, and S. L. White. 1982. Carbohydrate moieties of glycoproteins: a re-evaluation of their function. *Biochem. Biophys. Acta.* **650**:209-232.

55. Waechter, C. J., J. W. Schmidt, and W. A. Catterall. 1983. Glycosylation is required for maintenance of functional sodium channels in neuroblastoma cells. *J. Biol. Chem.* **258**:5117-5123.

56. Stone, G. C., and R. Hammerschlag. 1983. Glycosylation as a criterion for defining subpopulation of fast transported proteins. *J. Neurochem.* **40**:1124-1133.

57. Elam, J. S. 1979. Axonal transport of complex carbohydrates. In Complex Carbohydrates of Nervous Tissue. Plenum Press. New York. 235-252.

58. Haley, J. E., L. J. Tirri, and R. W. Ledeen. 1979. Axonal transport of lipids in the rabbit optic system. *J. Neurochem.* **32**:727-734.

59. Toews, A. D., J. F. Goodrum, and P. Morell. 1979. Axonal transport of phospholipids in the rat visual system. *J. Neurochem.* **32**:1165-1173.

60. Berry, R. W. 1980. Evidence of multiple somatic pools of individual axonally transported proteins. *J. Cell Biol.* **78**:379-385.

61. Garner, J. A., and H. R. Mahler. 1987. Biogenesis of presynaptic terminal proteins. *J. Neurochem.* **49**:905-915.

62. Loewy, A., W-S. Liu, C. Baitinger, and M. B. Willard. 1991. The major ^{35}S-methionine-labeled rapidly transported (superprotein) is identical to SNAP-25, a protein of synaptic terminals. *J. Neurosci.* **11**: 3412-3421.

63. Goodrum, J. F., and P. Morell. 1982. Axonal transport, deposition, and metabolic turnover of glycoproteins in the rat optic pathway. *J. Neurochem.* **38**:696-704.

64. Navon, F., P. Greengard, and P. De Camilli. 1984. Synapsin I in nerve terminals: Selective association with small synaptic vesicle. *Science* **226**:1209-1211.

65. Lariviere, L., and P. A. Lavoie. 1982. Calcium requirement for fast axonal transport in frog motoneurons. *J. Neurochem.* **39**:882-886.

66. Hammerschlag, R., F. A. Bolen, and R. C. Carlsen. 1983. Accumulation of fast transported AChE and adenylate cyclase at a nerve ligature is unaffected by conditions that inhibit accumulation of the ^{3}H-protein. *Soc. Neurosci. Abst.* **9**:149.

67. Cancalon, P., and I. M. Beidler. 1977. Difference in the composition of the polypeptides deposited in the axon and the nerve terminals by fast axonal transport in the garfish olfactory nerve. *Brain Res.* **121**:215-227.

68. Weiss, D. G., V. Krygier-Brevart, G. W. Gross, and G. W. Kreutzberg. 1978. Rapid axoplasmic transport in the olfactory nerve of the pike. II. Analysis of proteins by SDS gel electrophoresis. *Brain Res.* **139**:77-87.

69. Stone, G. C., R. Hammerschlag, and J. A. Bobinski. 1983. Differential delivery of sulfated proteins by fast axonal transport. *Soc. Neurosci. Abst.* **9**:149.

70. Huttner, W. B., and R. W. H. Lee. 1982. Protein sulfation on tyrosine residues. *J. Cell Biol.* **95**:389a.

71. Morin, P. J., N. Liu, R. J. Johonson, S. E. Leeman, and R. E. Fine, 1991. Isolation and characterization of rapid transport vesicle subtypes from rabbit optic nerve. *J. Neruochem.* **56**:335-341.

72. Kelly, R. B. 1993. Storage and release of neurotransmitters. *Cell.* **72**:43-53.

73. Jahn, R., and T. C. Südhof. 1994. Synaptic vesicles and exocytosis. *Annu. Rev. Neurosci.* **17**:219-246.

74. Schweizer, F. E., H. Betz, and G. J. Augustine. 1995. From vesicle docking to endocytosis: Intermediate reaction of exocytosis. *Neuron.* **14**:689-696.

75. Südhof, T. C., and R. Jahn. 1991. Proteins of synaptic vesicles involved in exocytosis and membrane recycling. *Neuron.* **6**:665-677.

76. Bennet, M. K, and R. H. Scheller. 1994. A molecular description of synaptic vesicles membrane trafficking. *Annu. Rev. Biochem.* **63**:63-100.

77. Stone, G. C., R. Hammerschlag, and J. A. Bobinski. 1983. Fast-transported glycoproteins and nonglycosylated proteins contain sulfate. *J. Neurochem.* **41**:1085-1089.

78. Lee, R. W., and W. B. Huttner. 1983. Tyrosine-o-sulfate proteins of PC12 pheochromocytoma cells and their sulfation by a tyrosylprotein sulfotransferase. *J. Biol. Chem.* **258**:11326-11334.

79. Söllner, T., S. W. Whiteheart, M. Brunner, H. Erdjument-Bromage, S. Geromanos, P. Tempst, and J. E. Rothman. 1993. SNAP receptors implicated in vesicle targeting and fusion. *Nature.* **362**:318-324.

80. Söllner, T., M. K. Bennett, S. W. Whitheart, R. H. Scheller, and J. E. Rothman. 1993. Protein assembly-disassembly pathway *in vitro* that may correspond to sequential steps by synaptic vesicle docking, activation, and fusion. *Cell.* **75**:409-418.

81. Huttner, W. B. 1993. Snappy exocytoxins [News; Comment]. *Nature.* **365**:104-105.

82. Montecucco, C., and G. Schiavo. 1994. Mechanism of action of tetanus and botulinum neurotoxins. *Mol. Microbiol.* **13**:1-8.

83. Foran, P., G. W. Lawrence, C. C. Shone, K. A. Foster, and J. O. Dolly. 1996. Botulinum neurotoxin C1 cleaves both syntaxin and SNAP-25 in intact and permeabilized chromaffin cells: Correlation with its blockade of catecholamine release. *Biochemistry.* **35**:2630-2636.

84. Schiavo, G., A. Santucci, B. R. Dasgupta, P. P. Mehta, J. Jontes, F. Benfenati, M. C. Wilson, and C. Montecucco. 1993. Botulinum neurotoxins serotypes A and E cleaves SNAP-25 at distinct COOH-terminal peptide bonds. *FEBS.* **335**:99-103.

85. Osen-Sand, A., M. Catsicas, J. K. Staple, K. A. Jones, G. Ayala, J. Knowles, G. Grennigloh, and S. Catscicas. 1993. Inhibition of axonal growth by SNAP-25 antisense oligonucleotides *in vitro* and *in vivo*. *Nature.* **364**:445-448.

86. Bark, I. C. 1993. Structure of the chicken gene for SNAP-25 reveals duplicated exons encoding distinct isoforms of the protein. *J. Mol. Biol.* **233**:67-76.

87. Bark, I. C., and M. C. Wilson. 1994. Regulated vesicular fusion in neurons: Snapping together the details. *Proc. Natl. Acad. Sci. U.S.A.* **91**:4621-5624.

88. Bark, I. C., K. M. Hahn, A. E. Raybinin, and M. C. Wilson. 1995. Differential expression of SNAP-25 protein isoforms during divergent vesicle fusion events of neural development. *Proc. Natl. Acad. Sci. U.S.A.* **92**: 1510-1514.

89. Boschert, U., C. O'Shaughnessy, R. Dickinson, M. Tessari, C. Bendotti, S. Catsicas, and E. M. Pich. 1996. Developmental and plasticity-related differential expression of two SNAP-25 isoforms in the rat brain. *J. Comp. Neurol.* **367**:177-193.

90. Willard, M., W. M. Cowan, and P. R. Vagelos. 1974. The polypeptide composition of intra-axonally transported proteins: evidence of four transport velocities. *Proc. Natl. Acad. Sci. U.S.A.* **71**:2183-2187.

91. Kelly, A., J. A. Wagner, and R. B. Kelly. 1980. Properties of individual nerve terminal proteins identified by two-dimensional gel electrophoresis. *Brain Res.* **185**:192-197.

92. Wagner, J. A., A. Schick-Kelly, and R. B. Kelly. 1979. Nerve terminal proteins of the rabbit visual relay nuclei identified by axonal transport and two-dimensional electrophoresis. *Brain Res.* **168**:97-117.

93. Hess, D. T., T. M. Slater, M. C. Wilson, and J. H. Pate Skene. 1992. The 25 kDa synaptosomal-associated protein SNAP-25 is the major methionine-rich in rapid axonal transport and a major substrate for palmitoylation in adult CNS. *J. Neurosci.* **12**:4634-4641.

94. Hess, E. J., K. A. Collins, and M. C. Wilson. 1996. Mouse model of hyperkinesis implicates SNAP-25 in behavioral regulation. *J. Neurosci.* **16**:3104-3111.

95. Hesyer, C. J., M. C. Wilson, and L. H. Gold. 1995. Coloboma hyperactive mutant exhibits delayed neurobehavioral developmental milestones. *Dev. Brain Res.* **89**:264-269.

96. Kang, C. M., P. A. Lavoie, and P. F. Gradiner. 1995. Chronic exercise increases SNAP-25 abundance in fast-transported proteins of rat motoneurones. *Neuroreport.* **6**:549-553.

97. Papasozomenos, S. C., L. Autilio-Gambetti, and P. Gambetti. 1983. Distribution of proteins migrating with the fast axonal transport. Their relationship to smooth

endoplasmic reticulum. *Brain Res.* **278**:232-235.

99. O'Farrell, P. H. 1975. High resolution two-dimensional electrophoresis of proteins. *J. Biol. Chem.* **250**:4007-4024.

100. Paxinos, G., and C. Watson. 1986. The rat brain in stereotaxic coordinates. Academic Press. Sydney.

101. Fujiki, Y., A. L. Hubbard, S. Fowler, an S., P. B. Lazarow. 1982. Isolation of intracellular membranes by means of sodium carbonate treatment: application of endoplasmic reticulum. *J. Cell. Biol.* **93**:97-102.

102. Garner, J. A. 1990. Cytoplasmic matrix proteins in central nervous system presynaptic terminals: turnover and effects of osmotic lysis. *Brain Res.* **526**:186-194.

103. Laemmli, U. K. 1970. Cleavage of structural proteins during the assembly of the head of bacteriophage T4. *Nature.* **27**:680-685.

104. Laskey, R. A., and A. D. Mills. 1975. Quantitative film detection of ^{3}H and ^{14}C in polyacrylamide gels by fluorography. *Eur. J. Biochem.* **56**:335-341.

105. Smith R. S., H. Chan H, and R. E. Snyder. 1991. Brefeldin A inhibits fast

axonal protein transport and disassembles Golgi Apparatus but does not diminish anterograde axonal vesicle transport. *Neurosci. Abst.* **17**:59.

106. Tooze, S. A., and W. Huttner. 1990. Cell-free protein sorting to the regulated and constitutive secretory pathways. *Cell.* **60**:837-847.

107. Baltinger, C., and M. Willard. 1987. Axonal transport of synapsin I-like proteins in rabbit retinal ganglion cells. *J. Neurosci.* **3**:2153-2163.

108. Jung, L. J., and R. H. Scheller. 1991. Peptide processing and targeting in the neuronal secretory pathway. *Science.* **251**:1330-1335.

109. Longo, F. M., and R. Hammerschlag. 1980. Relation of somal lipid synthesis to the fast axonal transport of protein and lipid. *Brain Res.* **193**:471-485.

110. Baitinger, C., J. Levine, T. Lorenz, C. Simon, P. Skene, and M. Willard. 1991. Characteristics of axonally transported proteins. In axoplasmic transport. Spring-Verlag, Berlin. 110-120.

111. Goodrum, J. F., P. and Morell. 1982. Axonal transport deposition, and metabolic turnover of glycoproteins in the rat optic pathway. *J. Neurochem.* **38**:696-704.

112. Toews, A. D., B. F. Saunders, and W. D. Blanker. 1983. Differences in the

kinetics of axonal transport for individual classes in rat sciatic nerve. *J. Neurochem.* **40**:555-562.

113. Towes, A. D., B. F. Saunders, and P. Morell. 1982. Axonal transport and metabolism of glycoproteins in rat sciatic nerve. *J. Neurochem.* **39**:1348-1355.

114. Stone, G. C., R. Hammerschlag, and J. A. Bobinski. 1984. Fast axonal transport of tyrosine sulfate containing proteins:preferentially routing of sulfoproteins toward nerve terminals. *Cell. Mol. Neurobiol.* **4**:249-262.

115. Rulli, R. D., and D. L. Wilson. 1987. Destination of some fast-transported proteins in sensory neurons of bullfrog sciatic nerve. *J. Neurochem.* **48**:134-140.

116. Gray, E. G., and V. P. Whittaker. 1960. The isolation of synaptic vesicles from the central nervous system. *J. Physiol.* **153**:35-37.

117. Gray, E. G., and V. P. Whittaker. 1962. The isolation of nerve endings from brain: An electron-microscopic study of cell fragments derived by homogenization and centrifugation. *J. Anat.* **96**:79-88.

118. Whittaker, V. P., I. A. Michaelson, and R. J. A. Kirkland. 1964. The separation of synaptic vesicles from nerve-ending particles (synaptosomes). *Biochem. J.* **90**:293-305.

119. Garner, J. A. 1990. Cytoplasmic matrix proteins in central nervous system presynaptic terminals: turnover and effects of osmotic lysis. *Brain Res.* **526**: 186-194.

120. Paxinos, G. 1985. Visual system. The Rat Nervous system - Forebrain and Midbrain. Academic Press, New York. **1**:169-221.

121. Jeffery, G., A. Cowey, and H. G. J. M. Kuypers. 1981. Bifurcating retinal ganglion cell axons in the rat demonstrated by retrograde double labelling. *Exp. Brain Res.* **44**:34-40.

122. Karlesson, J-O., and J. Sjöstrand. 1971. Synthesis, migration, and turnover of protein in retinal ganglion cells. *J. Neurochem.* **18**:749-767.

123. Hodge, A. J., and W. J. Adelman. 1980. The neuroplasmic network in Loligo and Hermissenda neurons. *J. Ultrastruct. Res.* **70**:220-241.

124. Dreher, B., S. J. Sefton, S. Y. K. Ni, and G. Nisbett. 1985. The morphology, number and distribution of class I cells in the retina of the albino and hooded rat. *Brain Behav. Evol.* **26**:10-48.

125. Munoz-Martinez, F. J., R. Nunez, and A. Sanderson. 1981. Axonal transport: a qualitative study of retained and transported protein fractions in the cat. *J. Neurobiol.* **12**:15-26.

126. Brimijoin S., J. M. Lundberg, E. Brodin, T. Hökflet, and G. Nilsson. 1980. Axonal transport of substance P in the vagus and sciatic nerves of the guinea pig. *Brain Res.* **191**:443-357.

127. Huttner, W. B. 1982. Sulphation of tyrosine residue: a widespread modification of proteins. *Nature.* **299**:273-276.

128. Linden, R., and V. H. Perry. 1983. Massive retinotectal projection in rats. *Brain Res.* **272**:145-149.

129. Fukuda, Y., T. Sugimoto, and T. Shirokawa. 1982. Strain differences in quantitative analysis of the rat optic nerve. *Exp. Neurol.* **75**:525-532.

130. Lam, K., A. J. Sefton, and M. R. Bennett. 1982. Loss of axons from the optic nerve of the rat during early development. *Dev. Brain Res.* **3**:487-491.

131. Sefton, A. J. 1968. The innervation of the lateral geniculate nucleus and anterior colliculus in the rat. *Vision Res.* **8**:867-881.

132. Hughes, A. 1977. The pigmented rat optic nerve: Fibre count and fibre diameter spectrum. *J. Comp. Neurol.* **176**:263-268.

133. Perry, V. H., Z. Henderson, and R. Linden. 1983. Postnatal changes in the retinal ganglion cell and optic axon populations in the pigmented rat. *J. Comp. Neurol.* **219**:356-368.

134. Gething, M. J. 1985. Protein transport and secretion. Cold Spring harbour laboratory, Cold Spring, NY.

135. Sefton, A. J., and M. Swinburn. 1964. Electrical activity of lateral geniculate nucleus and optic tract of the rat. *Vision Res.* **4**:315-328.

136. Bennett, G., L. DiGambrardino, H. L. Koenig, and B. Droz. 1973. Axonal migration of protein and glycoprotein to nerve endings. II. Radioautographic analysis of the renewal of glycoproteins in nerve endings of chicken ciliary ganglion after intracerebral injection of ^{3}H-fucose and ^{3}H-glucosamine. *Brian Res.* **60**:129-146.

137. Tessler, A., L. Autilio-Gambetti, and P. Gambetti. 1980. Axonal growth during regeneration: a quantitative autoradiographic study. *J. Cell Biol.* **87**:197-203.

138. Hendrickson, A. E. 1972. Electron microscopic distribution of axoplasmic transport. *J. Comp. Neurol.* **144**:381-398.

139. Schonbach, J., C. Schonbach, and M. Cuenod. 1971. Distribution of transported proteins in the slow phase of axoplasmic flow. An electron microscopical autoradiographic study. *J. Comp. Neurol.* **141**:485-498.

140. Harry, G. J., J. F. Goodrum, T. W. Bouldin, A. D. Toews, and P. Morell. 1989. Acrylamide-induced increases in deposition of axonally transported glycoproteins in rat sciatic nerve. *J. Neurochem.* **52**:1240-1247.

141. Bisby, M. A. 1985. Retrograde axonal transport of phospholipids in rat sciatic nerve. *J. Neurochem.* **45**:1941-1947.

142. Goldberg, D. J., J. H. Schwartz, and A. A. Sherbany. 1978. Kinetic properties of normal and perturbed axonal transport of serotonin in a single identified axon. *J. Physiol.* **281**:559-579.

143. Brimijoin, S., and M. J. Wiermaa. 1977. Direct comparison of the rapid axonal transport of norepinephrine and dopamine-ß-hydroxylase activity. *J. Neurobiol.* **8**:239-250.

144. Willard, M. W. 1983. Techniques for studying axonally transported proteins. In:

Current methods in cellular neurobiology. Wiley, New York. 2:35-84.

145. Lorenz, T., and M. Willard. 1978. Subcellular distribution of intraaxonally transported polypeptides in the rabbit visual system. *Proc. Natl. Acad. Sci. U. S. A.* **75**:505-509.

146. Levine, J., and B. Willard. 1980. The composition and organization of axonally transported proteins in the retinal ganglion cells of the guinea pig. *Brain Res.* **194**:137-154.

147. Tytell, M., M. M. Black, J. A. Garner, and R. J. Lasek. 1981. Axonal transport: each major rate component reflects the movement of distinct macromolecular complexes. *Science.* **214**:179-181.

148. Freeman, J. A., S. Bolcks, M. Deaton, B. McGuire, J. J. Norden, and G. J. Snipes. 1986. Axonal and glial proteins associated with development and response to injury to the rat and goldfish optic nerve. *Exp. Brain Res.* **13**:34-47.

149. Snipes, G.J., B. Costello, B. McGuire, B. N. Mayers, S. S. Bock, J. J. Norden, and J. A. Freeman. 1987. Regulation of specific neuronal and nonneuronal proteins during development and following injury in the rat central nervous system. *Prog. Brain. Res.* **71**:155-175.

150. Moya, K. L., L. I. Benwitz, S. Jhaveri, and S. A. Schneider. 1987. Enhanced visualization of axonally transported proteins in the immature CNA by suppression of systemic labeling. *Dev. Brain Res.* **31**:183-191.

151. Padilla, S. S., L. J. Roger, A. D. Toews, J. F. Goodrum, and P. Morell. 1979. Comparison of proteins transported in different tracts of the central nervous system. *Brain Res.* **176**:407-411.

152. Tytell, M., R. L. Gulley, R. J. Wenthold, and R. J. Lasek. 1980. Fast axonal transport in auditory neurons of the guinea pig: a rapidly turned-over glycoprotein. *Proc. Natl. Acad. Sci. U. S. A.* **77**:3042-3046.

153. Skene, J. H. P., and M. B. Willard. 1981. Axonally transported proteins associated with axon growth in rabbit central and peripheral nervous systems. *J. Cell Biol.* **89**:96-103.

154. Tashiro, T., H. Kasai, and M. Kurokawa. 1980. A calmodulin-related polypeptide rapidly migrates within the mammalian nerve. *Biomed. Res.* **1**:292-299.

155. Bisby, M. A. 1981. Reversal of axonal transport: similarity of proteins transported in anterograde and retrograde directions. *J. Neurochem.* **36**:741-745.

156. Perry, G. W., and D. L. Wilson. 1981. Protein synthesis and axonal transport during nerve regeneration. *J. Neurochem.* **37**:1203-1217.

157. Neale, J. H., D. S. Forman, D. B. Shibla, and S. A. Shortell, S. A. 1980. Comparative analysis of rapidly transported axonal proteins in sensory neurons of the frog and rat. *J. Neurochem.* **35**:838-843.

158. Oyler, G. A., G. A. Higgins, R. A. Hart, E. Battenberg, M. Billingsley, F. E. Bloom, and M. C. Wilson. 1989. The identification of a novel synaptosomal associated protein, SNAP-25, differentially expressed by neuronal subpopulations. *J. Cell Biol.* **109**:3039-3052.

159. Trimble, W. S., D. M. Cowan, and R. H. Scheller. 1988. VAMP-1: A synaptic vesicle-associated integral membrane protein. *Proc. Natl. Acad. Sci. U. S. A.* **85**:4538-4542.

160. Bennett, M. K., N. Calakos, and R. Scheller. 1992. Syntaxin: a synaptic protein implicated in docking of synaptic vesicles at presynaptic active zones. *Science.* **257**:255-259.

161. Matthew, W. D., L. Tsavaler, and L. F. Reichardt. 1981. Identification of a synaptic vesicle-specific membrane protein with a wide distribution in neuronal and neurosecretory tissue. *J. Cell Biol.* **91**:257-261.

162. Mollard, G. F. V., G. A. Mignery, M. Baumert, M. A. Perin, T. J. Hanson, M. P. Burger, R. Jahn, and T. C. Südhof. 1990. Rab 3 is a small GTP-binding protein exclusively localized to synaptic vesicles. *Proc. Natl. Acad. Sci. U. S. A.* **87**:1988-1992.

163. Horikawa, H. P. M., H. Saisu, T. Ishizuka, Y. Sekine, A. Tsugita, S. Odani, and T. Abe. 1993. A complex of rab3A, SNAP-25, VAMP/synaptobrevin-2 and syntaxins in brain presynaptic terminals. *FEBS Lett.* **330**:236-240.

164. Block, M. R., Glick, B. S., Wilcox, C. A., Wieland, F. T., and Rothman, J. E. 1988. Purification of an N-ethylmaleimide-senstive protein catalyzing vesicular transport. *Proc. Natl. Acad. Sci. U.S.A.* **85**:7852-7856.

165. Clarry, D. O., I. C. Griff, and J. E. Rothman. 1990. SNAPs, a family of NSF attachment proteins involved in intracellular membrane fusion in animals and yeast. *Cell* **61**:709-721.

166. Bray, J. J., C. M. Kon, and B. M. Breckenridge. 1971. Reversed polarity of rapid axonal transport in chicken motoneurons. *Brain Res.* **33**:560-564.

167. Abe, T., T. Haga, and M. Kurokawa. 1974. Retrograde axoplasmic transport: its continuation as anterograde transport. *FEBS Lett.* **47**:272-275.

168. Bisby, M. A. 1976. Orthograde and retrograde axonal transport of labeled proteins in motoneurons. *Exp. Neurol.* **50**:628-648.

169. Partlow, L. M., C. D. Ross, R. Motwani, and D. B. McDougal. 1972. Transport of axonal enzymes in surviving segments of frog sciatic nerve. *J. Gen. Physiol.* **60**:388-405.

170. Bisby, M. A., and V. T. Bulgr. 1977. Reversal of axonal transport at a nerve crush. *J. Neurochem.* **29**:313-320.

171. Farquhar, M. G. 1985. Progress in unraveling pathways of Golgi traffic. *Ann. Rev. Cell Biol.* **1**:447-488.

172. Kleinsmith, L. J., and V. M. Kish. 1988. Processing of proteins for secretion. In, Principles of cell biology. Harper and Raw, New York. 175-178.

173. Hammerschlag, R. 1982. Multiple roles of calcium in the initiation of fast transport of fast axonal transport. In, Axoplasmic Transport. Springer, New York. 279-286.

174. Hammerschlag, R., and G. C. Stone. 1987. Further studies on the initiation of fast axonal transport. In, Axonal Transport. Liss, A. R. 37-51.

175. Pryer, N. K., L. J. Wuestehube, and R. Schekman. 1992. Vesicle mediated protein sorting. *Annu. Rev. Biochem.* **61**:471-516.

176. Tooze, J., H. F. Kern, S. D. Fuller, and K. E. Howell. 1989. Condensation-sorting events in the rough endoplasmic reticulum of exocrine pancreatic cells. *J. Cell Biol.* **109**:35-50.

VITA

Name: Surafel Mulugeta
Birth: Addis Abeba, Ethiopia 04/19/59
Nationality: United States Citizen

Education

Undergraduate

B.A., Chemistry and Biology. Bluffton College, Bluffton, Ohio. May, 1982.

Graduate

Ph.D., Neuroscience. Department of Anatomy and Neurobiology, Eastern Virginia Medical School, Norfolk, Virginia. July, 1997.

Research Work

1994-1997

Studies of protein trafficking and targeting in the rat optic pathway. Expression of heat shock proteins in abnormal rats.

1993-1994

Investigation of thermo-tolerant and thermo-sensitive cells in their activation of DNA topoisomerase.

1992-1993

In vitro and *in vivo* studies of the induction and/or expression of heat shock proteins in neuronal cells and tissues. Studies of amyloid precursor protein and ß-amyloid protein in neuronal cells.

1991-1992

Characterization of heat shock proteins in T-lymphocytes.

Publications

Mulugeta, S., B. Tedeschi, M-T Maa, K. Guhl, N. Hawkins, S.R. Shenoy, J. Broccoletti and P.F. Aravich. 1997. Fawn-Hooded rats with congenital serotonin abnormalities express inducible 70 kDa heat shock protein (HSP72) in brown fat: implication for thermogenesis. *Soc. Neurosci. Abst.* In press.

Guhl, K., S. Mulugeta, B. Tedeschi, S.R. Shenoy, M-T Maa, N. Hawkins, J.J. Edwards, C-T Hsu, G.E. Goode, and P.F. Aravich. 1997. Stress Inducible 70 kDa heat shock protein (HSP72) expression in gastric mucosa of animal model of anorexia nervosa and gastric stress ulcers. *Soc. Neurosci. Abst.* In press.

Mulugeta, S., R.P. Ciavarra, and B. Tedeschi. 1996. Immunoprecipitation of specific subsets of fast and slow transported proteins with SNAP-25 in the rat primary visual pathway. *Mol. Biol. Cell abst.* 7:225a.

Mulugeta, S., B. Tedeschi, C-T Hsu, S.R. Shenoy, T. Coon, J. McCormick, M-T Maa, G.E. Goode, and P.F. Aravich. 1996. Stress inducible 70 kDa heat shock protein (HSP72) expression in adrenal glands of Fawn-Hooded rats with Congenital serotonin abnormalities. *Soc. Neurosci. Abst.* **22**:1146.

Mulugeta, S., M.E. Brown, R.P. Ciavarra, and B. Tedeschi. 1995. Trafficking of the fast axon transported retinal ganglion cell proteins. *Mol. Biol. Cell Abst.* **6**:70a.